

## Periodic layer formation during solid state reactions

**Citation for published version (APA):**

Rijnders, M. R. (1996). *Periodic layer formation during solid state reactions*. [Phd Thesis 1 (Research TU/e / Graduation TU/e), Chemical Engineering and Chemistry]. Technische Universiteit Eindhoven.  
<https://doi.org/10.6100/IR476735>

**DOI:**

[10.6100/IR476735](https://doi.org/10.6100/IR476735)

**Document status and date:**

Published: 01/01/1996

**Document Version:**

Publisher's PDF, also known as Version of Record (includes final page, issue and volume numbers)

**Please check the document version of this publication:**

- A submitted manuscript is the version of the article upon submission and before peer-review. There can be important differences between the submitted version and the official published version of record. People interested in the research are advised to contact the author for the final version of the publication, or visit the DOI to the publisher's website.
- The final author version and the galley proof are versions of the publication after peer review.
- The final published version features the final layout of the paper including the volume, issue and page numbers.

[Link to publication](#)

**General rights**

Copyright and moral rights for the publications made accessible in the public portal are retained by the authors and/or other copyright owners and it is a condition of accessing publications that users recognise and abide by the legal requirements associated with these rights.

- Users may download and print one copy of any publication from the public portal for the purpose of private study or research.
- You may not further distribute the material or use it for any profit-making activity or commercial gain
- You may freely distribute the URL identifying the publication in the public portal.

If the publication is distributed under the terms of Article 25fa of the Dutch Copyright Act, indicated by the "Taverne" license above, please follow below link for the End User Agreement:

[www.tue.nl/taverne](http://www.tue.nl/taverne)

**Take down policy**

If you believe that this document breaches copyright please contact us at:

[openaccess@tue.nl](mailto:openaccess@tue.nl)

providing details and we will investigate your claim.

**PERIODIC LAYER FORMATION  
DURING  
SOLID STATE REACTIONS**

**PROEFSCHRIFT**

ter verkrijging van de graad van doctor aan de Technische Universiteit Eindhoven, op gezag van de Rector Magnificus, prof.dr. M. Rem, voor een commissie aangewezen door het College van Dekanen in het openbaar te verdedigen op maandag 16 december 1996 om 16.00 uur

door

**Marco Raymond Rijnders**

geboren te Andijk

Dit proefschrift is goedgekeurd  
door de promotoren:

prof.dr. R. Metselaar  
en  
prof.dr. F.J.J. van Loo

Druk: Universiteitsdrukkerij, Technische Universiteit Eindhoven

CIP-DATA KONINKLIJKE BIBLIOTHEEK, DEN HAAG

Rijnders, Marco Raymond

Periodic layer formation during solid state reactions /  
Marco Raymond Rijnders.-Eindhoven: Technische  
Universiteit Eindhoven  
Thesis Technische Universiteit Eindhoven.-with ref.-  
With summary in Dutch.  
ISBN 90-386-0119-0  
Subject headings: solid state reactions / periodic layer  
formation / periodic phenomena

The work presented in this thesis has been carried out at the Vakgroep voor Vaste Stof Chemie en Materialen, Faculty of Chemical Engineering and Chemistry, Eindhoven University of Technology, the Netherlands.

The investigations were partly supported by SON (the Dutch foundation for chemical research) with financial aid from NWO (the Dutch organization for the advancement of scientific research).

## CONTENTS

<b>1. INTRODUCTION</b>	<b>1</b>
<b>1.1 Solid state reactions and solid state diffusion</b>	<b>1</b>
<b>1.2 Definition of the problem; periodic layer formation</b>	<b>2</b>
<b>1.3 Outline of this work</b>	<b>3</b>
References	4
<b>2. DIFFUSION AND THERMODYNAMICS</b>	<b>5</b>
<b>2.1 Thermodynamics of solids</b>	<b>5</b>
2.1.1 Introduction	5
2.1.2 Chemical potential and activity; Activity diagrams	6
2.1.3 The phase rule; Phase diagrams	8
<b>2.2 Defects</b>	<b>9</b>
2.2.1 Vacancies	9
2.2.2 Dislocations	10
2.2.3 Grain boundaries	13
2.2.4 Phase interfaces	14
<b>2.3 Solid state diffusion</b>	<b>14</b>
2.3.1 Atom movements	14
2.3.2 Reference frames	15
2.3.3 Reactive diffusion	16
<b>2.4 Mobility</b>	<b>17</b>
<b>2.5 The Kirkendall effect</b>	<b>19</b>
<b>2.6 The influence of stress on diffusion: mechanochemistry</b>	<b>22</b>
<b>2.7 Reaction layer morphologies and microstructure</b>	<b>23</b>
References	27

<b>3. CHEMICAL PERIODICITY</b>	<b>29</b>
<b>3.1 Internal reactions</b>	<b>29</b>
<b>3.2 The Liesegang phenomenon</b>	<b>31</b>
<b>3.3 Periodically layered oxide scales</b>	<b>32</b>
<b>3.4 Other periodic structures</b>	<b>33</b>
3.4.1 Oscillating reactions	33
3.4.2 Self-organisation (pattern formation) in solids	33
References	34
<b>4. EXPERIMENTAL METHODS</b>	<b>37</b>
<b>4.1 Materials</b>	<b>37</b>
4.1.1 The pure materials	37
4.1.2 Alloy and diffusion couple preparation	37
4.1.3 Determination of phase equilibria	38
<b>4.2 Annealing procedures</b>	<b>38</b>
<b>4.3 Diffusion couple cross-section preparation</b>	<b>39</b>
<b>4.4 Analysis</b>	<b>40</b>
<b>5. PERIODIC LAYER FORMATION: EXPERIMENTAL OBSERVATIONS</b>	<b>41</b>
<b>5.1 Introduction</b>	<b>41</b>
<b>5.2 Ag/Ti-foil/Si diffusion couples</b>	<b>41</b>
5.2.1 Introduction	41
5.2.2 Experimental details	42
5.2.3 Phase Equilibria in the Ag-Ti-Si system	42
5.2.4 The formation of periodic structures in the couples Ag/Ti-foil/Si	48
<b>5.3 Reactions of transition-metal silicides with zinc</b>	<b>55</b>
5.3.1 Reactions of iron-silicides with zinc	55
5.3.2 Reactions of cobaltdisilicide with zinc	59
5.3.3 Reactions of nickel-silicides with zinc	63
<b>5.4 Reactions of nickel-cobalt-iron alloys with magnesium</b>	<b>65</b>
<b>5.5 Reactions of non-carbide forming metals with silicon carbide</b>	<b>69</b>
5.4.1 Reactions of iron, cobalt or nickel with SiC	69
5.4.2 Reactions of platinum with SiC	71
5.4.3 Reactions of palladium with SiC	79
References	82

<b>6. MECHANISMS OF PERIODIC LAYER FORMATION DURING SOLID STATE REACTIONS</b>	<b>85</b>
<b>6.1 Proposed reaction mechanism leading to periodic pattern         formation in Ag/Ti-foil/Si diffusion couples</b>	<b>85</b>
<b>6.2 Periodic layer formation and the Kirkendall effect</b>	<b>90</b>
6.2.1 Evidence for Kirkendall effect driven periodic layer formation; Pt/SiC diffusion couples	90
6.2.2 Fluxes in metal silicide/Zn diffusion couples	95
6.2.3 Periodic layer formation in Ni-Co-Fe alloy/Mg diffusion couples	95
6.2.4 Sintering behaviour and band formation	96
6.2.5 Single-crystalline vs. polycrystalline substrate	96
<b>6.3 Appearance of loops</b>	<b>98</b>
References	98
<b>List of symbols and abbreviations</b>	<b>101</b>
<b>Summary</b>	<b>103</b>
<b>Samenvatting</b>	<b>105</b>
<b>Nawoord</b>	<b>107</b>
<b>Curriculum vitae</b>	<b>108</b>

# CHAPTER 1

## INTRODUCTION

### 1.1 SOLID STATE REACTIONS AND SOLID STATE DIFFUSION

When the universe was still young and very hot, it was inhabited by gaseous species only. Only after a few billion years the first solids started to appear and the universe became interesting for solid state chemists. However, it took another few billion years for small solid particles to cluster into a huge lump and for Man to appear on the face of it. Unaware of the large impact this would have, Man started to cast iron and bronze to produce weapons and tools. Solid state science had become inevitable.

Nowadays solid state science comprises an enormous field of fundamental knowledge and engineering, from mineralogy to quantum physics and from the design of high-temperature materials to the development of catalysts. A small part of it is devoted to the study of solid state reactions and it is in this field this thesis will make a contribution.

Appreciable chemical reaction of the solid state mostly takes place at temperatures well above room temperature. Knowledge of the chemistry of solids is therefore important for engineers who design and build equipment for operation at high temperatures, e.g. engines, turbines, drilling heads, linings of blast-furnaces etc. However, processes connected with solid state diffusion at room temperature pose engineering problems, too. Creep, atmospheric corrosion and embrittlement of low-melting solders are among the most prominent of those. With the downscaling of micro-electronic circuits, diffusion (electromigration) in these circuits will have to be taken into account. Notwithstanding the practical interest of solid state chemistry, this thesis will be more concerned with the fundamental aspects of certain types of solid state reactions.

A distinction should be made between reactions of the solid state and solid-solid reactions. The first comprises all possible reactions of a solid, from decomposition to catalytic activity. Only one of the reactants needs to be a solid. Solid-solid reactions occur between solids only, although the reaction products are not necessarily solids. E.g. reactions of non-nitride forming



metals with silicon nitride will produce gaseous nitrogen. It also often happens that the reaction temperature is higher than the melting point of one or more of the product phases, hence liquid will form. This thesis is concerned with solid-forming reactions only. The terms solid state reaction and solid-solid reaction will be used alternatively.

What makes solids different from liquids and gases, is their rigid (lattice) structure. Since chemical reaction needs the encounter of reactive species, the role of *diffusion* in solid-solid reactions is evident. For such reactions to proceed, atoms need to move through the lattice to arrive at a place where they can react. The *kinetics* of solid state reactions are therefore largely dependent on crystal structure and its defects. Another property of solid state reactions, as opposed to reactions of liquids and gases, is that, due to the rigidity of the lattice, solids may support stresses and hence (elastic) stresses may develop during the reaction. This imposes extra boundary conditions for the analysis of solid state reactions. When the solid is not able to accommodate the stresses, plastic deformation or cracking will occur. Finally, *anisotropy* is an important characteristic of solids. This makes the magnitude of physical properties like diffusion, elastic constants, reflection etc., direction dependent.

Whether or not a reaction may take place is predicted in the first instance by *thermodynamics*. The Gibbs energy of reaction under specified conditions should be negative for a reaction to proceed spontaneously. The *phase diagram* determines possible equilibria. However, many solid state reactions, although thermodynamically allowed, proceed at an almost negligible rate (at least at low temperatures) because of the kinetic constraints. This makes the study of the *reaction rates* or kinetics of solid state reactions essential. Kinetics describes the evolution in time of a non-equilibrium many-particle system towards equilibrium (or a steady state) [1]. From a fundamental viewpoint the study of kinetics will help to solve reaction mechanisms. For an engineer it is important to know and (if possible) to control the rate of reaction, e.g. to prevent catastrophic breakdown of coatings, joints, electrical contacts or structural materials.

Thermodynamics, kinetics and mechanics are at the basis of the research presented in this thesis.

## **1.2 DEFINITION OF THE PROBLEM; PERIODIC LAYER FORMATION**

Thinking of chemical reactions, we think about the conversion of a substance or substances into another substance. When reactants are brought together a reaction occurs during some time until equilibrium is reached (the time needed to reach equilibrium depends on kinetics). When the reaction is complete, we should find a homogeneous distribution of the reaction products in space, if we consider fluids or gases. The concentration of the product substance is monotonically rising with time. For solid-solid reactions this is equivalent to saying that the reaction product layer grows with time, i.e. although the concentration of components in the

solid reaction product is fixed, the amount of reaction product increases. It is common understanding that reaction product layers in a bulk diffusion couple grow simultaneously. Depending on the number of components, we may find single-phase, two-phase etc. product layers. Usually, of each product layer only one is present. To put it another way, if the composition of the reaction layer is measured from one end-member of the couple to the other, no oscillations are found. Once the composition has passed into another phase field, it will not go back to one which has already been passed.

There are, however, solid state reactions, which result in more than one layer of the same product. In the reaction zone we find a regular repeating pattern of reaction products. This is the so-called periodic layered structure. The number of periodic layers increases with time. This means, when crossing the reaction zone from the one end-member to the other, that the composition of the zone oscillates, or, in other words that the composition-line (*diffusion path*) in the equilibrium phase diagram has several loops into the same area.

The periodic structure is not a result of a periodic reaction (i.e. a reaction whose reaction products vary periodically with time). It may be the final (and stable) result of a solid state diffusion-reaction process.

Periodic layer formation is a complex and interesting solid state phenomenon. The aim of this thesis is to describe several actual periodic layered structures, to clarify the factors involved in periodic layer formation and, finally, to explain the mechanisms by which this structure may come about.

### 1.3 OUTLINE OF THIS WORK

The main objective of this work is to elucidate the mechanisms for the formation of reaction layers which are periodic in space and time in *solid state reactions*.

In order to provide adequate background, Chapter 2 considers briefly the basic theory involved. This covers diffusion, thermodynamics, the role of defects and stresses in solid state reactions. Reaction layer morphologies are considered. Special emphasis is put on the Kirkendall effect. Chapter 3 reviews the literature on chemical periodicity and periodic phenomena encountered in chemistry.

In Chapter 4 the experimental set-up of the investigations is given. More details on the experiments will appear throughout Chapter 5.

Chapter 5 is concerned with the experimental observation of the periodic layered morphology in several ternary systems and one quaternary system.

Chapter 6 elaborates on the possible mechanisms for periodic layer formation in view of the experimental observations given in Chapter 5.

## **References to Chapter 1**

- [1] H. Schmalzried: *Chemical Kinetics of Solids*, VCH Verlagsgesellschaft mbH, Weinheim, Germany, 1995

## ***Further reading***

*Treatise on solid state chemistry*, vol. 4, *Reactivity of solids*, N.B. Hannay, ed., Plenum Press, New York, 1976

H. Schmalzried: *Festkörperreaktionen, Chemie des Festen Zustandes*, Verlag Chemie GmbH, Weinheim, Germany, 1971

## CHAPTER 2

### DIFFUSION AND THERMODYNAMICS

This chapter covers some fundamental principles which are of importance to the following chapters. The background presented here remains extremely limited because of the large number of basic textbooks which treat those subjects in depth. A general bibliography is given at the end of this chapter.

#### 2.1 THERMODYNAMICS OF SOLIDS

##### 2.1.1 Introduction

Thermodynamics is concerned with energy balances and equilibrium. It relates various properties of chemical systems to certain state functions (like internal energy, entropy etc.) and changes in the system are described in terms of changes of those state properties. When two materials react, there is a change of total energy. We are interested in reactions at constant temperature and pressure, so the Gibbs energy ( $G \equiv H - TS$ ) of the system and changes herein will be the appropriate central state variable to consider. The Gibbs energy of reaction indicates the direction of spontaneous change.

In general, a chemical reaction is written:



where  $\nu_i$ ,  $\nu_j$  denote the stoichiometric coefficients,  $R_i$  the reactant species and  $P_j$  the product species.

The equilibrium constant  $K_r$  for this reaction is given by the *mass action law*:

$$K_r = \frac{\prod_j a_{P_j}^{\nu_j}}{\prod_i a_{R_i}^{\nu_i}} \quad (2.2)$$

where  $a_{s_i}$  is the *activity* of species  $i$  (see 2.1.2).

The relation between the *standard* Gibbs energy of reaction  $\Delta G_r^\ominus$  and  $K_r$  is:

$$\Delta G_r^\ominus = -RT \ln K_r \quad (2.3)$$

with R being the gas constant ( $8.314 \text{ J} \cdot \text{K}^{-1} \cdot \text{mol}^{-1}$ ) and T the absolute temperature (K). The standard energy of reaction is obtained by adding the proper standard Gibbs energies of formation of the reacting species:

$$\Delta G_r^\ominus = \sum_j \nu_j \Delta G_f^\ominus(\text{P}_j) - \sum_i \nu_i \Delta G_f^\ominus(\text{R}_i) \quad (2.4)$$

The standard state of a solid is established as the most stable form at a pressure of one atmosphere and a specified temperature.

### 2.1.2 Chemical potential and activity; Activity diagrams

Because of the different interaction energies between atoms of like and unlike type, adding or removing atoms of a certain type to a system, i.e. changing its composition, will alter its internal energy. If the composition is changed at constant pressure and temperature, the Gibbs energy of the system will change. This is expressed by:

$$\left( \frac{\partial G}{\partial n_i} \right)_{p, T, n_j \neq n_i} = \mu_i \quad (2.5)$$

The partial molar free energy (or molar Gibbs function), as expressed on the left-hand side, is assigned the symbol  $\mu_i$ , the *chemical potential*. Thus the chemical potential of i measures the rate of change of the Gibbs energy upon adding an infinitesimal amount of i to the system.

The chemical potential of i in a phase  $\pi$  at arbitrary conditions is defined through:

$$\mu_i^\pi(T, p, \underline{x}) = \mu_i^\ominus + RT \ln a_i^\pi(T, p, \underline{x}) \quad (2.6)$$

where  $\mu_i^\ominus$  is the standard molar Gibbs function,  $a_i^\pi$  the activity of i in phase  $\pi$ , and  $\underline{x}$  the total composition ( $\underline{x} = x_1, x_2, \dots$ , where  $x_i$  is the mole fraction of component i). At equilibrium the chemical potential of i is the same in all phases, so if the same standard state is chosen for i in every phase, also its activity will be equal in all phases. Conversely, if the chemical potential of i is not everywhere the same, the system is not in equilibrium and some kind of change has to take place. This change may be a chemical reaction, but it may also be mixing, unmixing, vaporization etc. In solids there will be a flow (diffusion) of component i in the direction where its chemical potential is lower (see 2.4). The concept of *local equilibrium*, frequently used in solid state chemistry, states that the chemical potential be a continuous function everywhere. This is equivalent to saying that nucleation of intermediate phases is

instantaneous and interface concentrations take their equilibrium values throughout [1]. If the pure component  $i$  is in its standard state, the second term of the right-hand side of (2.6) should be zero, hence  $a_i = 1$  in the standard state. The activity may be expressed as the product of the mole fraction of the component and an activity coefficient which is, in general, dependent on the conditions:

$$a_i(T, p, \underline{x}) = \gamma_i(T, p, \underline{x}) \cdot x_i \quad (2.7)$$

In ideal solutions the activity coefficient of a component is equal to 1, hence the activity of a component equals its mole fraction in ideal solutions. In general, at intermediate concentrations,  $\gamma$  is not a constant, nor is it a linear function of concentration. At low solute concentrations,  $a_{\text{solute}}$  does become linearly proportional to its mole fraction (Henry's law,  $\gamma_i = \text{constant}$ ) and  $a_{\text{solvent}}$  becomes equal to its mole fraction (Raoult's law). This situation is depicted in Fig. 2.1 for a binary system with complete solubility (e.g. Cu-Ni). This is the simplest example of an *activity diagram*, which gives us the activity of the components of a system as a function of composition at a fixed pressure and temperature.

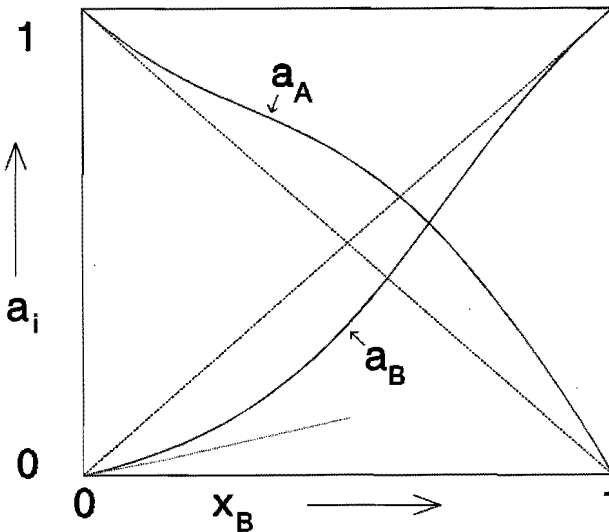


Fig. 2.1 Activity as a function of atomic fraction in a binary AB system

Activity diagrams for ternary systems may be calculated if thermodynamic data are available. These diagrams are more complicated to read but still conveniently plotted on paper. The activity of one of the components is plotted as a function of composition of the other two. A point to appreciate is that horizontal lines represent three-phase equilibria for which the activity of all three components is fixed. Single-phase fields appear as vertical lines (line-compounds) or areas (if there is a homogeneity range). Two-phase fields appear as areas. The use of such activity or potential diagrams has been explained by van Loo et al. [2].

### 2.1.3 The Phase Rule; Phase diagrams

The number of phases that may be present in a system at equilibrium is not arbitrary. If we define  $F$  as the number of variables that may be varied independently without changing the number of phases present, we have:

$$F = C - P + 2 \quad (2.8)$$

This is the so-called *phase rule* which was introduced, like most of the chemical thermodynamics, by J.W. Gibbs at the end of the 19th Century. The number 2 at the end stands for the variables temperature and pressure.  $C$  is the number of components present in the system and  $P$  the number of phases. Since in a *diffusion couple* (two pieces of solid clamped together and annealed for some time) also the activity of an element should be a variable, it follows that in binary diffusion couples only single-phase regions can exist, whereas in ternary couples also two-phase regions may occur (see 2.7).

*Phase diagrams* are the pictorial representations of possible equilibria between phases under varying conditions. They may be constructed from the knowledge of Gibbs energy curves as a function of their variables, but are, till the present, more easily accessible by experimentation. Since equilibria in complex systems are dependent on many different variables, a general phase diagram can be quite complicated. For representation on paper, two variables have to be chosen, with the other ones remaining fixed. The two-dimensionality of paper thus restricts the generality, but fortunately reduces the complexity of a phase diagram. Many choices for the independent variables are available to us (see, e.g. [3]).

Phase diagrams appearing throughout this thesis will be of either one of two types: 1) the binary composition vs. temperature diagram or 2) isothermal cross-section of a ternary composition vs. temperature diagram. It will be understood that for both types of diagram the total pressure is fixed; however, for solids there is little influence of the pressure on the phase diagram. From the last type of diagram we can read the compositions of the stable phases and their equilibrium compositions at one particular temperature and pressure. Tie-lines connect the equilibrium interface concentrations of two co-existing phases. In this type of diagram we can also plot a *diffusion path* [4], i.e. the locus of the compositions along the diffusion direction in a diffusion couple. The diffusion path shows us the actual sequence of phases in a diffusion couple. It cannot, in most cases, be predicted a priori. Kirkaldy and Brown [1] present a number of theorems on the properties of diffusion paths plotted on ternary isotherms. One of the most important should be repeated here: "a diffusion path on the ternary isotherm must cross the straight line joining the terminal compositions (of a diffusion couple) at least once". This is because the mass balance should be preserved.

In real diffusion couples a unique diffusion path is selected by the system, although it may have more solutions available [5].

## 2.2 DEFECTS

A perfect crystalline solid consists of an undistorted lattice of equilibrium positions wherein all the positions are occupied by the proper atoms. The perfect crystal is a theoretical concept only. In reality the perfect infinite array of lattice points is always more or less affected by distortions (not including thermal motion and elastic deformation). We call these distortions defects. The chemistry of solids cannot be understood without a proper knowledge of the nature and properties of defects. Defects of the lattice (we do not consider electronic and vibrational defects) can be classified according to their dimensions. We distinguish four categories:

1. Point defects (zero dimension): vacancies, interstitials and impurities, or a combination of these (e.g. Schottky defects, Frenkel pairs, divacancies, split interstitials). A vacancy is simply an empty equilibrium position of the lattice. Around a point defect, the lattice is distorted to some extent. Antisite defects, which are also point defects, are of a more subtle nature: an atom is sitting on a site in the "wrong" sublattice of a crystal. This is one of the possible defects to cause off-stoichiometry. It should be noted that interstitials may form an integral part of the crystal structure (as in  $\text{Fe}_3\text{C}$ ). In this case they should not be considered as defects.
2. Line defects (one dimension): dislocations.
3. Surface defects (two dimensions): external surfaces and internal surfaces: grain boundaries, interfaces (or phase boundaries), antiphase- and twin boundaries and stacking faults.
4. Macroscopic defects (three dimensions): pores, cracks, inclusions.

Each category has its own effects on the physical and chemical properties of the crystal. We will mainly consider the effects on diffusion. Defects always have a stress field and a certain energy associated with them. We can see this by introducing a defect in a perfect reference crystal: energy is needed to deform the crystal. The stress field causes the defects to interact.

### 2.2.1 Vacancies

Bulk diffusion normally proceeds by a vacancy mechanism, that is, atoms are moving by exchanging places with vacancies. Bulk diffusion may also proceed via an interstitial mechanism. No vacancies are needed in this case. We are not concerned with interstitial diffusion in this thesis.

Lattice vacancies are an equilibrium type of point defect. Their concentration is a function of temperature and pressure. In metals and alloys, near their melting point, the fraction of vacancies in the lattice is about  $10^{-3}$  to  $10^{-4}$ . An important property of vacancies is that they are not conserved; they can either be created at sources or annihilated at sinks (this fact allows lattice planes to move, the *Kirkendall-effect*, see 2.5). In the absence of a driving force, movement of vacancies in a solid is caused by random thermal motion. Every now and then an atom gains enough vibrational energy to jump into a neighbouring vacant space. This is the process of self-diffusion in solids [6]. Random thermal motion in alloys tends to level out concentration differences. The energy-barrier which must be overcome by the atom is called the activation energy for diffusion. It is due to the necessary distortion of the lattice



before the jump is possible. A special type of vacancy mechanism is called *relaxation mechanism*, proposed by Nachtrieb and Handler [7]. This occurs when distortion of the lattice around a vacancy (which is always present) can be compared to 'localized melting' of the crystal, allowing liquid-like diffusion for the atoms. According to Bocquet et al. [8], this model has now been abandoned. Vacancy mechanisms are predominant when the crystal structure is closely packed (not necessarily *close-packed*), because other mechanisms (e.g. interstitial movement) require much greater distortions of the lattice and hence a higher activation energy.

Compounds that show large deviations from stoichiometry may possess a high (structural) vacancy concentration on one of their sublattices (e.g. CoGa).

### **2.2.2 Dislocations**

Dislocations or line defects are present in each single- and polycrystalline material. In contrast to vacancies, a dislocation is not an equilibrium type of defect. This means that the number, size, type and arrangement of dislocations present is not a function of extensive thermodynamic variables, but depends rather on the thermal and mechanical history of the material. A dislocation (more precisely: dislocation line) is a line of distorted material inside the crystal. This distortion is a consequence of non-uniform slip of atomic planes across each other. The dislocation line is the boundary between slipped and unslipped areas of the crystal [9]. Two types of dislocations should be distinguished: edge- and screw dislocations. They are not basically different, strictly we should speak about a dislocation in the edge - or in the screw-orientation, but it is convenient to define them separately.

The edge-dislocation can be considered either as the boundary of a slipped atomic plane or as an extra atomic plane stashed into the lattice (Fig. 2.2a). The distortion (measured by the Burgers vector) is perpendicular to the dislocation line.

When we make a cut in a crystal, and shear the two edges of the cut, we produce a screw dislocation (Fig. 2.2b). In this case, the slip vector is parallel to the dislocation line. Going around the line, following the atomic plane, we make a step of the height of one atomic plane, hence the name screw dislocation. The crystal of Fig. 2.2b could be considered a single plane wound up like a spiral ramp.

A dislocation is uniquely defined by its burgers vector (unit slip vector)  $\bar{\mathbf{b}}$  and its direction vector  $\bar{\mathbf{s}}$ . An edge dislocation has its burgers vector perpendicular to its direction, a screw dislocation has its burgers vector parallel to its direction. A general dislocation line possesses both screw- and edge-character (Fig. 2.2c). It can be of any form, but it must either end at a surface or a node, or it must close on itself. When one dislocation ends at a surface it produces a step with a height equal to the projection of the Burgers vector normal to the surface. The material around a dislocation possesses residual strain because of the disregistry of the atoms in that region.

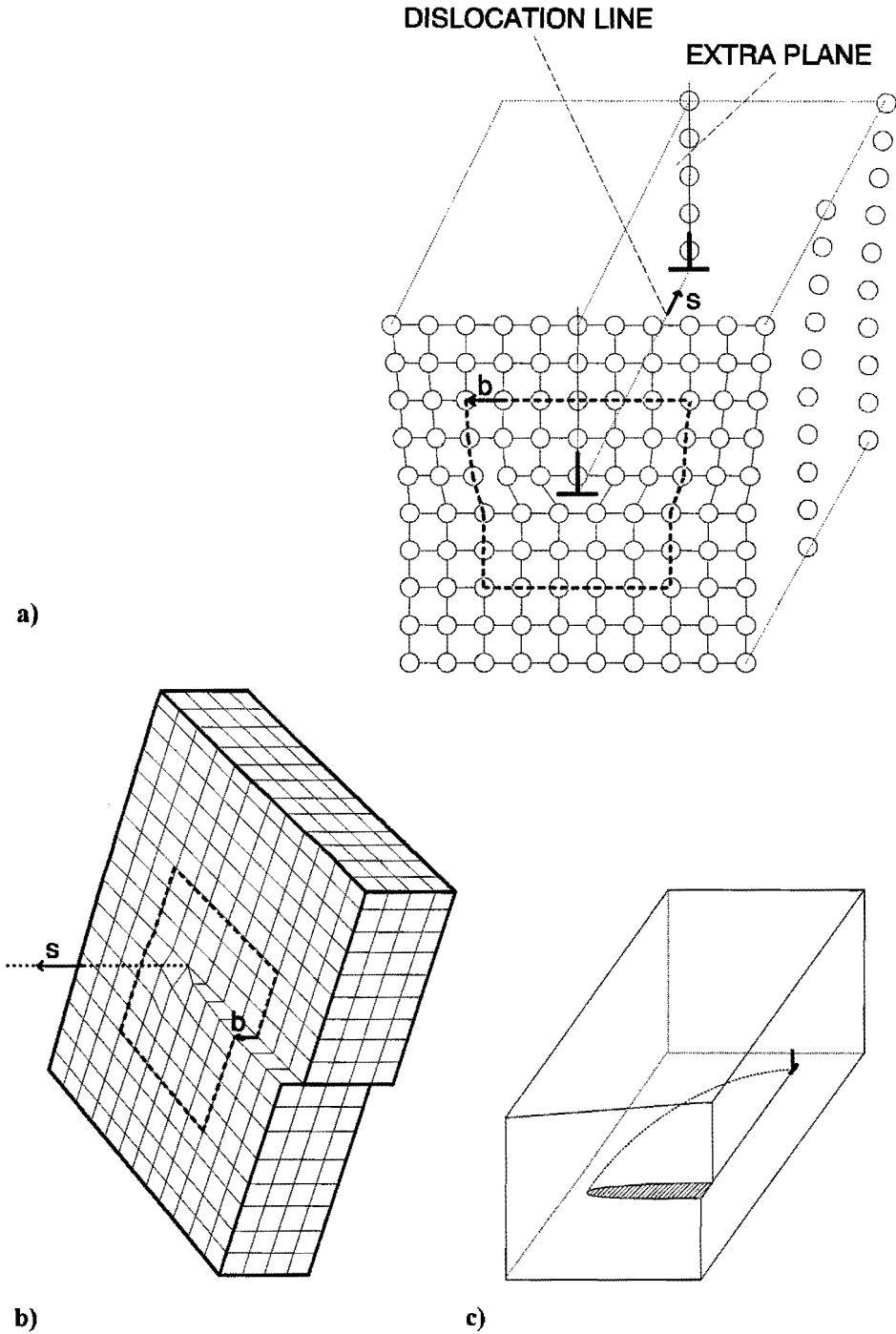


Fig. 2.2 Schematic view of dislocations; a) edge dislocation; b) screw dislocation; c) dislocation with mixed edge- and screw character

*Periodic layer formation during solid state reactions*

Motion of dislocation can be resolved into *glide* (conservative) and *climb* (non-conservative) components. Glide is the motion of a dislocation over a slip plane. In climb atoms have to move, so diffusion is involved in the process. *Plastic deformation* of a material always involves the glide of dislocations, i.e. a material can change its shape permanently when it is subjected to a stress that causes dislocation glide. The ductility of a material is, among others, determined by the number of *slip systems*, i.e. directions of easy glide, available to its crystal structure.

The process of growth or shrinkage of an edge dislocation by adding or removing vacancies is called climb. The motion of a screw is always glide. Dislocations can act as a source or sink for vacancies, especially at jogs and kinks (Fig. 2.3). Dislocations can also act as nucleation/precipitation sites by providing a stress field, which interacts with the misfit strain produced by the formation of a nucleus [10]. The stress field of dislocations provides a driving force for diffusion as well. Edge dislocations can provide a fast diffusion "pipe" because they border a dilated region of the crystal.

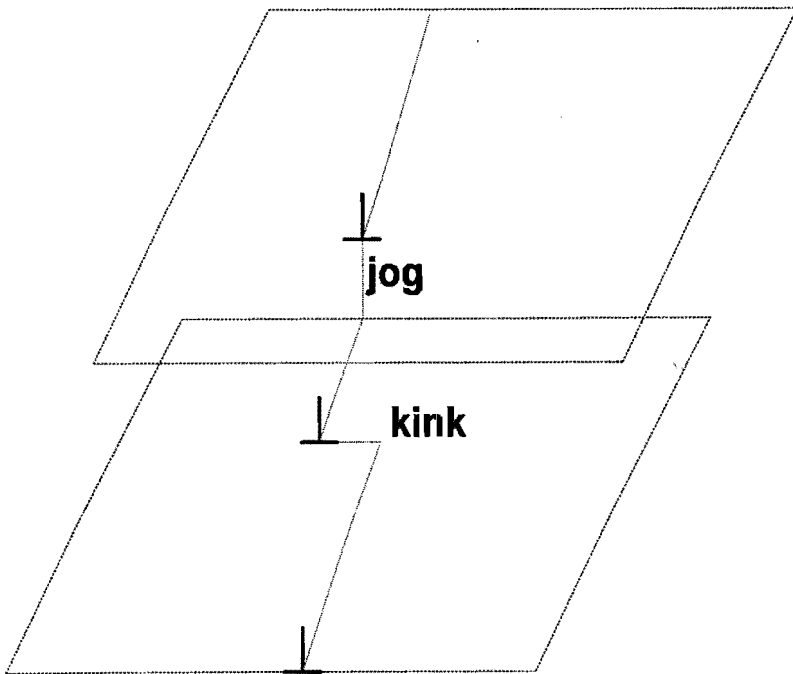


Fig. 2.3 *Schematic view of a kink and a jog in a dislocation*

To account for the large plastic deformation that can be produced in (metal) crystals, it is necessary to have regenerative multiplication of dislocations [9]. Multiplication of dislocations can be brought about either by glide, as in the Frank-Read and multiple cross-glide mechanisms, or by climb.

The operation of a *Frank-Read source* [11] is illustrated in Fig. 2.4. An initially straight segment of a dislocation, pinned at two points A and B, may bow out under the action of a stress. Pinning may be caused by impurities or nodes of dislocations. When the stress is greater than a certain critical stress, the dislocation expands through the positions shown in Fig. 2.4. As rotation about the pinning points continues, the dislocation closes on itself, annihilating over a portion of its length [12]. A closed dislocation loop is formed and the original situation is restored. This process may be repeated indefinitely, whereby more loops are created.

A similar mechanism operates via climb. This is the so-called Bardeen-Herring source [13]. Planes of atoms are added extending a stretch of dislocation as a loop like in the Frank-Read mechanism. This mechanism requires a vacancy supersaturation and therefore operates during quenching of a material.

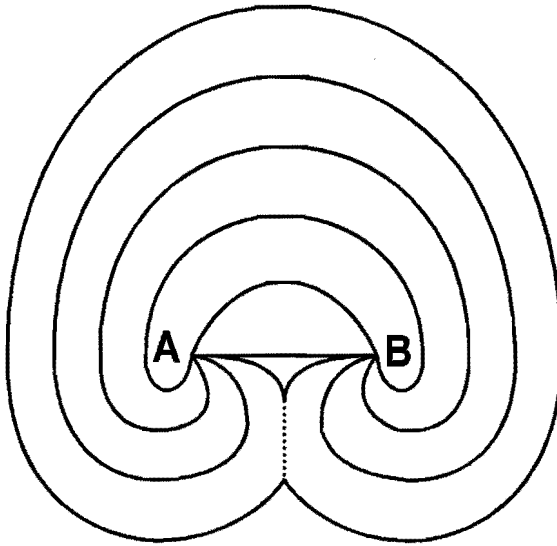


Fig. 2.4 *Frank-Read source for multiplication of dislocations*

### 2.2.3 Grain boundaries

Grain boundaries are two-dimensional non-equilibrium (evidenced by irreversible grain growth at high temperatures) defects in a solid. They are part of the *microstructure* of a material.

Grain boundaries can perform the same functions as dislocations. They provide a low energy barrier path for diffusion, because of the lower bonding energy for solute and tracer atoms. With finer grains, this effect is more obvious. The diffusivity in a grain boundary is dependent on the grain boundary orientation angle.

## **2.2.4 Phase interfaces**

Phase interfaces play an important role in heterogeneous reactions. Matter has to be transported across them in the course of reaction. The structure of a phase interface may be coherent (no or slight lattice mismatch between the phases), semi-coherent or incoherent. A semi-coherent interface exists of matching (epitaxial) lattice parts, separated by misfit dislocations.

An interphase interface will act as a source or sink for vacancies, as shown formally by van Loo et. al [14] by an explicit consideration of the atomic and vacancy fluxes during interdiffusion.

## **2.3 SOLID STATE DIFFUSION**

In the following sections diffusion will be treated as a one-dimensional problem. Vector notation will be avoided. It is only used to stress the generality of some basic equations.

### **2.3.1 Atom Movements**

Diffusion in solids is the movement of atoms or ions under the influence of some driving force. The nature of this force may be thermal, chemical, mechanical, electrical etc., or a combination of these. Solid state diffusion is different from diffusion in gases and fluids because of structural constraints imposed by the solid. Flow of matter in solids can also be caused by plastic deformation. This is not diffusion, but convective flow. Since a force is always equal to the gradient of a potential (field), the driving force for diffusion must be a derivative of a so-called 'diffusion potential' or (preferably) 'generalized chemical potential' [15]. All factors contributing to this potential influence diffusion. The main contributors to *isothermal* diffusion in the absence of an electrical field are the chemical potential and the (elastic) stress-field. This is so if we consider the chemical potential as a potential arising solely from compositional differences.

Solid state diffusion and reaction exist by virtue of defects and their mobility (see Section 2.4). Solid state diffusion is divided into two major categories: *volume* or *bulk diffusion* and *short-circuit diffusion*. The former is predominant at high temperature and may be due to several different diffusion mechanisms (Fig. 2.5). The latter is predominant at low temperatures ( $T < 0.5 T_m$  for pure materials) and associated with grain boundaries. In a perfect single crystal only volume diffusion can occur, whereas in polycrystalline materials short circuit diffusion will also play a role.

No solid state reaction can occur without diffusion. Other solid state phenomena where diffusion is of importance are e.g. the homogenization of alloys at high temperatures, sintering, recrystallization and grain growth, and precipitation of second-phase particles in solids.

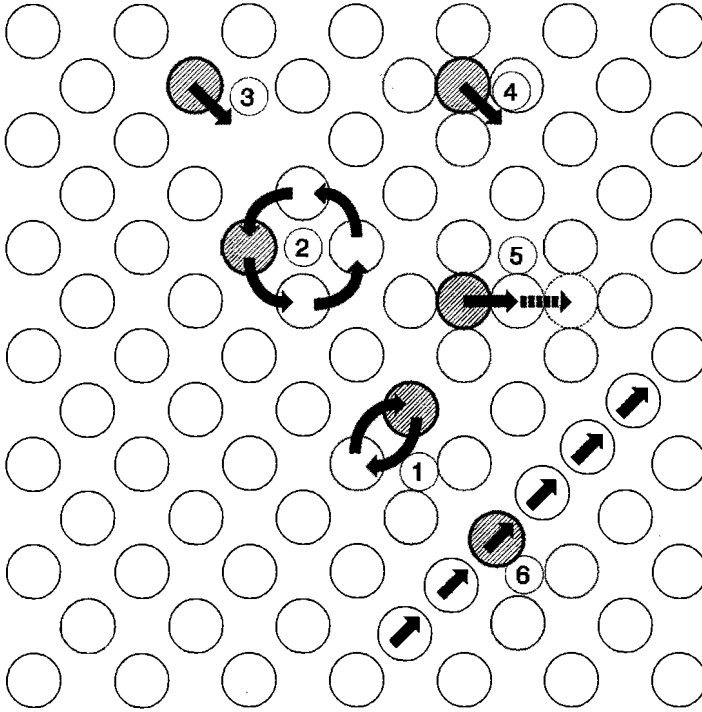


Fig. 2.5 Diffusion mechanisms in the solid state (after [16]); 1. direct exchange; 2. ring exchange; 3. vacancy mechanism; 4. direct interstitial; 5. indirect interstitial; 6. "crowdion"

### 2.3.2 Reference frames

Diffusion involves the motion of atoms, i.e. a flux of matter. Motion always has to be defined relative to some suitable origin or *frame of reference*. The diffusion coefficient is thus dependent on the choice of reference frame. If the flux is viewed from the position of an observer, we speak about the *laboratory frame of reference*. This frame may be considered to be fixed in space. If we consider diffusion in one dimension (as is common for the analysis of diffusion couples) we have to define a section or plane, perpendicular to this direction, relative to which the rate of transfer of the diffusing species is measured [17]. A general formulation defining such a frame is [18]:

$$\sum_{i=1}^n \alpha_i J_i = 0 \quad (2.9)$$

where  $J_i$  denotes the flux of  $i$  and  $\alpha_i$  are appropriate coefficients (e.g. partial molar volumes for a volume-fixed frame). All these frames will have a certain velocity with respect to the laboratory fixed frame. The *Matano plane* is the plane through which equal quantities (in

moles) of matter have been transported. If volume changes during interdiffusion are ignored, this plane identifies the position of the original contact plane.

Another possibility is to define the diffusive motion relative to a plane of inert markers which indicates the gross convective flow of matter. This is comparable to measuring a diffusion flux of salt in flowing water relative to some chips placed on the water which move with the flow velocity [19]. In such a case we speak about the *Kirkendall* frame of reference (see also 2.5). The Kirkendall frame of reference is moving with respect to the laboratory frame and true (intrinsic) diffusion is measured relative to it. From the above it is obvious that the numeric value of a diffusion coefficient in itself is a relative number. One has to know the frame of reference in which it is defined.

A flux in the laboratory frame is related to the flux through any other (moving) plane by:

$$J_i = j_i + C_i v_{rf} \quad (2.10)$$

where  $j_i$  is the flux with respect to the reference frame,  $C_i$  is the concentration and  $v_{rf}$  is the velocity of the reference frame with respect to the laboratory frame.

### 2.3.3 Reactive Diffusion

Reactive diffusion is characterized by the appearance of one or more new phases at the original interface between two phases  $\alpha$  and  $\beta$  (heterogeneous reaction), hence spatial separation of these phases occurs. In such a process, at least two interfaces are formed and the formation of phases at one or more of those interfaces depends on the supply of reactants, i.e. diffusing species. Reactive diffusion therefore comprises two steps: 1. the formation of phases (chemical reaction); this step involves nucleation, and 2. diffusion of components through the reaction (product) layer. Reaction requires rearrangement of the atoms at the interface and may involve a reaction barrier. If this barrier limits the growth rate of the product layer the reaction is said to be interface controlled or reaction controlled. When the solid state reaction is driven by a large  $\Delta G_r^\ominus$ , nucleation is easy and does not form a limitation to the process [20]. If the kinetics are limited by the arrival of species at the interface, the reaction is said to be diffusion controlled. In this case, the growth of a reaction product is governed by the flux equations and it will be parabolic with time if the local equilibrium interface chemical potentials are maintained. The formation of a phase AB in a binary diffusion couple can only continue by diffusion of A, or B, or both through the reaction layer. Depending on the ratio of the mobilities, the product can either grow at the A/AB interface, the B/AB interface, or both. In multiphase diffusion each separate reaction product layer grows parabolically with time. This leads to an overall parabolic time law for the thickness of the total reaction layer [21]:

$$(\Delta \xi)^2 = 2 k_p \cdot t \quad (2.11)$$

where  $\Delta\xi$  is the total reaction layer thickness,  $k_p$  the overall parabolic rate constant, and  $t$  is the time. The growth rate of an individual product layer is dependent on the fluxes in the neighbouring phases.

## 2.4 MOBILITY

Diffusion in inhomogeneous binary materials is often considered to be the result of a concentration gradient, or, in terms of Fick's first law (in one dimension):

$$\tilde{J}_i = -\tilde{D}_i \frac{\partial C_i}{\partial x} \quad (2.12a)$$

where  $\tilde{J}_i$  is the interdiffusion flux of species  $i$  ( $\text{mol} \cdot \text{m}^{-2} \cdot \text{s}^{-1}$ ),  $C_i$  its concentration ( $\text{mol} \cdot \text{m}^{-3}$ ). The constant of proportionality,  $\tilde{D}$ , is the *interdiffusion coefficient* (sometimes called chemical diffusion coefficient) and has units of  $\text{m}^2 \cdot \text{s}^{-1}$ .  $x$  (m) is a position coordinate measured in the direction of diffusion.

If we consider the flux with respect to the Kirkendall frame of reference, we define the so-called intrinsic flux as:

$$J_i = -D_i \frac{\partial C_i}{\partial x} \quad (2.12b)$$

where  $D_i$  denotes the intrinsic diffusion coefficient of  $i$ .  $D_i$  is generally different for different  $i$ . The interdiffusion coefficient and the intrinsic diffusion coefficient are related through [22,23]:

$$\tilde{D} = C_1 \bar{V}_1 D_2 + C_2 \bar{V}_2 D_1 \quad (2.13a)$$

where  $\bar{V}_i$  is the partial molar volume of component  $i$ . If the  $\bar{V}_i$ 's are equal, which means  $\bar{V}_i = V_m$ , then:

$$\tilde{D} = x_1 D_2 + x_2 D_1 \quad (2.13b)$$

where  $x_i$  is the mol fraction of component  $i$ . The interdiffusion coefficient in a binary system can be determined from the concentration profile of a diffusion couple by a conventional Boltzmann-Matano analysis [16]. At the position of the Kirkendall interface the values of  $D_i$  can be calculated. The Matano-Boltzmann method, however, does involve a concentration gradient and is therefore not applicable to diffusion couples containing phases with a very



narrow, and therefore unknown, region of homogeneity (line compounds). To circumvent this problem, Wagner [24] developed the concept of the *integrated diffusion coefficient*,  $D_{int}$ . This materials constant is defined as the interdiffusion coefficient integrated over its (unknown) limits of homogeneity:

$$D_{int} = \int_x^{x''} D dx \quad (2.14)$$

If the binary diffusion couple only contains layers of line-compounds, the interdiffusion coefficient of phase i can be written as:

$$D_{int}^i = (x^i - x^-) \frac{(x^+ - x^i) (\Delta x^i)^2}{x^+ - x^-} \frac{1}{2t} + \frac{\Delta x^i}{2t} \bullet \left[ \frac{(x^+ - x^i) \sum_{v=2}^{v=i-1} \frac{V_m^i}{V_m^v} (x^v - x^-) \Delta x^v + (x^i - x^-) \sum_{v=i+1}^{v=n-1} \frac{V_m^i}{V_m^v} (x^i - x^v) \Delta x^v}{x^+ - x^-} \right] \quad (2.15)$$

The phases are numbered sequentially by i, starting with i = 1 for one endmember and finishing with i = n for the other.  $x^i$  is the mole fraction of one of the components in phase i. The superscripts + and - pertain to the mole fraction of that component in the endmembers of the diffusion couple.  $\Delta x$  is the layer thickness, t the annealing time. In fact, Eq. 2.15 amounts to a summation of rectangular areas in the diffusion profile [25]. Once  $D_{int}$  of a phase is determined, the thickness of a layer of that phase occurring in any other diffusion couple may be calculated, since  $D_{int}$  is a materials constant. Eq. 2.15 has been used for the determination of interdiffusion coefficients in the Ti-Ag system and the Ti-Si system (s. Chapter 5) and for the Ni-Si system [25].

More correctly, diffusion should be considered the result of the action of some force. As noted in 2.1 this force is the gradient of a diffusion potential, or  $F = - \nabla V$ . It is found empirically that this potential gradient gives rise to a mean diffusion velocity  $v$ . This is mathematically expressed by the equation:

$$v = B.F \quad (2.16)$$

B is called *mobility* and has units of velocity per unit force.

A diffusion flux  $J$  is equal to the product of this diffusion velocity and the concentration:

$$\mathbf{J} = \mathbf{v} \cdot \mathbf{C} = B \cdot \mathbf{C} \cdot \mathbf{F} \quad (2.17)$$

If we consider the effect of the chemical potential only and ignore the contribution of all other possible potential fields, we may write, analogous to Fick's first law in the Kirkendall frame of reference:

$$J_i = -L_i \left( \frac{\partial \mu_i}{\partial x} \right) \quad (2.18)$$

$L_i$  is called the *transport coefficient*. Comparing with Eq. 2.17, we see  $L_i = B_i C_i$ . We may equate 2.12b and 2.18. Since  $C_i = (\partial C_i / \partial \ln C_i)$ , we find:

$$D_i = B_i \frac{\partial \mu_i}{\partial \ln C_i} = B_i \frac{\partial \mu_i}{\partial \ln x_i} \quad (2.19)$$

(The last equality holds since  $C_i / C = x_i$ , hence  $d \ln C_i = d \ln x_i$ , provided  $C$ , and thus the total volume, remains constant).

Since  $d\mu = RT \, d \ln a$  (Eq. 2.5) =  $RT \, d \ln x + RT \, d \ln \gamma$ , we find:

$$D_i = B_i RT \left( 1 + \frac{d \ln \gamma_i}{d \ln x_i} \right) \quad (2.20)$$

This relation links the thermodynamics to kinetics.

The relation  $D_i = B_i RT$  (when the system behaves ideally) is the so-called Nernst-Einstein relation.

## 2.5 THE KIRKENDALL EFFECT

Consider a closed tube containing two gases, A and B, separated by a semi-permeable membrane which is free to move without friction. The membrane only allows the passage of B. If mixing of A and B is thermodynamically favourable, B will diffuse into the A compartment. The number of B in the right-hand compartment, and therefore the pressure, will decrease. Now the membrane will move towards the right hand side of the container to equalize the pressure. This simple thought experiment serves to illustrate the Kirkendall-effect in solid state reactions.

*Periodic layer formation during solid state reactions*

Consider a binary bulk diffusion couple A/B in which the binary compound AB is formed (Fig. 2.6). When the intrinsic diffusivities of the components are different, mass flow will take place relative to the original joining surface. That is, if  $D_A > D_B$ , more atoms of A will end up

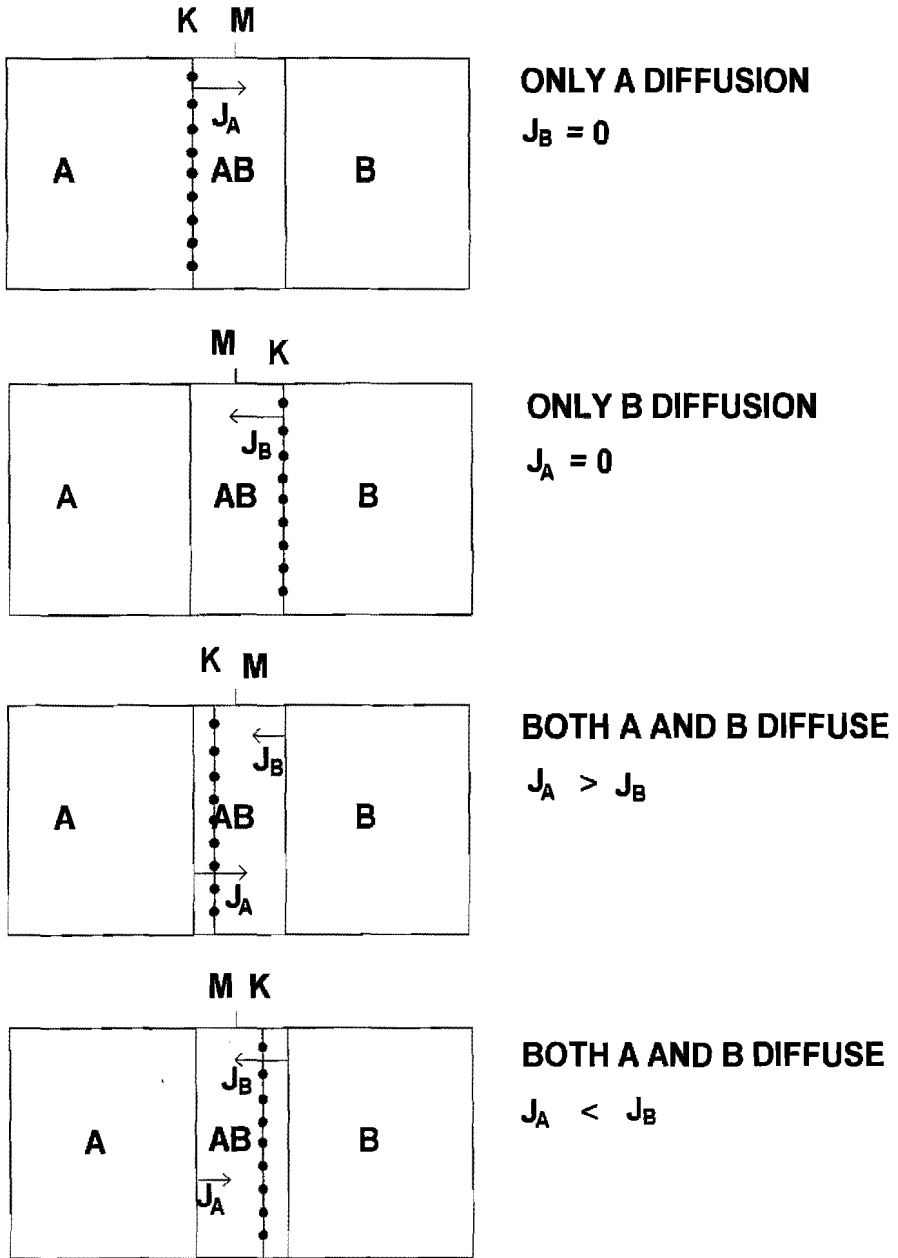


Fig. 2.6 Schematic view of the Kirkendall effect for a diffusion couple A/B and the reaction  $A + B = AB$ , with different mobilities of A and B

to the right of the plane marked K in Fig. 2.6 than atoms of B to the left. This causes the original joining plane to move relative to a fixed laboratory frame of reference, indicated by M in Fig. 2.6. Kirkendall was the first to note this, in a series of papers on the diffusion of zinc and copper in  $\alpha$ - and  $\beta$ -brass [26-28]. The term "Kirkendall effect" for the shift of the original weld plane was introduced by R.F. Mehl in the discussion following [28].

The Kirkendall effect may be considered as the addition of atomic planes on one side of the interface and removal of them on the other side (see, e.g. [13]) which causes the original interface (also called Kirkendall plane) to wander relative to the laboratory frame of reference. The position of the Kirkendall plane relative to its original position (the Matano plane) gives information about the relative mobilities of the components. This is especially true for binary diffusion couples, but also for higher order systems. In practice, the position of the Kirkendall plane is usually marked by inert marker particles or wires which are placed at the interface between the original diffusion couple halves before annealing. The particles have no interaction with the diffusing components but move as a whole as the atoms around them are diffusing. Another method of marking is to put a row of indentations perpendicular to the original interface. Even if no markers are used on purpose, the Kirkendall plane may be detected as a row of pores or a line of polishing debris inside the reaction zone. This role of "natural marker" may also be played by sintering additives. The movement of the Kirkendall interface relative to its original position (the Matano plane) can be determined if the sides of the diffusion couple do not react (which is often the case in practice). This is illustrated in Fig. 2.7

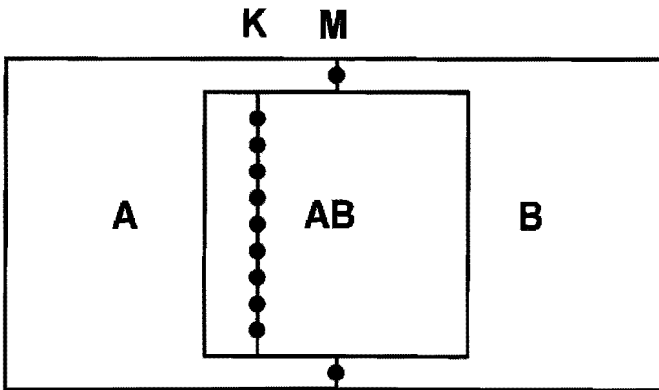


Fig. 2.7 *Determination of the displacement of the Kirkendall plane relative to the Matano plane*

In multiphase diffusion several reaction layers exist. Since the fluxes are expected to differ from each other in all phases, a Kirkendall plane must exist in each phase. Only one of those (the original contact interface) may be observed experimentally [14]. Since the motion of each Kirkendall plane is determined by the fluxes inside the product phases, the planes will, in

general, have a different velocity relative to each other. Their relative motion may even be *in opposite directions* inside a diffusion couple. As will be shown in subsequent chapters, this fact is crucial to the formation of the periodic layered reaction morphology.

## **2.6 THE INFLUENCE OF STRESS ON DIFFUSION: MECHANOCHEMISTRY**

If a solid is stressed, (elastic) energy is added to it. Therefore, its Gibbs energy will be different from that in the unstressed state. This in turn means that stress will influence diffusion, since diffusion is dependent on the gradients of the Gibbs energies of the components. Thus stress is one of the forces that may be incorporated into the thermodynamic potential for diffusion. The relaxation of stress takes place via diffusion (creep), plastic deformation or, in the worst case, via cracking.

Stress may be applied externally (e.g. shear, tension, compression, thermal stress) or generated internally by the diffusion-reaction process. In the latter case we speak about *self-stress*. In the following important sources of self-stress are considered.

In general, intrinsic diffusivities of components in a diffusion couple are different. This means that there will be a net flow of matter (Kirkendall effect, see 2.5). Volume is displaced in the direction of the flow, since more atoms cross the Kirkendall-plane in the one direction than in the other. This will cause one couple half to shrink and the other to expand. Since the couple halves are joined, i.e. elastically coupled, shrinkage will lead to tensile stress in the couple half and compressive stress in the other. Such a diffusion couple will have a tendency to bend, and indeed it does if it is not constrained by its own mass or external force, as exemplified by papers of Stevens and Powell (Ag-Au, [29]), Beke and Szabó (Ni-Mo, [30]), Daruka et al. (Ti-Zr, [31]), Osinski (Fe<sub>3</sub>Si-Zn, [32]) and this work (Fig. 5.15). The appearance of new phases between the couple halves complicates the treatment because of different molar volumes and the appearance of new interfaces. To our knowledge, no quantitative treatment of this case has been given.

When the couple does not bend, internal stresses develop inside the couple: a compressive stress, directed perpendicular to the diffusion direction in the "receiving" couple half and a tensile one in the shrinking one.

Even if the fluxes across the original contact plane were equal in magnitude (but of opposite direction) changes in molar volume would give rise to an imbalance in "volume" transport. This causes a so-called stress-free strain [33] in a constrained diffusion couple.

If a new interface is created (as in reactive diffusion), this interface may be a source of stress, even if it is non-coherent. Phase volume changes and internal precipitation are a source of stress as well.

If a foreign atom of different atomic size is incorporated in a lattice (another form of volume transport), local dilation or compression of the lattice occurs, resulting in local stress.

A general aspect of diffusion and stress is the feedback mechanism: diffusion may generate stress (self-stress) and stress may cause diffusion (e.g. the Gorsky effect [34]). This means that equations for diffusion and stress potentials are coupled.

Stresses play an important role in the formation of oxide scales (viz. 3.3).

## 2.7 REACTION LAYER MORPHOLOGIES AND MICROSTRUCTURE

In a binary system, the formation of two-phase zones at a fixed temperature and pressure is forbidden by the phase rule. A non-planar interface would imply a varying surface tension and with the temperature and pressure fixed there is simply no degree of freedom for this variable. Therefore we expect only single-phase layers with straight interfaces in binary diffusion couples [35]. The sometimes observed nonplanar interfaces may be due to grain-boundary diffusion [36], a crystallographic orientation effect [37] or very small amounts of impurity (making the system ternary).

What kind of reaction zone morphologies would be possible in a ternary diffusion couple? The phase rule allows single-phase and two-phase regions. If there is only one reaction product, we obviously have a single-phase layer. This is only possible when a ternary phase is present on the mass-balance line, as in the classical case of spinel formation  $AO + B_2O_3 = AB_2O_4$ . If there are more reaction products (Eq. 2.1, with  $i, j \geq 2$ ), we speak about *multiphase diffusion* and we have several possibilities.

Let's consider a hypothetical diffusion path on the isothermal cross-section of a hypothetical A-B-C phase diagram (Fig. 2.8, after [4]). A diffusion path a-n is plotted between the endmembers  $\alpha$  (at composition a) and C. The corresponding diffusion couple is drawn below the phase diagram. A solid line crossing a single-phase field (e.g. a-b) denotes an existing layer of that phase in the diffusion couple. A dashed line parallel to a tie-line in a two-phase field (g-h) represents a straight interface between two single-phases. A solid line crossing tie-lines (b-c) represents a locally equilibrated two-phase zone. A solid line entering a two-phase field and returning to the same phase-field (d-e-f) represents a region of isolated precipitates. When the volume fraction of one of the reaction products is small compared to that of the other, a two-phase zone with precipitates may develop. The actual morphology of a two-phase zone cannot be exactly deduced from the diffusion path.

Rapp et al. [38], and Yurek et al. [39], following Wagner [40,41] have shown that a solid state displacement reaction resulting in two reaction products may develop either a layered arrangement of single-phase layers with straight interfaces (e.g.  $Cu_2O/Co$ ) or an aggregate two-phase zone. This two-phase zone may be either lamellar (e.g.  $Fe/Cu_2O$ ) or interwoven (e.g.  $Fe/NiO$ ). The interwoven arrangement dominates when there is non-negligible solubility of the reaction products in the reactants. In order to predict which of the arrangements will occur, additional information on the mobilities of the components in the product phases is needed, next to the thermodynamic data.

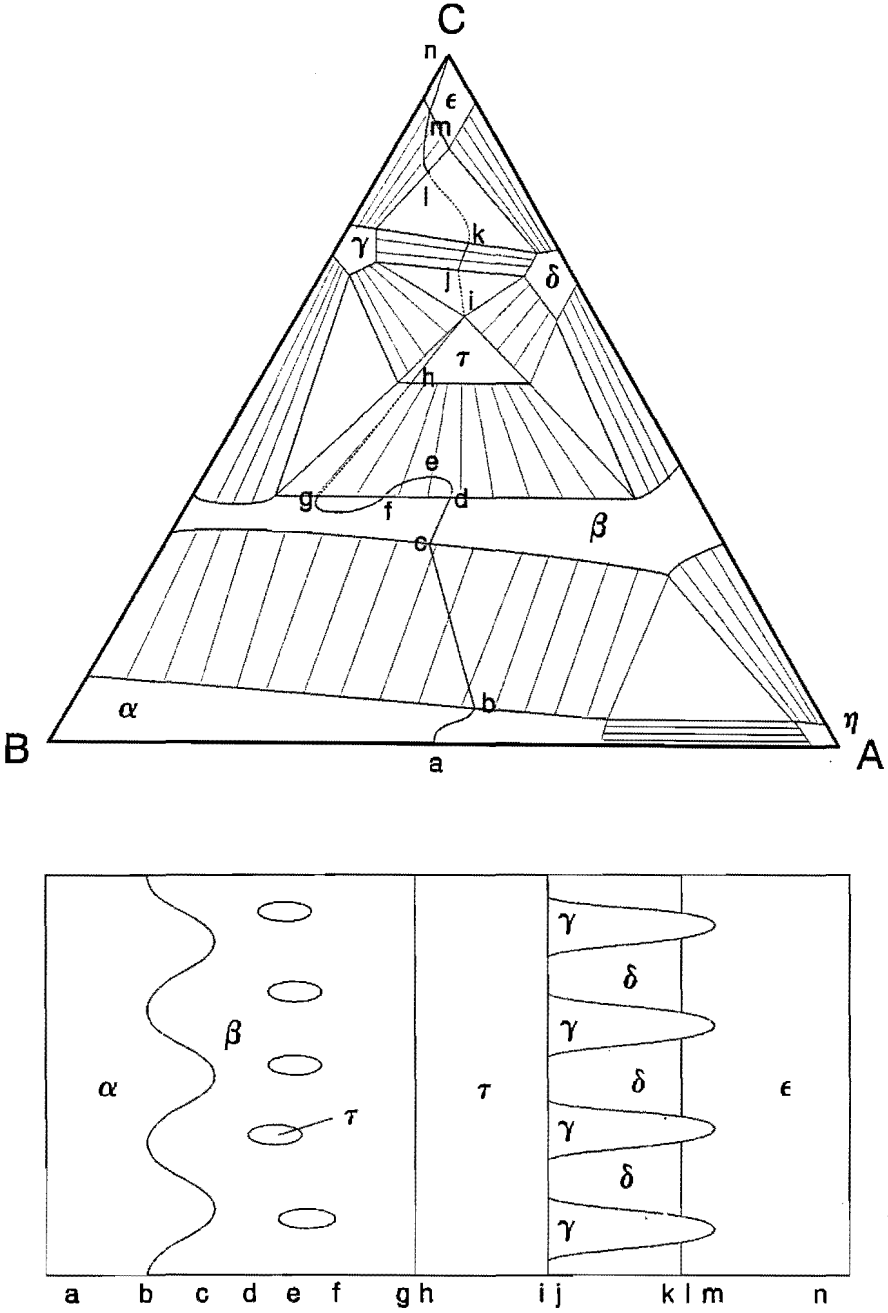


Fig. 2.8 Hypothetical diffusion path in a ternary system and corresponding reaction layer morphologies (after [4])

An important factor determining the growth of single-phase or two-phase reaction products is the substrate/product interface stability. If this interface is stable against small perturbations, it will remain flat. If not, distortions of the interface may grow into a macroscopically observable wavy interface, or, finally into a two-phase zone [41].

Consider a hypothetical diffusion couple BO/A (Fig. 2.9), with two reaction product layers, AO and B. We assume tentatively the interface between the products to be wavy. Assume further that the growth of AO takes place at the AO/B interface. Then we need diffusion of A through AO and diffusion of O through B. Since the diffusion rates are not equal, one of the two has to be rate-limiting. If the diffusion of A through AO is rate-limiting, more A arrives at position I than at position II. Therefore AO grows faster at I and a planar interface will be stable. If, on the other hand, the diffusion of O through B is rate-limiting, the layer will grow faster at position II, and the aggregate morphology will be stable. Schmalzried [21] summarizes this by noting that an interface is morphologically unstable when it moves against the flux of the rate-determining component.

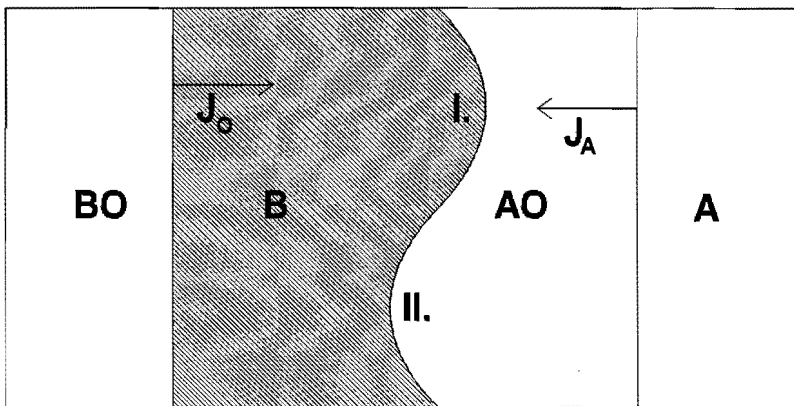


Fig. 2.9 *Formation of straight or wavy interfaces in a ternary diffusion couple depends on the relative mobilities of the diffusing components*

In addition to the prediction of morphology, van Loo et al. [2,42,43] were able to predict the *product layer sequence* for some displacement reactions on the basis of thermodynamic arguments. Both sequences BO/B/AO/A and BO/AO/B/A have been observed. In the latter case only planar interfaces are present, because O does not move from its lattice.

A more recently observed reaction layer morphology which may be added as a separate class is the periodic layered morphology. This morphology is characterized by a more or less regular repetition of bands of precipitates of one reaction product embedded in a matrix phase (another reaction product). Details and mechanisms of formation of this morphology will be considered in depth in Chapters 5 and 6.

A general scheme of the elementary morphologies is given in Fig. 2.10.



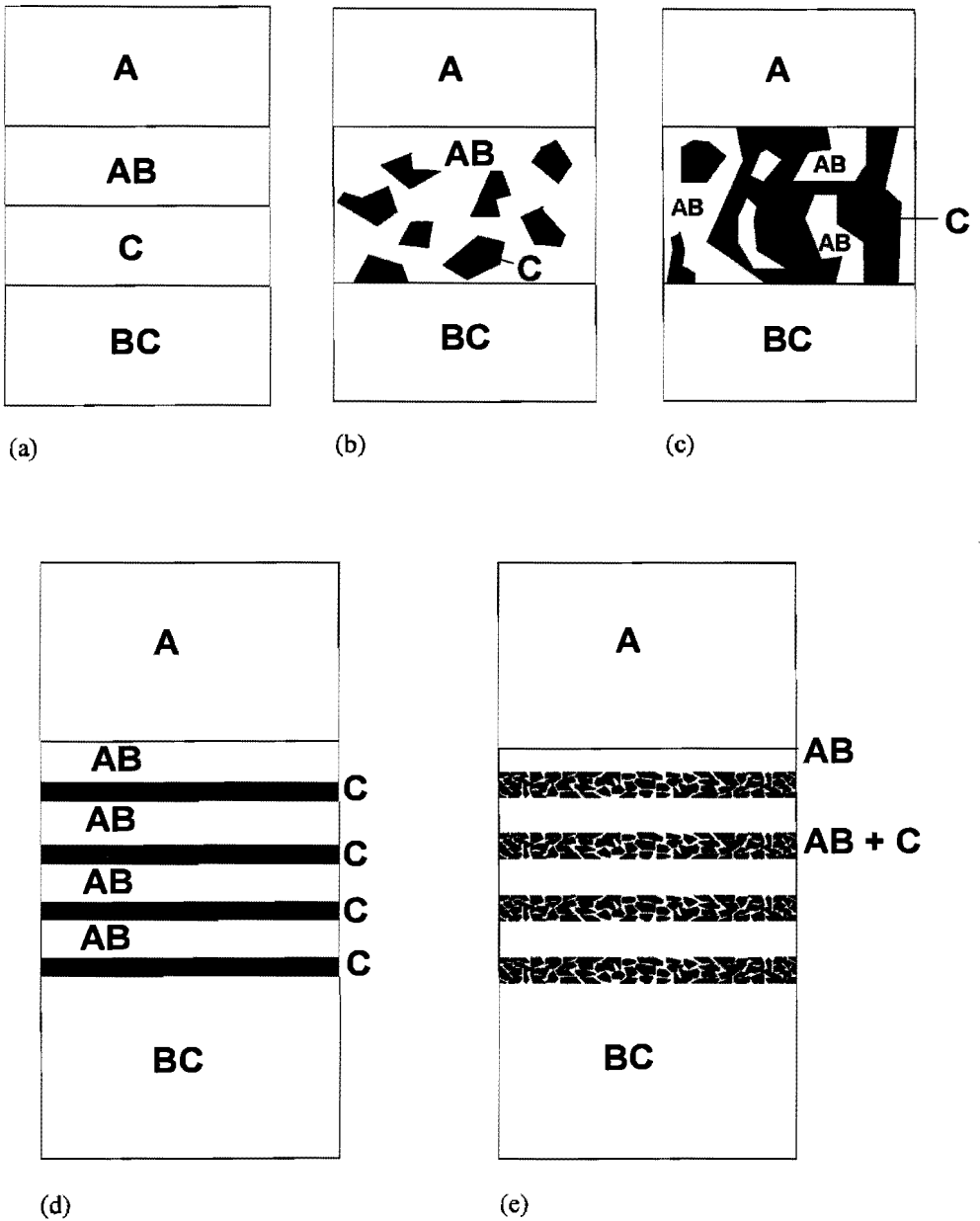


Fig. 2.10 Overview of possible reaction layer morphologies in ternary solid state diffusion couples; a) simple layered; b) isolated precipitates; c) interwoven; d) periodic layered with single-phase layers; e) periodic layered with two-phase layers

## References to Chapter 2

- [1] J.S. Kirkaldy, L.C. Brown: Diffusion behaviour in ternary multiphase systems, *Can. Metallurgical Quart.* **2** (1963), 89-117
- [2] F.J.J. van Loo, J.A. van Beek, G.F. Bastin, R. Metselaar: The role of thermodynamics and kinetics in multiphase ternary diffusion, in: Conference proceedings TMS-AIME, M.A. Dayananda, G.E. Murch, eds., 1984
- [3] A.D. Pelton, H. Schmalzried: On the geometrical representation of phase equilibria, *Met. Trans.* **4** (1973), 1395-1404
- [4] J.B. Clark: Conventions for plotting the diffusion paths in multiphase ternary diffusion couples on the isothermal section of a ternary phase diagram, *Trans. Met. Soc. AIME* **227** (1963), 1250-1251
- [5] P. Maugis, W.D. Hopfe, J.E. Morral, J.S. Kirkaldy: Multiple interface velocity solutions for ternary biphase infinite diffusion couples, *Acta Met.*, to be published (1996),
- [6] S. Mrowec: Defects and diffusion in solids, an introduction, Materials Science Monographs 5, Elsevier, 1980
- [7] N.H. Nachtrieb, G.S. Handler: A relaxed vacancy model for diffusion in crystalline metals, *Acta Met.* **2** (1954), 797-802
- [8] J.L. Bocquet, G. Brébec, Y. Limoge: Diffusion in metals and alloys, in: Physical Metallurgy I, R.W. Cahn, P. Haasen, eds., North-Holland physics publishing, Amsterdam, 1983, 385-474
- [9] D. Hull, D.J. Bacon: Introduction to dislocations, 3rd edition, Pergamon Press, 1984
- [10] F. Larché: Nucleation and precipitation on dislocations, in: Dislocations in solids **4**, F.N. Nabarro, ed., North-Holland Publishing Co. Amsterdam, 1979
- [11] F.C. Frank, W.T. Read, jr. Multiplication processes for slow moving dislocations, *Phys. Rev.* **79** (1950), 722-723
- [12] J.P. Hirth, J. Lothe: Theory of dislocations, 2nd edition, Krieger Publishing Comp. Malabar, 1992
- [13] J. Bardeen, C. Herring: Diffusion in alloys and the Kirkendall effect, in: Imperfections in nearly perfect crystals, W. Shockley, et al. eds., Wiley, New York, 1952, 261-288
- [14] F.J.J. van Loo, B. Pieraggi, R.A. Rapp: Interface migration and the Kirkendall-effect in diffusion-driven phase transformations, *Acta Metall. Mater.* **38** (1990), 1769-1773
- [15] J. Philibert: Atom movements, diffusion and mass transport in solids, les éditions de physique, les Ulis, 1991
- [16] Y. Adda, J. Philibert: La diffusion dans les solides, Tome I & II, Institut National des Sciences et Techniques nucléaires, Saclay, 1966
- [17] G.S. Hartley, J. Crank: Some fundamental definitions and concepts in diffusion processes, *Trans. Farad. Soc.* **45** (1949), 801-818
- [18] J.E. Lane, J.S. Kirkaldy: Diffusion in multicomponent metal systems. VIII. Kinetic calculation of the Onsager L coefficients in substitutional solid solutions, *Can. J. Phys.* **42** (1964), 1643-1657
- [19] L.S. Darken: Diffusion, mobility and their interrelation through free energy in binary metallic systems, *Trans. Met. Soc. AIME* **175** (1948), 184-201
- [20] F.M. d'Heurle: Nucleation of new solid phases from chemical interactions at an interface, *J. Vac. Sci. Technol. A* **7** (1989), 1467-1471
- [21] H. Schmalzried: Chemical kinetics of solids, VCH Verlagsgesellschaft, Weinheim, Germany, 1995
- [22] R.W. Balluffi: On the determination of diffusion coefficients in chemical diffusion, *Acta Met.* **8** (1960), 871-873
- [23] L.E. Trimble, D. Finn, Cosgarea, Jr. A mathematical analysis of diffusion coefficients in binary systems, *Acta Met.* **13** (1965), 501-507
- [24] C. Wagner: The evaluation of data obtained with diffusion couples of binary single-phase and multiphase systems, *Acta Met.* **17** (1969), 99-107
- [25] J.H. Gülpen, A.A. Kodentsov, F.J.J. van Loo: Growth of silicides in Ni-Si and Ni-SiC diffusion couples, *Z. Metallkde.* **86** (1995), 530-539

- [26] E.O. Kirkendall, Thomassen, Upthegrove: Rates of diffusion of copper and zinc in alpha brass, *Trans. AIME* **133** (1939), 186-203
- [27] E.O. Kirkendall: Diffusion of zinc in alpha brass, *Trans. AIME* **147** (1942), 104-110
- [28] A.D. Smigelskas, E.O. Kirkendall: Zinc diffusion in alpha brass, *Trans. Met. Soc. AIME* **171** (1947), 130-134
- [29] D.W. Stevens, G.W. Powell: Diffusion induced stresses and plastic deformation, *Met. Trans. A* **8A** (1977), 1531-1541
- [30] D.L. Beke, I.A. Szabó: Effect of stress on diffusion, in: Diffusion in materials, DIMAT-92, M.Koiwa et al. ed., Trans Tech Publications, Zürich, 1992, 537
- [31] I. Daruka, I.A. Szabó, D.L. Beke, C. Cserhádi, A.A. Kodentsov, F.J.J. van Loo: Diffusion induced bending of thin sheet couples: theory and experiments in Ti-Zr system, *submitted to Acta Mater.* (1996)
- [32] K. Osinski: The influence of aluminium and silicon on the reaction between iron and zinc, *PhD. Thesis*, Eindhoven University of technology, Eindhoven, the Netherlands, 1983
- [33] G.B. Stephenson: Deformation during interdiffusion, *Acta Met.* **36** (1988), 2663-2683
- [34] G. Alefeld, J. Völkl, G. Schaumann: Elastic diffusion relaxation, *Phys. Stat. Sol.* **37** (1970), 337-351
- [35] F.J.J. van Loo: Multiphase diffusion in binary and ternary solid state systems, *Prog. Sol. State Chem.* **20** (1990), 47-99
- [36] M.M.P. Janssen, G.D. Rieck: Reaction diffusion and Kirkendall-effect in the nickel aluminum system, *Trans. Met. Soc. AIME* **239** (1967), 1372-1385
- [37] J.A. van Beek, S.A. Stolk, F.J.J. van Loo: Multiphase diffusion in the systems Fe-Sn and Ni-Sn, *Z. Metallkde.* **73** (1982), 439-444
- [38] R.A. Rapp, E. Ezis, G.Y. Yurek: Displacement reactions in the solid state, *Met. Trans.* **4** (1973), 1283-1292
- [39] G.J. Yurek, R.A. Rapp, J.P. Hirth: Kinetics of the displacement reaction between iron and Cu<sub>2</sub>O, *Met. Trans.* **4** (1973), 1293-1300
- [40] C. Wagner: Über den Mechanismus von doppelten Umsetzungen durch Reaktion im festen Zustand, *Z. Anorg. Allgem. Chem.* **236** (1938), 320-338
- [41] C. Wagner: Oxidation of alloys involving noble metals, *J. Electrochem. Soc.* **103** (1956), 571-580
- [42] J.A. van Beek, P.M.E. de Kok, F.J.J. van Loo: Solid-state displacement reactions in the Fe-Ni-S and Cu-Ni-S systems between 400 °C and 500 °C, *Oxid. Met.* **22** (1984), 147-160
- [43] F.J.J. van Loo, J.A. van Beek, G.F. Bastin, R. Metselaar: On the layer sequence and morphology in solid-state displacement reactions, *Oxid. Met.* **22** (1984), 161-180

### **Further reading**

- W. Bollmann: Crystal defects and crystalline interfaces, Springer Verlag, Berlin, 1970
- H.G. van Bueren: Imperfections in crystals, North-Holland Publishing Co. Amsterdam, 1960
- W. Jost: Diffusion in solids, liquids, gases, Academic Press inc. New York, 1960
- W.T. Read, jr. Dislocations in crystals, int. series in pure and applied physics, McGraw-Hill, New York, 1953
- P.G. Shewmon: Diffusion in solids, McGraw-Hill, New York, 1963
- R.A. Swalin: Thermodynamics of solids, John Wiley & Sons, Inc. New York, 1972
- Diffusion and stresses, proceedings of the 1st international workshop on diffusion and stresses, Balatonfüred, Hungary, 1995, D.L. Beke, I.A. Szabó, eds, Defect and diffusion forum, Vols. 129-130, Scitec Publications, Zürich, Switzerland, 1996

## CHAPTER 3

### CHEMICAL PERIODICITY

This chapter deals with literature on periodic structures encountered in chemistry in a broad sense. Stable periodic patterns formed by chemical reaction are met in many areas of chemistry. The first two sections of this chapter consider the relatively mature science of band formation during chemical reaction. The following sections give a short overview of the more general science of pattern formation.

#### 3.1 INTERNAL REACTIONS

The formation of a product AB from the reaction of solid A with solid B can, in principle, occur in two ways [1]. The first way is for AB to nucleate at the A/B interface and form a product layer whereby A and B get separated. This occurs in bulk (semi-infinite) diffusion couples and is dealt with in Chapter 2. The second way is for the molecule AB to precipitate inside a solvent (or matrix) and grow by diffusional addition of A and B to the precipitate. The latter type of reaction is called *internal reaction*. A change in temperature or pressure with subsequent oversaturation with respect to one of the components may cause this type of reaction inside an originally homogeneous phase. Internal oxidation [2] and internal nitridation, occurring with alloys containing a less noble element as a solute (in small quantity), also belong to the category of internal reactions.

Yet another type of internal reaction occurs when two components counterdiffuse in a non-reactive (inert) solvent phase. AB will nucleate when the maximum solubility product is exceeded. In the framework of this thesis, the latter type is the most important. The principle of this internal reaction is sketched in Fig. 3.1. The figure shows four stages of the internal reaction. Components A and B diffuse into the inert matrix C. The usual error function concentration profiles are set up. Once the profiles start to overlap, the product  $c_{ACB}$  starts to rise. At  $t^*$  and  $x^*$  the maximum solubility product is reached and AB starts to precipitate out. In ref. [3] a model for this type is described. The position of first precipitation, growth of the nuclei and morphological development of a band of precipitates is considered in terms of parameters like interdiffusion coefficients, molar volumes and activity products.

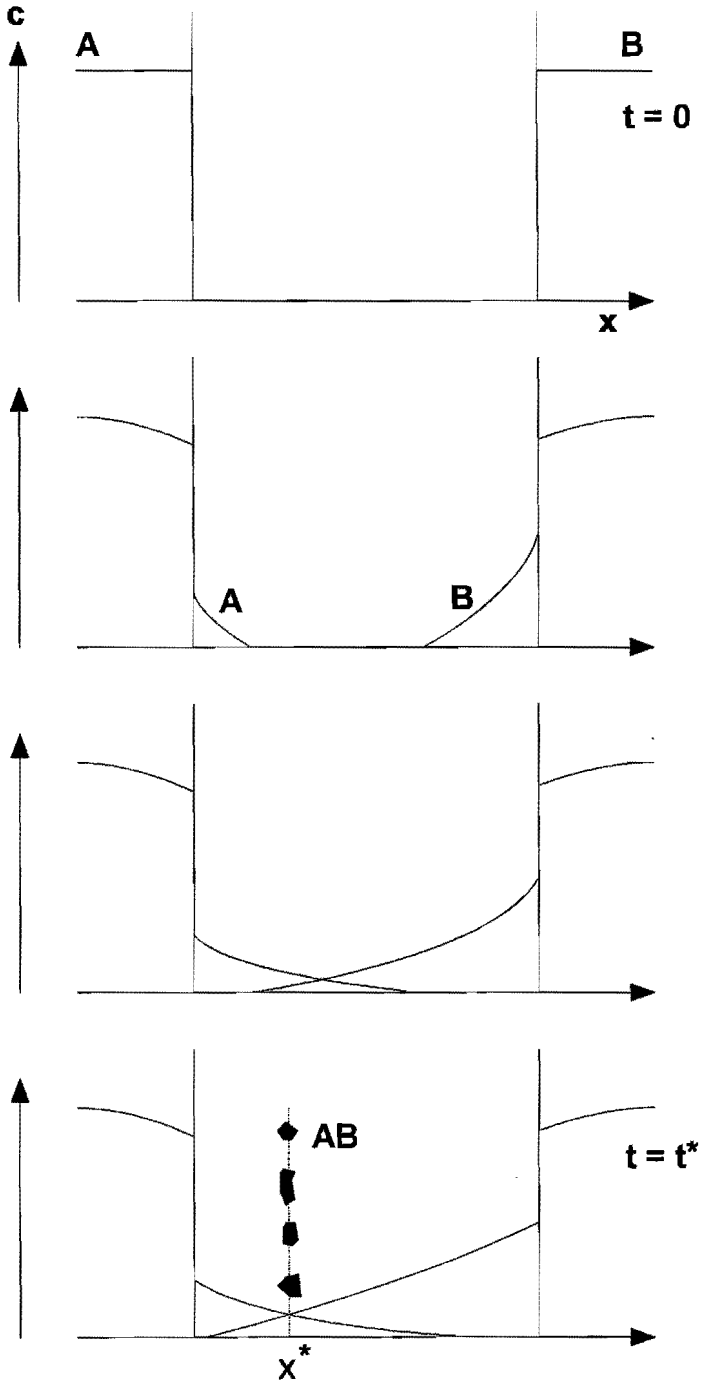


Fig. 3.1 Schematic concentration profiles at different diffusion times for the internal reaction  $A + B = AB$ , AB precipitating in matrix phase

Internal precipitates may appear either randomly distributed, as a single band or as multiple bands (periodic precipitation, e.g. AlAs bands in a copper matrix [4] or  $\text{CaTiO}_3$  bands in  $\text{NiO}$  [5]). All types of internal reactions in non-metallic systems were discussed by Schmalzried and Backhaus-Ricoult [6].

### 3.2 THE LIESEGANG PHENOMENON

At the time of writing of this thesis we witness the 100<sup>th</sup> anniversary of the Liesegang phenomenon (and that of the modern Olympic Games). Liesegang [7] was the first one to observe a periodic precipitation of a compound inside a solvent. When he placed a drop of concentrated solution of silver nitrate (the "outer electrolyte") in water on a dilute solution of ammonium dichromate (the "inner electrolyte") in gelatine he observed concentric rings of silver dichromate with relatively clear spaces between the rings. When this experiment is done in a test tube, discs (or, when viewed from the side, bands) of precipitates are observed. The spacing between these discs increases with distance to the original contact surface, but a few cases of "revert-spacing" have been reported [8,9]. Since then, a large number of systems was observed to show this particular behaviour and it may be conjectured that any salt may be precipitated from a supersaturated matrix in the form of rings or discs if the conditions are favourable. That the phenomenon is indeed a general one, may be deduced from the fact that Liesegang rings or bands (or, preferably *periodic precipitation*) have been observed in gel-solution systems (e.g., [10], the majority of studies concentrates on these), in liquid-liquid systems (e.g., [11] describes 40 cases), in gas-gas reactions [12,13], solid-gas reactions [14,15] and solid-solid reactions ([4,5], this work).

A comprehensive review of the early theories on Liesegang ring formation has been given by Hedges [16] in 1932. By this time Hedges had collected already 482 references on the phenomenon. He discussed four existing theories (the supersaturation theory, the adsorption theory, the coagulation theory and the diffusion wave theory) on the phenomenon. An overview of the history and profound discussion of the Liesegang phenomenon may be found in [17].

A 1953 review by Stern [18] adds another 41 studies which have been conducted since the appearance of Hedges' book, including Wagner's mathematical analysis [19] which now forms the basis of analysis of periodic precipitation. Wagner's analysis later has been slightly modified by Prager [20] and amended by Kahlweit [21], who took account of the growth rate of the precipitates. Surprisingly, the oldest proposed mechanism for Liesegang band formation, due to Wi. Ostwald [22], is currently accepted. Ostwald proposed the occurrence of supersaturation and the existence of a metastable solubility limit beyond which precipitation should occur. A compound will not precipitate from solution until its maximum solubility product is reached. In practice it is found that many compounds may be held in solution for a long time, even if their concentration exceeds this maximum value (i.e. the solution is

supersaturated). When supersaturation is increased the compound will eventually precipitate out of the solution until the equilibrium concentration is established.

Ostwalds' interpretation of Liesegang band formation is as follows. When a solution (containing A) and a gel (containing B) are placed in contact, the outer electrolyte (A) diffuses into the gel. A supersaturated solution is formed behind the diffusion front. When AB starts to precipitate out of solution, both A and B will diffuse towards the fresh nuclei. This will leave a space which is depleted of B. With continuing diffusion of A, this zone will remain free of precipitates since there can be no supersaturation of AB. Therefore a new supersaturated zone will build up some distance from the original precipitate and in this way a new band or ring of precipitates is formed.

Both analytical and numerical methods have been used to quantify periodic precipitation. Numerical methods [23,24] have mimicked the features of periodic precipitation quite well, but are usually not fed by data from actual systems. The Liesegang phenomenon and its modelling continue to attract scientific interest as evidenced by recent publications. Newer models include the nucleation rate (which is strongly dependent on the supersaturation) and particle growth [23,25,26] and/or take into account diffusion of the precipitated product [27] and depletion of the reservoir [28]. Modelling specifically fit for periodic precipitation in solids has not been done. The model of Henisch et al. [24] is a good candidate for this task.

Although at the moment the interest in the Liesegang phenomenon is academic, a practical interest might be the synthesis of anisotropic multilayer ceramics. Adair et al. have successfully attempted to use periodic precipitation to produce a multilayered ceramic material [29].

Liesegang band formation has been considered by some authors to be part of a more general phenomenon: spontaneous pattern formation [9,30,31].

### **3.3 PERIODICALLY LAYERED OXIDE SCALES**

When a metal is oxidized, a layer of one or more oxides (an oxide scale) will grow on its surface. The scale may be a regular closed layer, but sometimes appears as a stack of many layers. This phenomenon, called lamination or striation, has been observed in the oxidation of, e.g., tantalum [32], niobium [33] and titanium [34,35].

Mechanical failure of a scale during oxidation is due to the development of stresses (either tensile or compressive) in the scale during the growth. These stresses are caused by the difference in molar volume between the scale and the adjoining substrate. Whether the stresses lead to failure is dependent on the mechanical properties of the scale and the metal/scale interface. Compressive stresses will lead to blistering or flaking, whereas tensile stresses may cause wedge-like cracks in the scale. In a continued oxidation experiment, blistering will expose a fresh metal surface to the oxidizing species and repeated scale growth/blistering cycles will give the scale a periodic layered morphology.

## 3.4 OTHER PERIODIC STRUCTURES

### 3.4.1 Oscillating reactions

It is well known that reacting systems in far-from-equilibrium conditions show complex dynamics and patterning. The earliest and best-known example is the Belousov-Zhabotinsky (B-Z) reaction (see, e.g. [36,37]). Patterns and concentration oscillations in this reaction (and other related ones), if carried out in a closed vessel, are of transient nature; they occur during a short period of time and finally disappear as the reaction goes to completion. On the other hand, oscillation may be sustained indefinitely if a reactor is continuously fed [38]. The system is then in a stable stationary state, but not in an equilibrium state.

The literature on this subject is highly mathematical, except in the simplest cases. Spatiotemporal concentration patterns arise as solutions of a set of coupled diffusion and reaction equations under specified boundary conditions (see, e.g. [39,40]). A necessary condition for oscillations is *feedback*. An example is autocatalysis, in which some step in the reaction sequence influences the rate of a step earlier in the sequence. Feedback may also arise when the heat of reaction is not adequately removed from the system. Since reaction rates are strongly temperature dependent (via the Arrhenius law), heating of the system will enhance or inhibit certain steps in the reaction sequence.

In contrast to the Liesegang phenomenon, periodic patterns in this type of reaction result from concentration oscillations in time and space, i.e. they are not stationary. Up till now oscillating reactions have been observed in liquid solutions. Although in theory there will be no reason for solids not to exhibit such behaviour, the first solid state oscillator remains yet to be discovered. Experimental difficulties defy the possibility for observation of fluctuating concentrations of solids inside solids *in situ*. The observed patterns in the reaction zone of  $\text{Co}_2\text{Si}/\text{Zn}$  diffusion couples (Fig. 5.17) are reminiscent of those observed in the B-Z reaction. Also, the parallel bands observed perpendicular to the diffusion direction bear resemblance to waves. The observed patterns consist of particles of one solid in equilibrium with the matrix solid. This means that no diffusion-reaction process is going on inside the reaction zone of the diffusion couple. Reaction-diffusion is going on at the reaction front, where the patterns must have been formed. Models of the B-Z reaction, like the Brusselator [41] involve autocatalysis. Moreover, the "far from equilibrium" situation is stressed in the literature. Although the reaction mechanisms are not exactly known, autocatalysis is not likely to occur in the simple solid state reactions considered in this work, and contrary to the B-Z reaction models, local equilibrium is assumed. Therefore we will not draw upon the theories for oscillating reactions in this thesis to explain the occurrence of periodic layered reaction zones in diffusion couples.

### 3.4.2 Self-organization (pattern formation) in solids

The oscillating reactions described in the previous section form *patterns* in space and time. Initially homogeneous materials or phases may spontaneously develop intricate patterns (resulting from the reaction  $\alpha = \beta + \gamma$ ) when they are (put) in a "far from equilibrium" state. A good example of this apparent "self-organization" [42] is the formation of lamellar eutectic



structures like pearlite (see, e.g. [43-47]) or peritectic ones [48]. The formation of cellular or dendritic microstructures and Widmanstätten colonies can also be considered as a process of self-organization [49].

Naturally, the periodic structures found in diffusion couples strike us as being patterns. However, since they do not precipitate from a homogeneous solid solution they cannot be treated within the framework of the theory of pattern formation.

Although pattern formation and oscillating chemical reactions present many interesting features and unresolved questions, treatment of this matter falls outside the scope of this thesis.

### References to Chapter 3

- [1] H. Schmalzried: Chemical kinetics of solids, VCH Verlagsgesellschaft, Weinheim, Germany, 1995
- [2] J.L. Meijering: Internal oxidation in alloys, *Adv. in Mat. Res.* **5** (1971), 1-81
- [3] M. Backhaus-Ricoult, H. Schmalzried, R.J. Tarento: Internal solid state reactions of the type  $A + B = AB$ : Diffusion-controlled formation of AB from A and B dissolved in a crystalline host matrix, *Ber. Bunsenges. Phys. Chem.* **95** (1991), 1593-1610
- [4] J.E. Gerrard, M. Hoch, F.R. Meeks: Counterdiffusion of aluminum and arsenic in copper, *Acta Met.* **10** (1962), 751-758
- [5] H. Schmalzried, T. Frick: Internal solid state reaction: formation of perovskite in NiO-matrix, *Ber. Bunsenges. Phys. Chem.* **99** (1995), 914-919
- [6] H. Schmalzried, M. Backhaus-Ricoult: Internal solid state reactions, *Prog. Sol. St. Chem.* **22** (1993), 1-57
- [7] R.E. Liesegang: Ueber einige Eigenschaften von Gallerten, *Naturw. Wochenschr.* **11** (1896), 353-362
- [8] E.S. Hedges, R.V. Henley: The formation of Liesegang rings as a periodic coagulation phenomenon, *J. Chem. Soc.* (1928), 2714-2726
- [9] M. Flicker, J. Ross: Mechanism of chemical instability for periodic precipitation phenomena, *J. Chem. Phys.* **60** (1974), 3458-3465
- [10] T. Isemura: Studies on rhythmic precipitates, *Bull. Chem. Soc. Jap.* **14** (1939), 180-237
- [11] H.W. Morse: Periodic precipitation in ordinary aqueous solutions, *J. Phys. Chem.* **34** (1930), 1554-1577
- [12] C.F. Goodeve, A.S. Eastman, A. Dooley: The reaction between sulphur trioxide and water vapours and a new periodic phenomenon, *Trans. Farad. Soc.* **30** (1934), 1127-1133
- [13] E.L. Spatz, J.O. Hirschfelder: Liesegang ring formation arising from diffusion of ammonia and hydrogen chloride gases through air, *J. Chem. Phys.* **19** (1951), 1215
- [14] Y.S. Shen, E.J. Zdanuk, R.H. Krock: The influence of additives on the formation of periodic precipitation (Liesegang bands) in the Ag-Cd system, *Met. Trans.* **2** (1971), 2839-2844
- [15] R.L. Klueh, W.W. Mullins: Periodic precipitation (Liesegang phenomenon) in solid silver, *Acta Met.* **17** (1969), 59-76
- [16] E.S. Hedges: Liesegang rings and other periodic structures, Chapman & Hall Ltd. London, 1932
- [17] H.K. Henisch: Crystals in gels and Liesegang rings, Cambridge University Press, Cambridge, 1988
- [18] K.H. Stern: The Liesegang phenomenon, *Chem. Rev.* **54** (1954), 79-99
- [19] C. Wagner: Mathematical analysis of the formation of periodic precipitations, *J. Colloid Sci.* **5** (1950), 85-97
- [20] S. Prager: Periodic precipitation, *J. Chem. Phys.* **25** (1956), 279-283

- [21] M. Kahlweit: Über die Kinetik der Phasenbildung in kondensierten Systemen. V. Periodische Fällungen und ein Modellversuch zur inneren Oxydation von Metallegierungen, *Z. Phys. Chem. Neue Folge* **32** (1962), 1-26
- [22] W. Ostwald: Lehrbuch der allgemeinen Chemie, An.Engelman Verlag, Leipzig, 1897, 778
- [23] M. Bensetti, M. Lallemand: Improved approach to Liesegang phenomena, *Sol. State Phenomena* **41** (1995), 21-36
- [24] H.K. Henisch: Liesegang ring formation in gels, *J. Cryst. Growth* **76** (1986), 279-289
- [25] P.S. Braterman, C. Tan, S. Yang: Periodic precipitation in a competitive particle growth model, *Mat. Res. Bull.* **29** (1994), 287-292
- [26] G.T. Dee: Patterns produced by precipitation at a moving reaction front, *Phys. Rev. Lett.* **57** (1986), 275-278
- [27] J.B. Keller, S.I. Rubinow: Recurrent precipitation and Liesegang rings, *J. Chem. Phys.* **74** (1981), 5000-5007
- [28] H.K. Henisch, J.M. García-Ruiz: Crystal growth in gels and Liesegang ring formation; I. Diffusional relationships; II. Crystallization criteria and successive precipitation, *J. Cryst. Growth* **75** (1986), 195-211
- [29] J.H. Adair, S.A. Touse, P.J. Melling: Chemically derived multilayer ceramics, *Am. Ceram. Soc. Bull.* **66** (1987), 1490-1494
- [30] D. Feinn, P. Ortoleva, W. Scalf, S. Schmidt, M. Wolff: Spontaneous pattern formation in precipitating systems, *J. Chem. Phys.* **69** (1995), 27-39
- [31] P. Ortoleva: Nonlinear physico-chemical phenomena, in: Periodicities in chemistry and biology, Theoretical Chemistry, vol. 4, H. Eyring, D. Henderson, eds., Academic Press, New York, 1978, 235-286
- [32] J. Stringer: The oxidation of tantalum at high temperatures: geometrical effects, *J. Less Comm. Metals* **16** (1968), 55-64
- [33] J.A. Roberson, R.A. Rapp: The observation of markers during the oxidation of columbium, *Trans. Met. Soc. AIME* **239** (1967), 1327-1331
- [34] J. Stringer: The oxidation of titanium in oxygen at high temperatures, *Acta Met.* **8** (1960), 758-766
- [35] G. Bertrand, K. Jarraya, J.M. Chaix: Morphology of oxide scales formed on titanium, *Oxid. Met.* **21** (1983), 1-19
- [36] A.N. Zaikin, A.M. Zhabotinsky: Concentration wave propagation in two-dimensional liquid-phase self-oscillating system, *Nature* **225** (1970), 535-537
- [37] R.J. Field: Chemistry of inorganic systems exhibiting nonmonotonic behaviour, in: Periodicities in chemistry and biology, Theoretical chemistry, vol. 4, H. Eyring, D. Henderson, eds., Academic Press, New York, 1978, 53-110
- [38] P. Gray, S.K. Scott: Chemical oscillations and instabilities; nonlinear chemical kinetics, Clarendon Press, Oxford, 1994
- [39] R. Kapral: Pattern formation in chemical systems, *Physica D* **D86** (1995), 149-157
- [40] H. Malchow, H. Rosé, C. Sattler: Spatial and spatio-temporal reaction-diffusion patterns in heterogeneous media, *J. Non-equilib. Thermodyn.* **17** (1992), 41-52
- [41] I. Prigogine, R. Lefever: Symmetry breaking instabilities in dissipative systems. II, *J. Chem. Phys.* **48** (1968), 1695-1700
- [42] J.S. Kirkaldy, D.J. Young: Diffusion in the condensed state, the Institute of Metals, London, 1987
- [43] R. Vilella: (reproduced by L.S. Darken and W.C. Leslie), in: Decomposition of austenite by diffusional processes, V.F. Zackay, H.I. Aaronson, eds., Interscience, New York, 1962, 253-
- [44] A.D. Doherty: Diffusive phase transformations in the solid state, in: Physical Metallurgy, Vol. II, R.W. Cahn, P. Haasen, eds., North-Holland Physics Publishing, Amsterdam, 1983, 933-1030
- [45] E. Hornbogen: Physical metallurgy of steels, in: Physical Metallurgy, Vol. II, R.W. Cahn, P. Haasen, eds., North-Holland Physics Publishing, Amsterdam, 1983, 1075-1138
- [46] J.D. Livingston, J.W. Cahn: Discontinuous coarsening of aligned eutectoids, *Acta Met.* **22** (1974), 495-503

*Periodic layer formation during solid state reactions*

- [47] V.K. Heikkinen: The formation of planar band colonies in vanadium-bearing mild steels, *Acta Met.* **21** (1973), 709-714
- [48] R. Trivedi: Theory of layered structure formation in peritectic systems, *Met. Trans. A* **26A** (1995), 1583-1590
- [49] J.S. Kirkaldy: Spontaneous evolution of spatiotemporal patterns in materials, *Rep. Prog. Phys.* **55** (1992), 723-795

## **CHAPTER 4**

### **EXPERIMENTAL METHODS**

Throughout the investigations use was made of the *diffusion couple* technique. Basically, this technique consists of: (1) preparing the materials; (2) cutting and preparing of suitably sized pieces; (3) clamping together of two pieces of the materials; (4) annealing run; (5) cutting of the joint pieces parallel to the diffusion direction; (6) preparation of the cross-section for microscopic examination; (7) microscopic examination and analysis.

For examination of isothermal cross-sections of the ternary phase diagrams use was made of the powder pellet technique. Pressed powder pellets of suitable compositions were annealed in evacuated silica capsules at the temperature of interest. After quenching, the pellets were prepared for microscopic examination and X-ray analysis.

A general overview of materials, procedures and equipment used is given here. Details of the experiments may be found in the separate sections of Chapter 5.

#### **4.1 MATERIALS**

##### **4.1.1 The pure materials**

The pure materials were used either directly as a couple half or to melt desired alloys or intermetallics. In table 4.1 the materials are listed which were obtained from a supplier.

##### **4.1.2 Alloy and diffusion couple preparation**

Alloys were prepared by arc-melting under an argon atmosphere. The elements are cut (metal foils) or crushed (silicon) to suitably sized pieces, weighed to the desired composition and molten together into an ingot of about 5 g. In order to improve homogenization, remelting is sometimes necessary. Three of those ingots are molten into a cylindrical bar. This bar is then homogenized in an evacuated silica capsule for 1 to 2 weeks at a temperature close to the melting point of the alloy. The capsule is then taken from the furnace and allowed to cool to room temperature. Composition was checked by quantitative SEM.

Slices of a thickness of about 2 mm were cut from the homogenized bars by a high speed saw with carborundum blade. Before placing the slices together in a sample holder they were

ground planparallel on SiC abrasive paper. Planparallelity is the single most important factor for having a good contact of the faces that are to be joined, especially so when the materials are not ductile. It was checked by clamping the slices in a micrometer. When viewed in the direction of a light source, no light should pass through the joining surfaces. Before mounting, the couple halves were cleaned ultrasonically in acetone.

#### **4.1.3 Determination of phase equilibria**

Solid state phase relations in ternary systems are determined by a powder pellet method. Powdered constituents (elements or compounds) of the constituting binary diagrams are thoroughly mixed in predetermined proportions and pressed into a pellet. This pellet is then annealed for a long time at the temperature of interest, allowing the mixture to equilibrate. The resulting phases are then examined by EPMA for composition and by XRD for structure.

### **4.2 ANNEALING PROCEDURES**

Pure metals with a high vapour pressure, like Zn and Mg, cannot be annealed in vacuum. Diffusion couples containing these elements were annealed in a flowing inert gas atmosphere (He or Ar). The couple halves are held together in a specially designed sample holder, made of alumina (Fig. 4.1). This sample holder is loaded into a quartz tube. The tube is closed and flushed with inert gas for half an hour to drive out the air. The whole assembly is then heated in a horizontal electroresistance furnace equipped with a Pt/Pt(15%Rh) thermocouple. A temperature control of  $\pm 3^\circ$  is attained in this kind of furnace. The metal spring on the end of the pressure bar serves to provide a good contact between the couple halves during the initial stage of the anneal. It is outside the hot zone. After annealing, the tube is taken from the furnace and allowed to cool to room temperature. No controlled cooling rates were applied. Diffusion couples that do not have the problem of volatile components were annealed in vacuum furnaces under a constant load. The assembly is shown in Fig. 4.2.

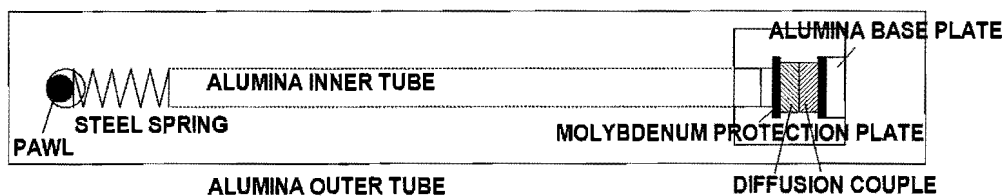


Fig. 4.1 *Tube clamp used for keeping couple halves together; used for Zn - or Mg-containing diffusion couples*

To observe diffusion couples *in situ* a simple furnace was constructed existing of a quartz tube wound with kantal resistive wire. Both ends of the tube were fitted with a rubber plug, allowing the positioning of a chromel-alumel thermocouple and the passage of He gas.

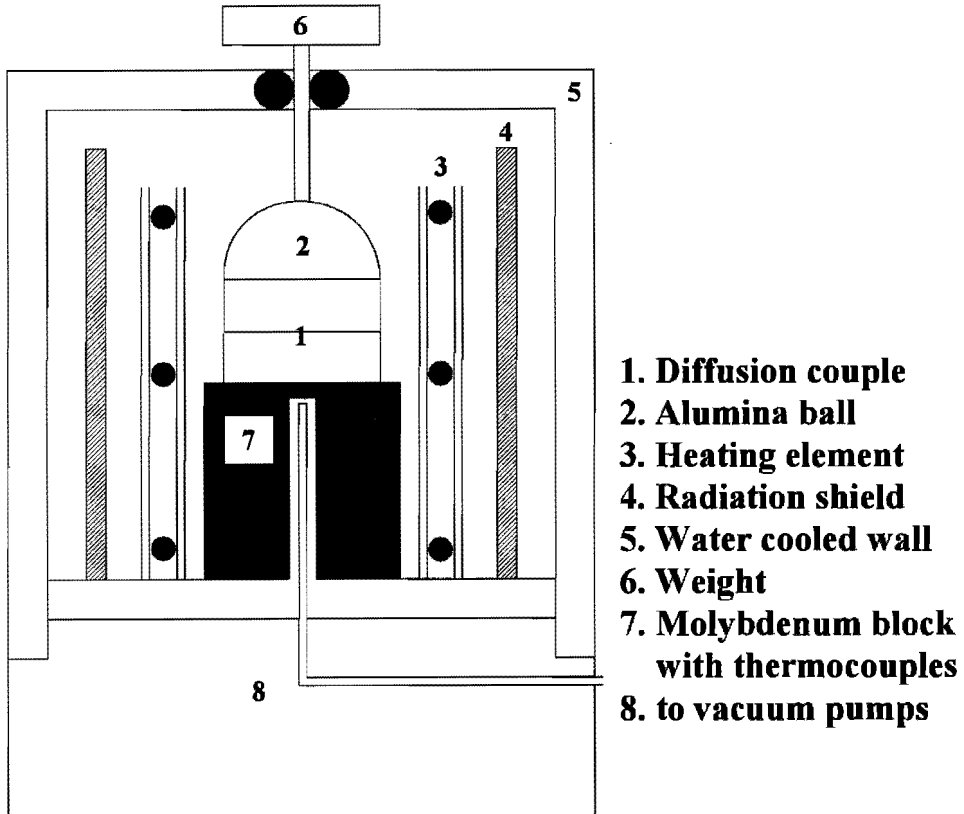


Fig. 4.2 Vacuum furnace used for diffusion experiments

#### 4.3 DIFFUSION COUPLE CROSS-SECTION PREPARATION

Cross-sections of the diffusion couples were prepared by cutting the couple on a slow-speed saw with a diamond wafering blade. After embedding in a conductive resin, the cross-section was ground on SiC-paper to 1200 grit and then polished with diamond paste. A surface finish of 1  $\mu\text{m}$  is usually satisfactory. Sometimes a final polishing step with a 0.25  $\mu\text{m}$  alumina powder slurry was carried out.

If necessary, the samples were etched with a suitable etchant (e.g. dilute HCl for  $\text{Fe}_3\text{Si}/\text{Zn}$  couples).

#### 4.4 ANALYSIS

All samples were inspected first by optical microscopy. Reaction layer thicknesses were measured and morphologies studied. Polarized light was used to identify non-cubic phases and their grain-structure.

Elemental analysis was performed on a SEM (JEOL 840A) equipped with an electron dispersive X-ray (EDX) detector. Most micrographs were taken on this machine. The SEM was operated at an acceleration voltage of 20 kV and a beam current of 1.6 nA. For accurate measurements an electron probe microanalyser (EPMA, JEOL JXA 8600 superprobe) was used. This machine is equipped with five wavelength dispersive X-ray (WDS) detectors.

X-ray diffraction was performed on both diffusion couples and pellets on a Philips PW1120 diffractometer using Cu K $\alpha$  radiation with the aid of a cylindrical texture camera.

Material	Type	Thickness or diameter	Purity	Supplier
Ag	Foil	several	99.99	Goodfellow (UK)
Co	Plate	0.7 mm	99.98	Goodfellow (UK)
Fe	Plate	several	99.99	Goodfellow (UK)
Mg	Rod	6 mm	99.9	Aldrich (USA)
Ni	Plate	1.0 mm	99.98	Goodfellow (UK)
Pt	Foil	0.25 mm	99.9	Alfa Products (Germany)
Si	Rod	15 mm	99.98	Hoboken (Belgium)
Ti	Foil	several	99.98	Goodfellow (UK)
Zn	Bulk	several	99.9	Budelco (Netherlands)
SiC	Polycryst.	pieces	unknown	ESW (Netherlands)
SiC*	Rod, HIPSiC	9 mm	>99.5	ESK (Germany)
SiC	Rod, HIPSiC	9 mm	>99.5	ESK (Germany)

\* Hot isostatic pressed, sintering additive 0.25% alumina

Table 4.1 List of the as-bought materials used in this investigation

## CHAPTER 5

### PERIODIC LAYER FORMATION: EXPERIMENTAL OBSERVATIONS

#### 5.1 INTRODUCTION

This chapter and the following will describe the formation of a periodic layered reaction zone in several ternary systems and one quaternary system. Detailed observations on the morphology are given. In general, the periodic layered morphology is characterized by a regular array of repeating alternating layers. These layers are either single-phase bands (Section 5.2) or bands of particles embedded in an intermetallic matrix phase (Sections 5.3 and further).

#### 5.2 Ag/Ti-foil/Si DIFFUSION COUPLES<sup>1</sup>

##### 5.2.1. Introduction

The present study was initially aimed at the experimental determination of the isothermal cross-section of the ternary Ag-Ti-Si phase diagram at 1123 K. The practical interest for this system lies in the fact that Ag-Ti binary alloys are used as a base in commercial filler metals for brazing various Si-containing ceramics (e.g. SiC, Si<sub>3</sub>N<sub>4</sub>). Knowledge of this system is needed in order to predict the reaction products which can be formed within the brazing seam during fabrication or during high-temperature exposure of the joints.

Using both the semi-infinite diffusion couple technique (mainly with multiphase alloys as end-members) and finite "sandwich" diffusion couples like Ag/Ti-foil/Si the isothermal cross-section through the ternary Ag-Ti-Si diagram at 1123 K was constructed. Using the *finite* sandwich couple technique, a periodic layered structure was found. This gave rise to an additional investigation parallel to the initial phase diagram study.

---

<sup>1</sup> Section 5.2 is a modified part of a paper which was published in *Z.Metallkd.* **87**(9) (1996), 732-739



## **5.2.2 Experimental Details**

Pure silver, titanium and silicon (details, see Ch. 4.2) were used as initial materials. Alloy ingots of nominal composition  $\text{Ti}_{80}\text{Ag}_{20}$ ,  $\text{Ti}_{60}\text{Ag}_{40}$ ,  $\text{Ti}_{75}\text{Si}_{25}$  were prepared by arc-melting under argon. The specimens were annealed in evacuated silica capsules at 1123 K for 120 h and quenched in water. The temperature was controlled within  $\pm 3$  degrees.

From the annealed ingots slices of approximate dimensions  $5 \times 5 \times 1.5 \text{ mm}^3$  were cut and their bonding faces were ground and polished to a final finish with  $0.25 \mu\text{m}$  alumina slurry.

Before bonding, all samples were ultrasonically cleaned in ethanol and then dried using a hot air blower. The diffusion couples were heat-treated in a vacuum furnace ( $5 \times 10^{-6}$  mbar) under an external load of 2 MPa. Temperature control was performed within  $\pm 2$  degrees accuracy. The actual temperature at the place of the sample might deviate  $\pm 5$  degrees from the values reported in this paper.

After annealing and standard metallographic preparation the diffusion couples have been examined by polarized light microscopy, scanning electron microscopy (SEM) and electron probe microanalysis (EPMA).

## **5.2.3 Phase Equilibria in the Ag-Ti-Si System at 1123 K**

### *Reactions between two-phase Ti-Ag alloys and Si at 1123 K*

The microstructure of the transition zone between silicon and a two-phase ( $\alpha\text{-Ti} + \text{Ti}_2\text{Ag}$ ) alloy with the nominal composition  $\text{Ti}_{80}\text{Ag}_{20}$  after annealing at 1123 K for 120 h is given in Fig. 5.1a. Continuous layers of the intermetallic compounds  $\text{TiSi}_2$  and  $\text{TiSi}$  were found at the Si-side of the diffusion couple and continuous layers of the binary intermetallics  $\text{TiAg}$  and  $\text{Ti}_2\text{Ag}$  were observed next to the initial two-phase alloy. The  $\text{TiAg}$  layer is separated from the titanium silicides by a thin layer of pure silver (Fig. 5.1b).

When a two-phase alloy  $\text{Ti}_{60}\text{Ag}_{40}$  consisting of  $\text{Ti}_2\text{Ag}$  and  $\text{TiAg}$  was used as end-member the reaction with silicon at 1123 K for 120 h led to the formation of three layers of titanium silicides:  $\text{TiSi}_2$ ,  $\text{TiSi}$  and  $\text{Ti}_5\text{Si}_4$  (Fig. 5.2a). Next to the initial two-phase alloy a continuous layer of  $\text{TiAg}$  was formed. Again this layer is separated from the titanium silicides by a layer of silver (Fig. 5.2b). The solubility of silver in the silicide phases as well as that of silicon in the intermetallic compound  $\text{TiAg}$  is below the detection limit of EPMA.

The formation of a continuous layer of Ag between  $\text{Ti}_5\text{Si}_4$  and  $\text{TiAg}$  is a strong indication that at this temperature the titanium silicides  $\text{TiSi}_2$ ,  $\text{TiSi}$  and  $\text{Ti}_5\text{Si}_4$  cannot be in equilibrium with  $\text{TiAg}$ .

In both couples the position of the Kirkendall plane nearly coincides with the Si/ $\text{TiSi}_2$  interface, showing that the total reaction layer is formed by diffusion of Si into the original two-phase alloys.

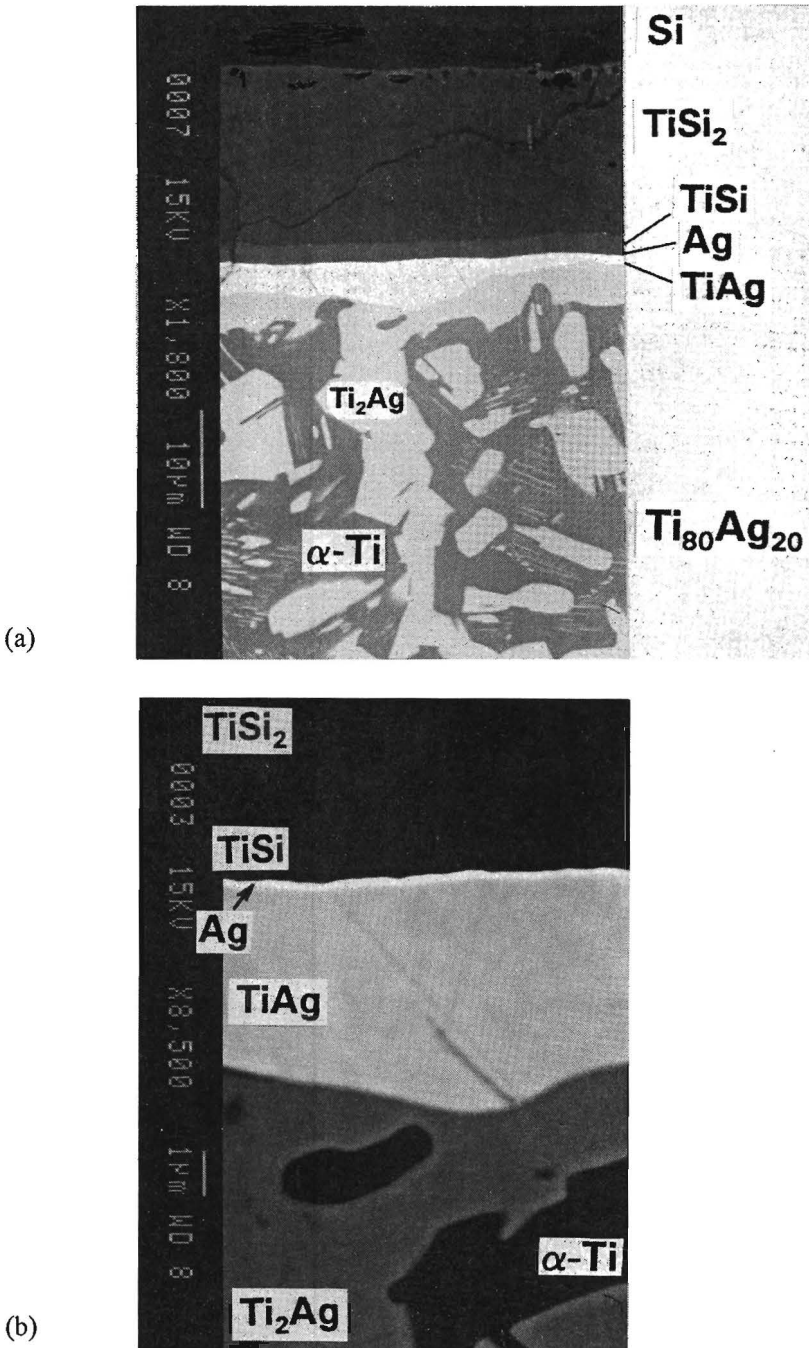


Fig. 5.1 Reaction zone of a Si/( $\alpha$ -Ti +  $Ti_2Ag$ )-alloy diffusion couple annealed for 120 h at 1123 K in vacuum (Backscattered Electron Images (BEI)); a) general view; b) magnified area showing the thin continuous silver layer

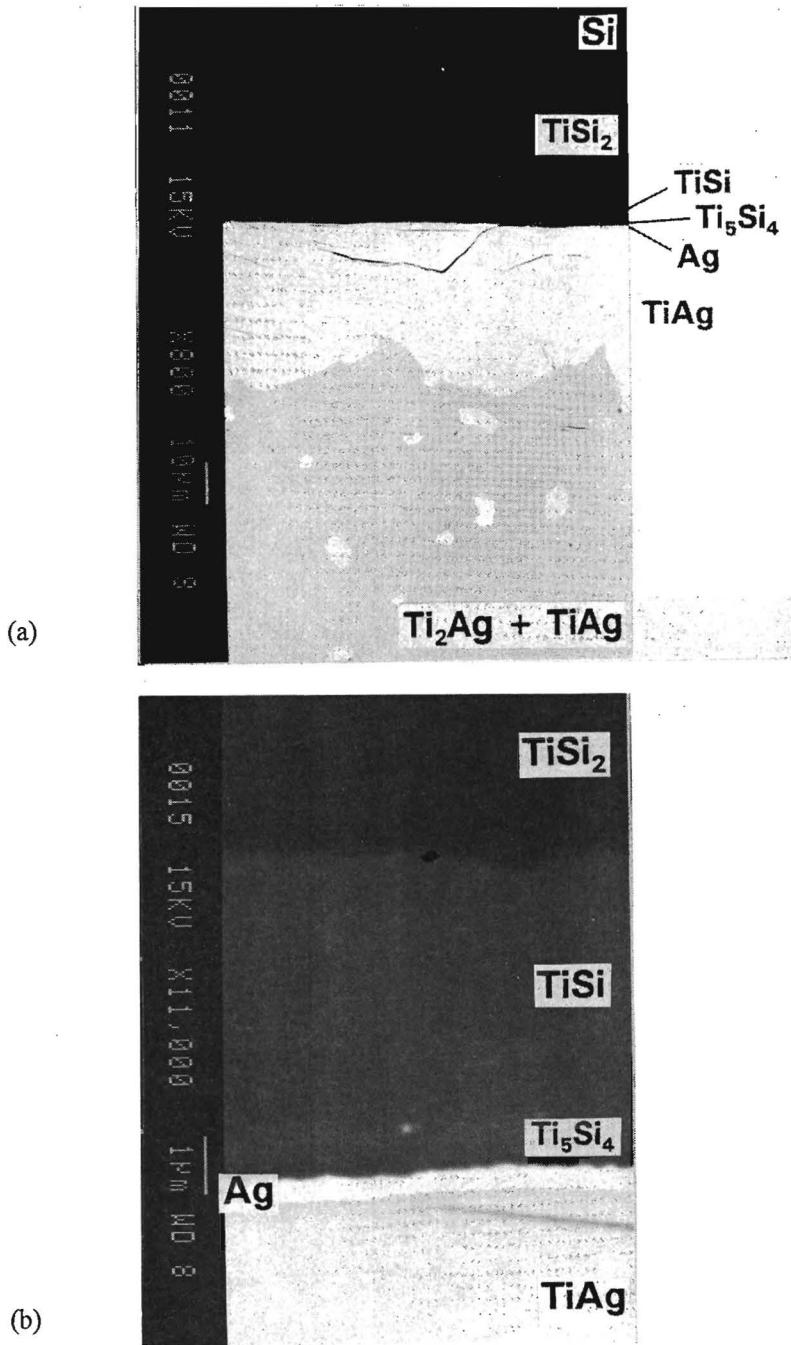


Fig. 5.2 Reaction zone of a Si/(Ti<sub>2</sub>Ag + TiAg)-alloy diffusion couple (BEI) annealed for 120 h at 1123 K in vacuum; a) general view; b) magnified area showing the thin continuous silver layer

*The interaction between silver and a non-equilibrated Ti<sub>75</sub>Si<sub>25</sub> alloy at 1123 K*

In Fig. 5.3 the microstructure of the reaction zone in the diffusion couple Ti<sub>75</sub>Si<sub>25</sub>/Ag after annealing at 1123 K for 144 h is given. A rim of Ti<sub>3</sub>Si around the Ti<sub>5</sub>Si<sub>3</sub> particles in the initial alloy underlines the peritectoid reaction  $\beta\text{-Ti} + \text{Ti}_5\text{Si}_3 \rightarrow \text{Ti}_3\text{Si}$  in the binary TiSi system as shown in Fig. 5.4 [1]. The morphology of the alloy can therefore be attributed to a non-equilibrium situation. Obviously the heat-treatment of the Ti<sub>75</sub>Si<sub>25</sub> alloy for 120 h at 1123 K was not sufficient to equilibrate the alloy. For a phase diagram investigation this is not necessarily a disadvantage. For instance, it can be seen from Fig. 5.3 that the particles of Ti<sub>5</sub>Si<sub>3</sub> originally present in the starting binary alloy still can coexist inside the reaction zone with silver and TiAg, but not with Ti<sub>2</sub>Ag. On the other hand, Ti<sub>3</sub>Si coexists with both intermetallics TiAg and Ti<sub>2</sub>Ag and with  $\alpha\text{-Ti}$ . This proves the presence of the three-phase equilibria Ti<sub>5</sub>Si<sub>3</sub> + TiAg + Ag, Ti<sub>5</sub>Si<sub>3</sub> + Ti<sub>3</sub>Si + TiAg, Ti<sub>3</sub>Si + TiAg + Ti<sub>2</sub>Ag and Ti<sub>3</sub>Si + Ti<sub>2</sub>Ag +  $\alpha\text{-Ti}$  in the Ag-Ti-Si system at 1123 K.

No evidence was found for the presence of ternary phases and all equilibria found in the described experiments are consistent with the ternary Ag-Ti-Si isotherm shown in Fig. 5.5. Theoretically it is possible that ternary phases exist in this system which did not nucleate in our samples, but in view of the consistency of the proposed isotherm with the finite sandwich experiments described in Section 5.2.4 this is very improbable.

The same phase relations are obtained from a thermodynamic assessment of the Ag-Ti-Si system as is shown in the next paragraphs.

*Thermodynamic aspects of the Ag-Ti-Si system*

Values for the standard Gibbs energy of formation of the intermetallic compounds in the Ti-Si system at 1123 K as given in Table 5.1 were derived from [2], except the one for Ti<sub>3</sub>Si as will be explained later. The data on the Ti-Ag system are the same as used in our previous work on the Ag-Fe-Ti system [3]. All intermetallic phases were treated as line compounds.

Compound	TiSi <sub>2</sub>	TiSi	Ti <sub>5</sub> Si <sub>3</sub>	Ti <sub>5</sub> Si <sub>4</sub>	Ti <sub>3</sub> Si	Ti <sub>2</sub> Ag	TiAg
$\Delta G_f^\circ / \text{kJ} \cdot \text{mol}^{-1}$	-163.4	-136.1	-647.0	-582.1	-197.0	-4.2	-3.4

Table 5.1 Standard Gibbs energy of formation for the compounds of the Ag-Ti-Si system at 1123 K

When using the value  $\Delta_f G^\circ(\text{Ti}_3\text{Si}) = -214.5 \text{ kJ} \cdot \text{mol}^{-1}$  as derived from Ref. [2] the phases Ti<sub>3</sub>Si and Ag should be in equilibrium which conflicts with our experimental results. If we do not want to change the data for the other phases and we want to get a negative standard Gibbs energy for the reactions  $3 \text{Ti}_3\text{Si} + 4 \text{Ag} \rightarrow \text{Ti}_5\text{Si}_3 + 4 \text{TiAg}$  and  $\text{Ti}_5\text{Si}_3 + 4 \text{Ti}_2\text{Ag} \rightarrow 3 \text{Ti}_3\text{Si} + 4 \text{TiAg}$ , as required by the experimentally determined isotherm, we need to have

$-198.5 < \Delta_f G^\ominus(\text{Ti}_3\text{Si}) < -195.1 \text{ kJ} \cdot \text{mol}^{-1}$ . The value of  $-197.0 \text{ kJ} \cdot \text{mol}^{-1}$  appearing in Table 5.1 is the value chosen by us. This is not an unrealistic procedure in view of the large influence of impurities on the stability of  $\text{Ti}_3\text{Si}$  with respect to  $\alpha\text{-Ti}$  and  $\text{Ti}_5\text{Si}_3$  [4]. With this adjustment the experimental results on the Ag-Ti-Si system are in agreement with the thermodynamic predictions. The calculated activities of the elements in the three-phase fields are presented in Table 5.2.

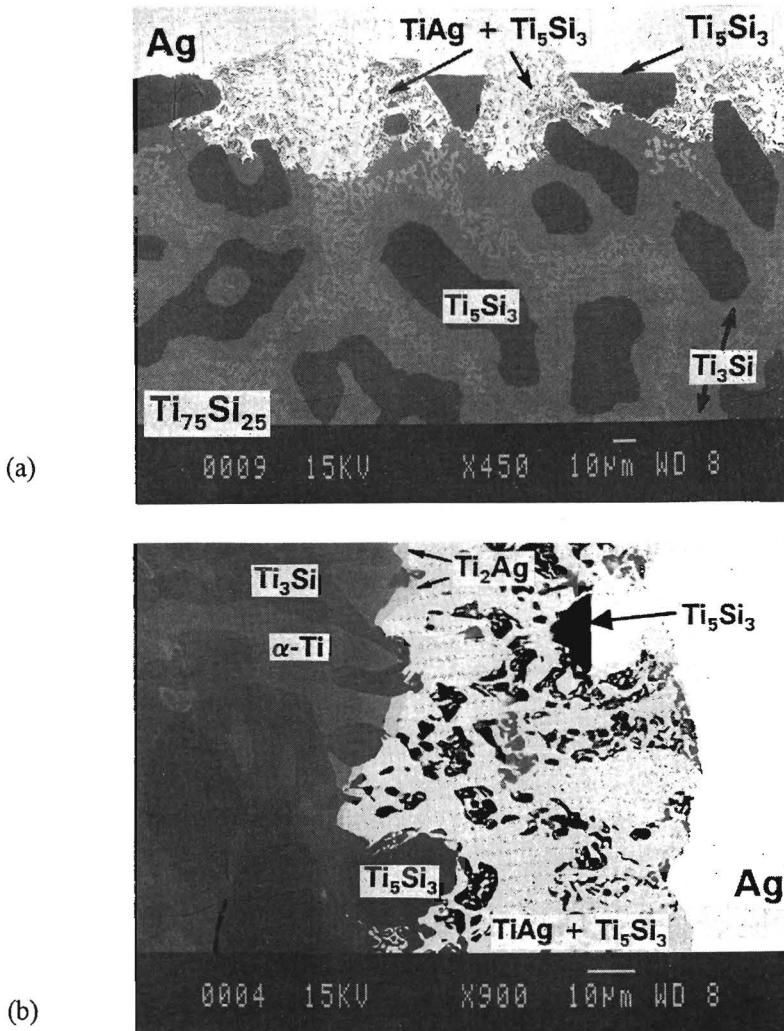


Fig. 5.3 Reaction zone of a Ag/ $\text{Ti}_{75}\text{Si}_{25}$ -alloy (nominal composition) diffusion couple (BEI); a) general view; b) magnified interfacial region

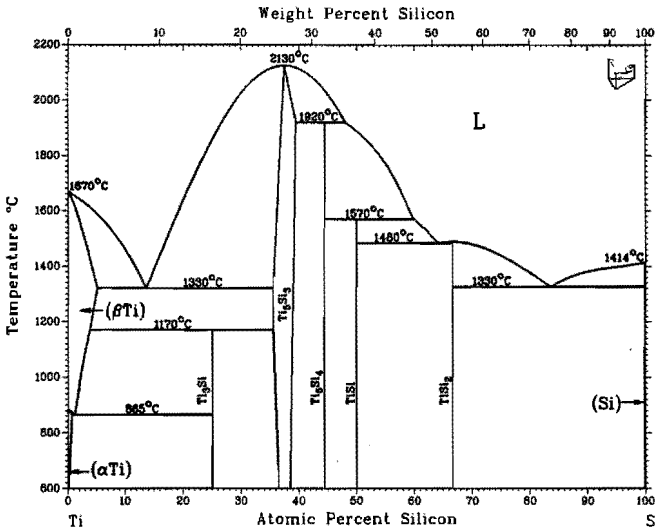


Fig. 5.4 Binary Ti-Si diagram according to [1]

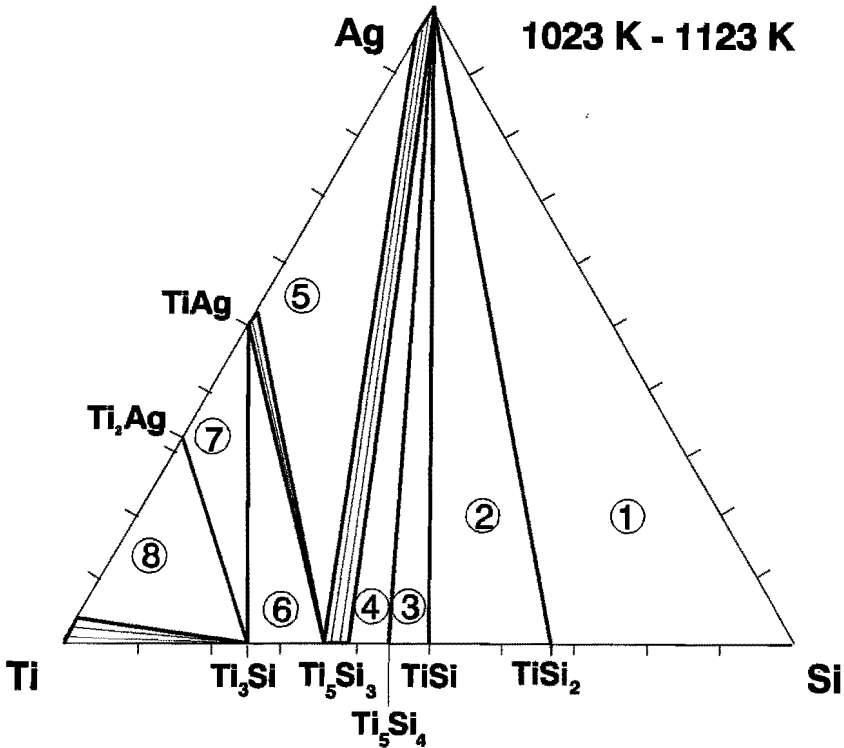


Fig. 5.5 Isothermal cross-section through the Ag-Ti-Si phase diagram, valid in the temperature range 1023-1123 K as determined in the present study

Area <sup>(2)</sup>	Activity <sup>(1)</sup>			Area <sup>(2)</sup>	Activity <sup>(1)</sup>		
	a <sub>Si</sub>	a <sub>Ti</sub>	a <sub>Ag</sub>		a <sub>Si</sub>	a <sub>Ti</sub>	a <sub>Ag</sub>
1	1	2.1*10 <sup>-8</sup>	1	5	1.6*10 <sup>-9</sup>	0.72	0.96 <sup>(3)</sup>
2	0.05	9.3*10 <sup>-6</sup>	1	6	1.4*10 <sup>-9</sup>	0.79	0.94
3	0.027	1.74*10 <sup>-5</sup>	1	7	8.9*10 <sup>-10</sup>	0.92	0.76
4	9.7*10 <sup>-4</sup>	2.47*10 <sup>-4</sup>	1	8	7.8*10 <sup>-10</sup>	0.96 <sup>(3)</sup>	0.69

<sup>(1)</sup> Activities calculated using the stable pure elements as the reference state:

<sup>(2)</sup> corresponding numbers are depicted in Fig. 5.5

<sup>(3)</sup> calculated assuming Raoult's behaviour

Table 5.2 The chemical activities of the elements in the three-phase fields of the Ag-Ti-Si system at 1123 K

## 5.2.4 The Formation of Periodic Structures in the Couples Ag/Ti-foil/Si

### *On solid state diffusion in the Ag-Ti-Si system*

Binary diffusion couples Ti/Si and Ti/Ag and sandwich samples Ti/Ag(foil)/Si were used to obtain information on the diffusion kinetics and the growth of intermetallic compounds in the Ag-Ti-Si system at 1123 K. In Fig. 5.6 the microstructure of the reaction zone in a binary diffusion couple Ti/Si after annealing in vacuum for 415 h at 1123 K is shown. TiSi<sub>2</sub> and TiSi are the predominant layers. Ti-rich silicides (Ti<sub>3</sub>Si, Ti<sub>5</sub>Si<sub>3</sub> and Ti<sub>5</sub>Si<sub>4</sub>) were found to grow much slower. The Kirkendall plane is revealed by the row of pores located close to the Si/TiSi<sub>2</sub> interface. These pores result from the removal (during polishing) of small HfO<sub>2</sub> particles (0.25-0.5 μm) which had been placed as inert markers on the surface of Ti prior to joining. The position of the Kirkendall-plane shows that silicon is the main diffusing species in the TiSi<sub>2</sub> phase.

Reaction of Ti in the diffusion couple with Ag at 1123 K leads to the formation of two continuous layers TiAg and Ti<sub>2</sub>Ag (Fig. 5.7). The Kirkendall plane is visible as a row of pores that coincides with the Ag/TiAg interface, proving that silver is by far the most mobile species in TiAg.

The thicknesses of the phases formed in the diffusion couple are directly related to the interdiffusion coefficients in these phases. As explained in section 2.4, when an intermetallic compound with a very narrow region of homogeneity grows during the reaction diffusion, the conventional Matano-Boltzmann analysis for evaluating interdiffusion coefficients cannot be applied. Since this is the case in Ti-Ag and Ti-Si diffusion couples, the method of Wagner was applied to determine integrated diffusion coefficients in these systems.

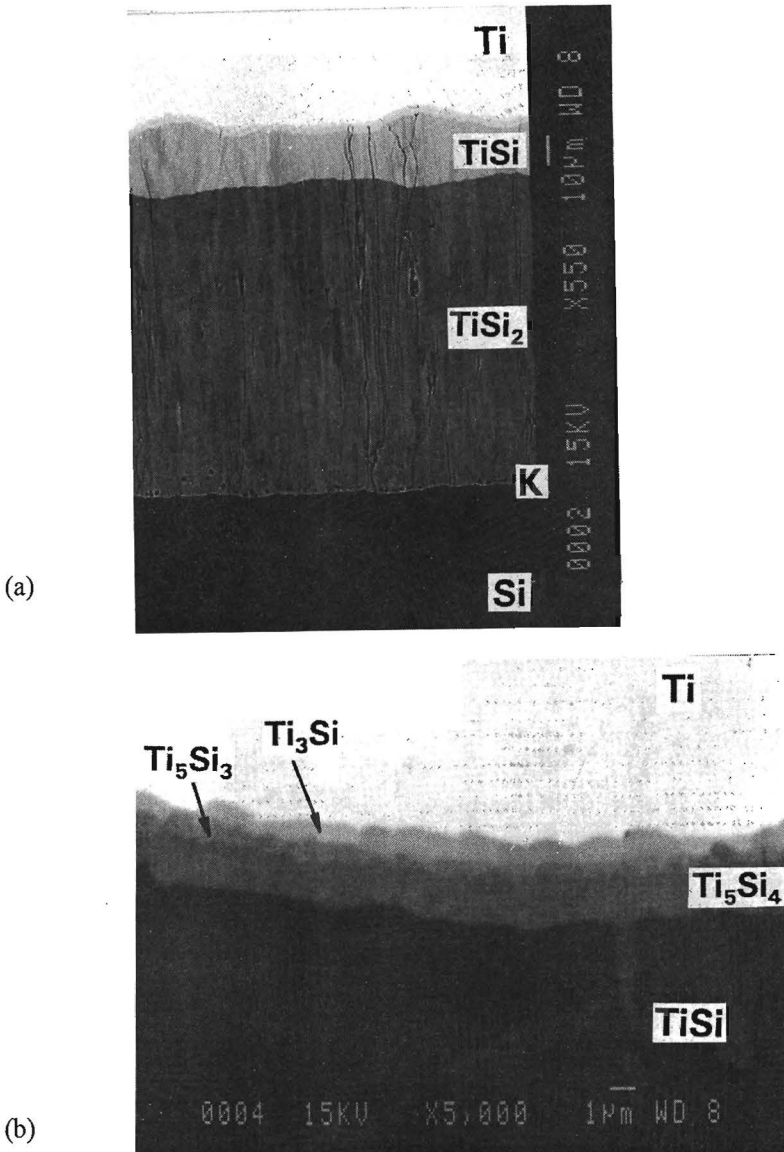


Fig. 5.6 *Reaction zone of a Ti/Si diffusion couple (BEI) annealed for 415 h at 1123 K in vacuum; a) general view; b) magnified area of the Ti/Ti-silicide interfacial region*

In Table 5.3 values of the average integrated diffusion coefficient in different intermetallic compounds of the Ag-Ti-Si system at 1123 K are listed. They are calculated using average layer widths in all couples; differences in molar volumes of the phases were taken into account.



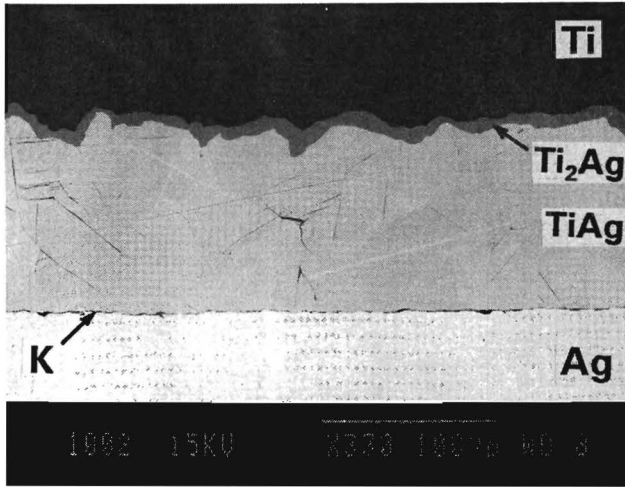


Fig. 5.7 Reaction zone of a Ti/Ag diffusion couple (BEI) annealed for 196 h at 1123 K in vacuum; K indicates the position of the Kirkendall plane

Knowledge of the values of the integrated diffusion coefficients makes it possible to calculate the thicknesses of the layers formed in a binary diffusion couple no matter which starting materials are used. The same is true in a ternary system in the absence of ternary phases or ternary solid solutions as is the case for the present Ag-Ti-Si system, but then the activities of the elements at the phase interfaces should be known [5] as are given in Table 5.2.

Ti-Si system			Ti-Ag system		
Phase	$V_m / 10^{-5} \text{ m}^3/\text{mole}$ of atoms	$D_{\text{int}} / 10^{-18} \text{ m}^2 \cdot \text{s}^{-1}$	Phase	$V_m / 10^{-5} \text{ m}^3/\text{mole}$ of atoms	$D_{\text{int}} / 10^{-18} \text{ m}^2 \cdot \text{s}^{-1}$
Ti <sub>3</sub> Si	1.00	4 ± 2	Ti <sub>2</sub> Ag	1.04	70 ± 30
Ti <sub>5</sub> Si <sub>3</sub> *	0.92	5 ± 2	TiAg *	1.03	1830 ± 200
Ti <sub>5</sub> Si <sub>4</sub>	0.91	11 ± 3	Ag	1.03	
TiSi	0.90	120 ± 50	Si	1.21	
TiSi <sub>2</sub>	0.85	890 ± 50	Ti	1.06	

\* Ti<sub>5</sub>Si<sub>3</sub> and TiAg have been treated as line compounds

Table 5.3. Experimentally determined integrated diffusion coefficients in the binary phases of the Ag-Ti-Si system

When 100  $\mu\text{m}$  foil of silver was pressed between slices of silicon and titanium (of a few mm thickness) and annealed in vacuum at 1123 K for 64 h, the formation of Ti-silicides was found close to the TiAg/Ag interface (Fig. 5.8). This indicates that silicon diffuses much faster through solid silver than titanium does.

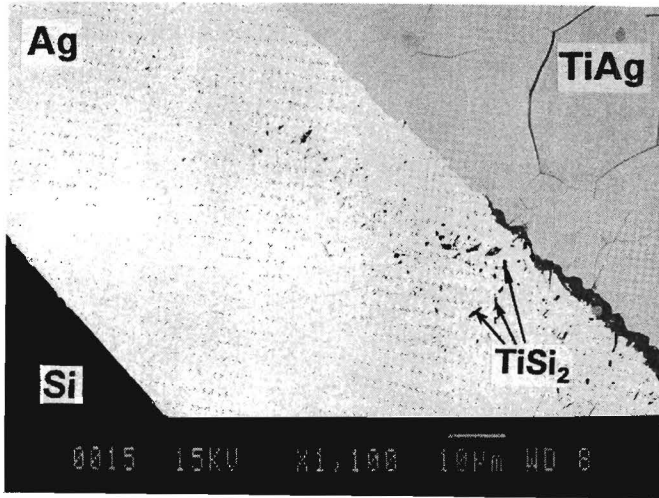


Fig. 5.8 *BEI of a part of the reaction zone in the "sandwich" sample Ti/Ag-foil (100  $\mu\text{m}$ )/Si annealed for 64 h at 1123 K in vacuum showing the formation of Ti-silicide precipitates inside the silver foil*

*Morphological evolution of the diffusion zone in Ag/Ti-foil/Si diffusion couples*

When a "sandwich" sample Ag/Ti-foil/Si was heat-treated for a sufficiently long time (depending on the thickness of the Ti-foil) the formation of a periodic structure in the reaction zone was observed (Fig. 5.9).

The microstructure consists of a continuous layer of  $\text{TiSi}_2$  adjacent to the silicon and a layer of TiAg next to the initial Ag end-member. The two-phase zone between those layers consists of alternating layers of Ti-silicides and pure silver parallel to the original interface. The morphology of the silver bands within this structure is an intermittent layer arrangement while the Ti-silicide layers exhibit an interconnected and slightly tortuous pattern. A continuous layer of silver was found next to TiAg. This layer always separates TiAg from the titanium silicides.

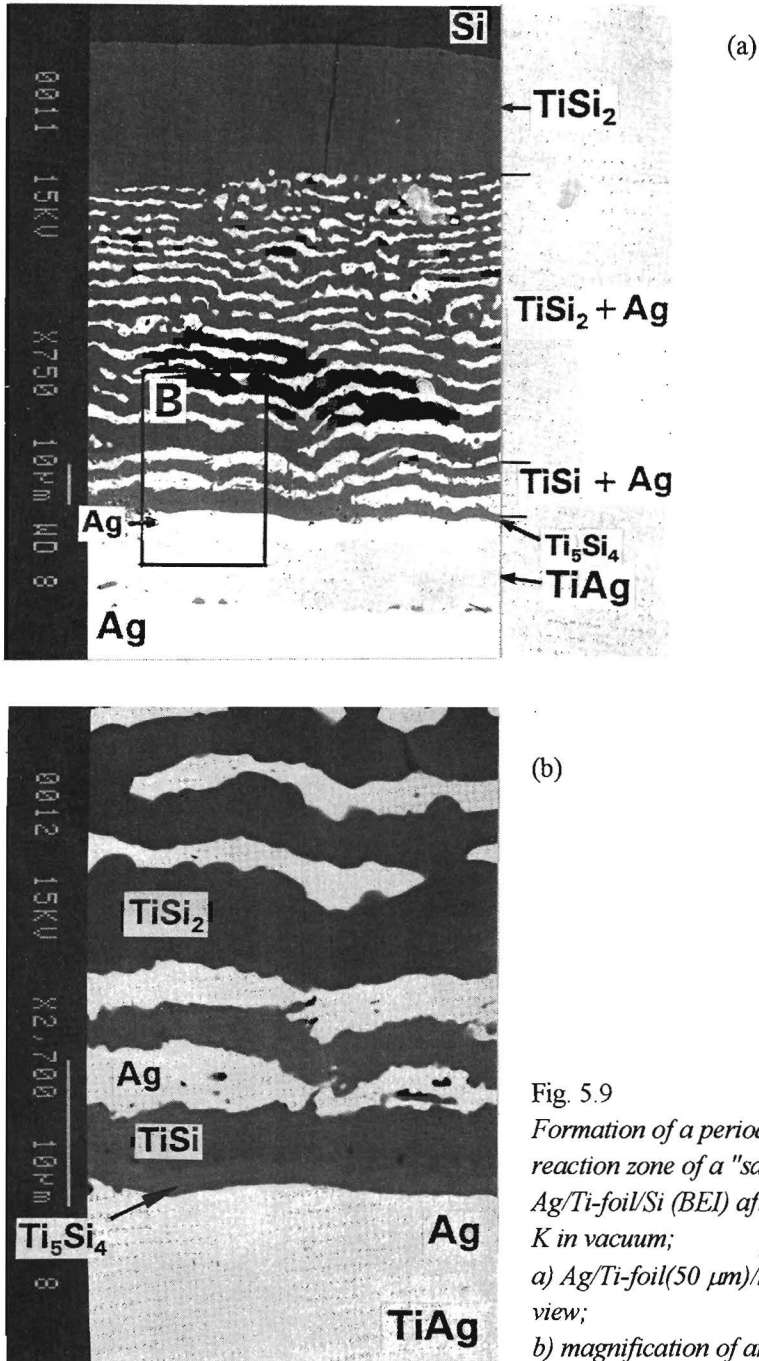
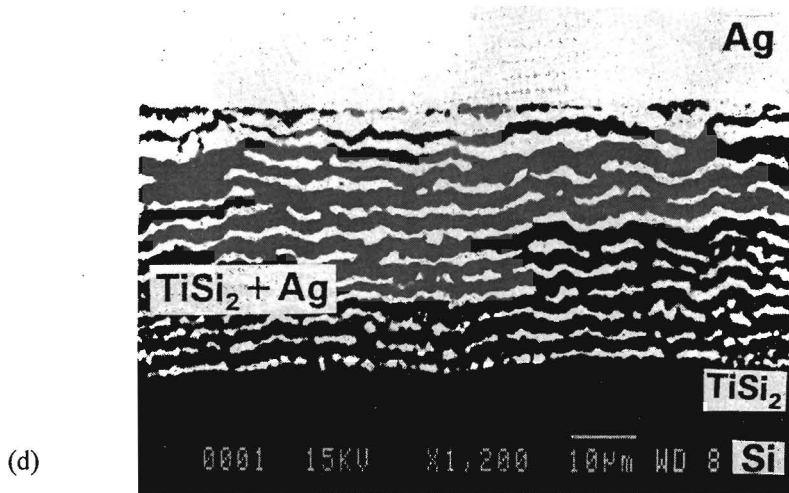
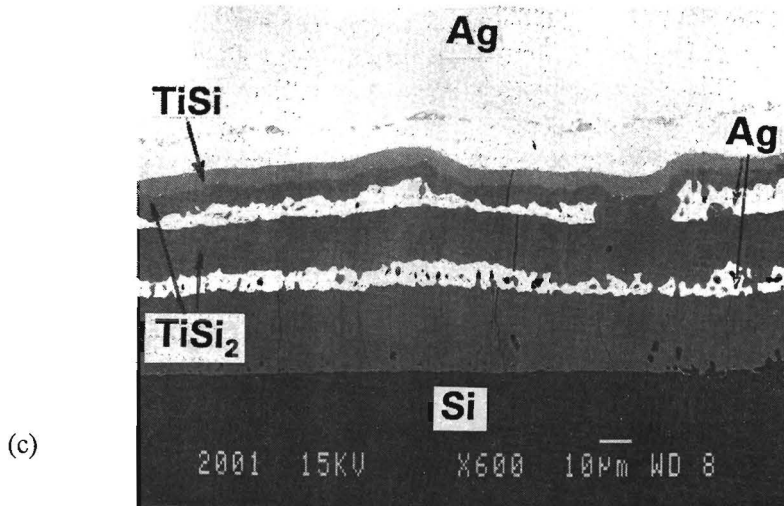


Fig. 5.9  
 Formation of a periodic structure in the reaction zone of a "sandwich" couple Ag/Ti-foil/Si (BEI) after annealing at 1123 K in vacuum;  
 a) Ag/Ti-foil(50  $\mu\text{m}$ )/Si, 600 h, general view;  
 b) magnification of area B in Fig. 5.9a

Fig. 5.9 (continued); c) Ag/Ti-foil(25  $\mu\text{m}$ )/Si, 300 h; d) Ag/Ti-foil(15  $\mu\text{m}$ )/Si, 168 h

The silicides present inside the periodic structure are TiSi<sub>2</sub> (adjacent to the continuous layer of TiSi<sub>2</sub>), TiSi and, for a number of samples, Ti<sub>5</sub>Si<sub>4</sub>, depending on the initial thickness of the Ti-foil and on the annealing time at a specified temperature. Whether or not a TiAg layer is present in the diffusion zone depends on the thickness of Ti-foil used and the annealing time, because the TiAg layer is consumed in the course of the reaction. The microstructure shown in Fig. 5.9d is the final stage (equilibrium structure) of such a morphological evolution. The titanium initially present in the diffusion zone has been completely converted into TiSi<sub>2</sub>.

In the binary Ag-Si system a eutectic melting point is found at 1118 K and 11 at.% Si [1]. No indication of a liquid phase formation was found in the sandwich couples annealed at  $1123 \pm 5$  K, in accordance with the fact that no Si was detected in the silver bands formed in the reaction zone. However, in order to be sure that no liquid phase might be involved in the periodic pattern formation a number of similar experiments were performed at 1023 K and 1073 K, far below the eutectic isotherm in the Ag-Si system. They all showed the same reaction layer morphology (Fig. 5.10).

A discussion and explanation of the observed phenomena will be offered in chapter 6. The formation of a periodic layered structure in Ag/Ti-foil/Si diffusion couples will be considered as a Liesegang phenomenon, see also Ch. 3.2.

Since, in general, zirconium behaves chemically in much the same way as titanium does, a diffusion couple of Ag/Zr-foil(100 $\mu$ m)/Si was prepared. Indeed a very distinct periodic layered reaction zone was found in this couple (Fig. 5.11).

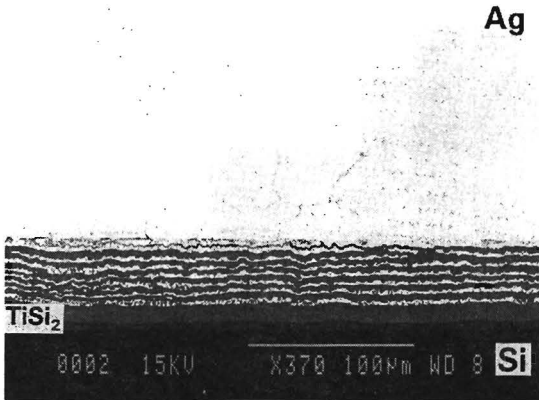


Fig. 5.10 Reaction zone of a sandwich couple Si/Ti-foil(15  $\mu$ m)/Ag annealed for 721 h at 1023 K in vacuum

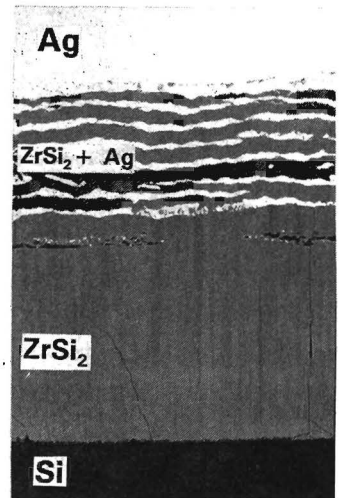


Fig. 5.11 Reaction zone of a sandwich couple Si/Zr-foil(100  $\mu$ m)/Ag annealed for 600 h at 1103 K in vacuum

### 5.3 REACTIONS OF TRANSITION METAL-SILICIDES WITH ZINC

The original discovery of this type of periodic layer formation was a consequence of the study of galvanizing of silicon-containing iron by Osinski [6,7]. The reaction of silicon-containing iron with zinc, at temperatures near the melting point of the latter, has iron-silicides and iron-zinc compounds as reaction products. The morphology of the reaction zone between Fe(Si) solid solution and zinc depends markedly on the silicon-content of the original substrate. There is no sharp transition between the reaction zone with isolated precipitates and the periodic layered reaction zone. Osinski's results are summarized in table 5.4.

Si-content (at.%)	Reaction products sequence	Morphology
0.15-0.4	$\Gamma/\Gamma_1/\delta/\zeta$	simple layered; perturbed $\delta/\zeta$ interface
2.3-6.3	$\delta/(\delta,\zeta)/\zeta$	simple layered; $(\delta,\zeta)$ two-phase zone FeSi (?) particles in $\zeta$
9.0	$(\delta,Fe_3Si)/\delta/\zeta$	$(\delta,Fe_3Si)$ two-phase layer, FeSi precipitates in $\zeta$
17.9	$(\delta,FeSi)/(\zeta,FeSi)$	FeSi precipitates throughout reaction zone
23.2	$(\delta,FeSi)/(\zeta,FeSi)$	short bands of FeSi particles
25.0	$(\delta,FeSi)/(\zeta,FeSi)$	periodic layered

Table 5.4. Summary of reaction layer morphologies of Fe(Si)/Zn diffusion couples at 395 °C,  $\delta \sim FeZn_{10}$ ,  $\zeta \sim FeZn_{13}$

#### 5.3.1 Reactions of iron-silicides with zinc

In Fig. 5.12 the reaction zone of a diffusion couple  $Fe_3Si/Zn$  after annealing at 663 K for 121 h is shown. The reaction layer itself consists of two main layers which are the  $\delta$ - $FeZn_{10}$  and  $\zeta$ - $FeZn_{13}$  phases (revealed by slightly etching the couple with dilute HCl). Inside these phases thin bands of interwoven FeSi particles (Fig. 5.12c) are found, i.e. two-phase layers. Some particles can also be found in between the bands. The bands can be continuous over hundreds of microns. Inside the  $\zeta$ -phase the bands tend to be irregular towards the zinc-side. This is also true for short annealing times. The width of the bands is 1.5-2  $\mu m$ . Inside  $\zeta$  they are somewhat narrower. The average distance (spacing) between the bands inside the  $\delta$ -phase is 16  $\mu m$ , inside  $\zeta$  it is 10-11  $\mu m$ . The band spacing is weakly dependent on the  $Fe_3Si$  grain orientation, as can be seen from Fig. 5.12a,b. A grain boundary in the (cubic)  $Fe_3Si$  (Fig. 5.12b) meets the reaction zone in point A and is extended as a boundary inside the reaction zone with different spacings of the layers on both sides.

The "lifting off" of the bands is observed to take place close to the  $Fe_3Si$ /reaction layer interface, i.e. the  $Fe_3Si$  is permanently covered by a very thin two-phase layer of FeSi and  $\delta$

(fig. 5.12d). After they have lifted of the substrate, the particles behave like inert markers in the diffusion zone, as they are in thermodynamic equilibrium with the matrix phases. This is evidenced by the fact that the bands continue through the  $\delta/\zeta$  interface.

The reaction layer growth is parabolic (Fig. 5.13), indicating diffusion controlled kinetics. The parabolic growth constant  $k_p$  (Eq. 2.11) is  $1489 \mu\text{m}^2\text{h}^{-1}$ . The Kirkendall plane is revealed by a row of pores close to the  $\text{Zn}/\zeta$  interface, proving that inside the  $\zeta$ -phase zinc is by far the most mobile diffusing species.

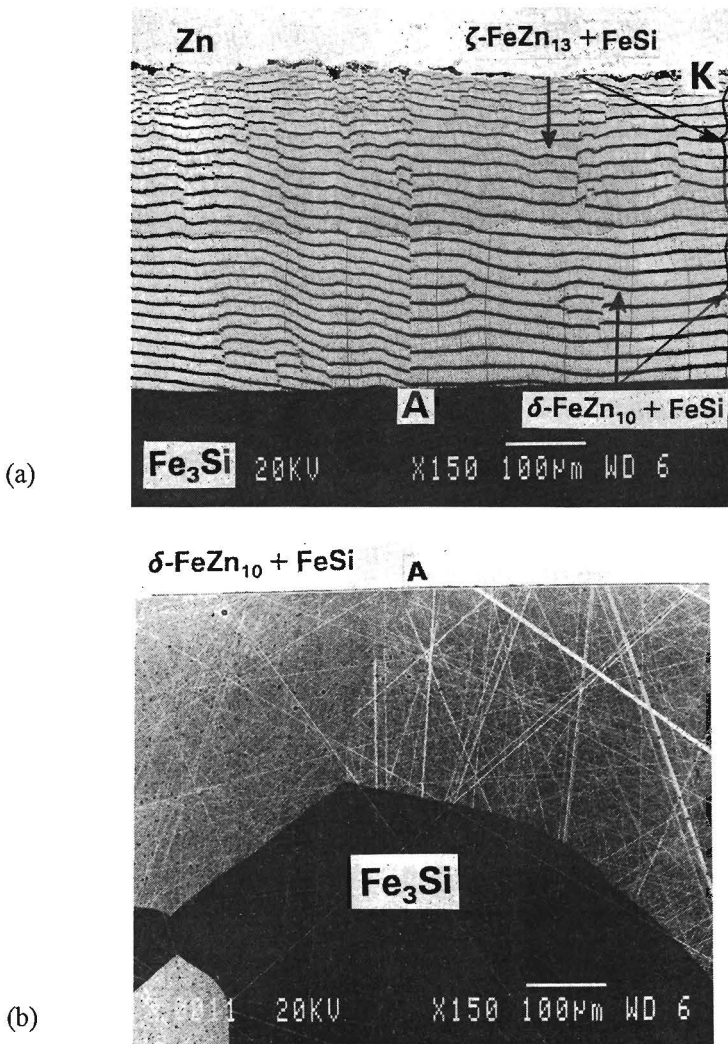
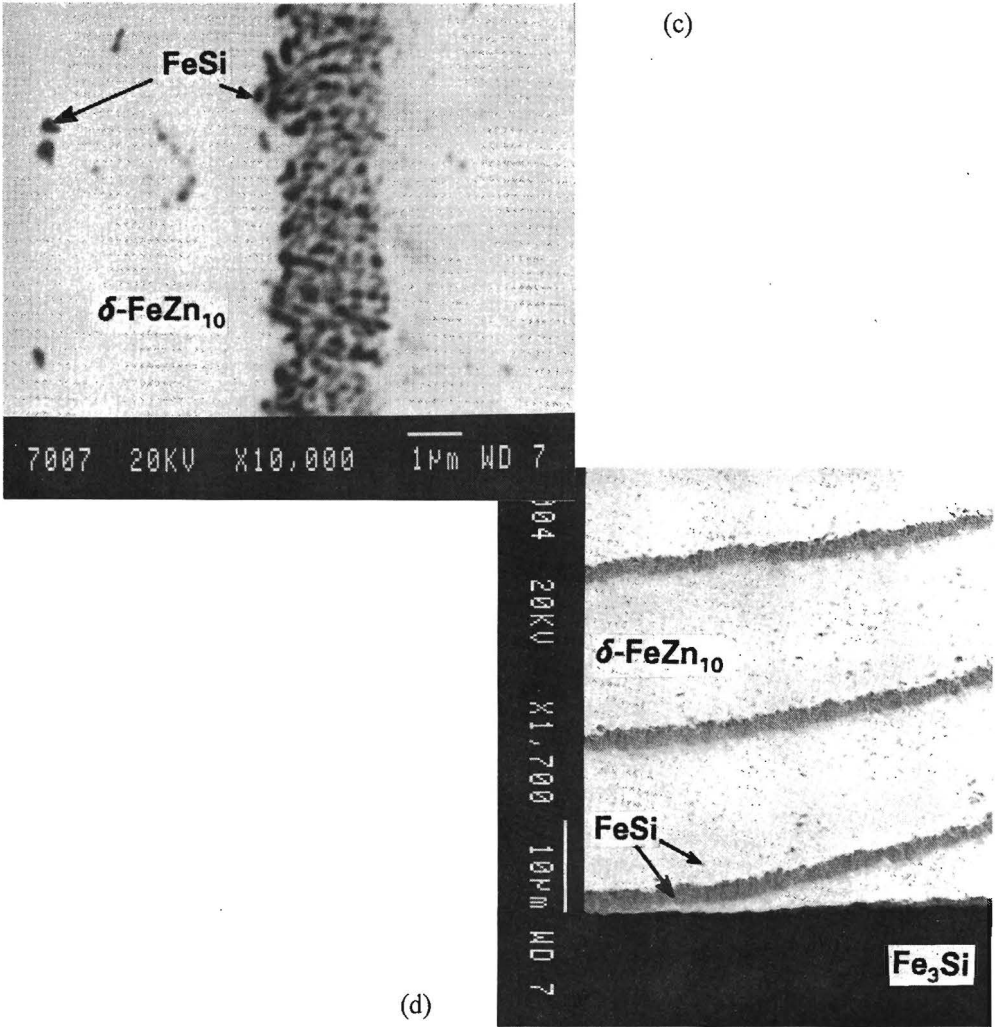


Fig. 5.12 BEI of the reaction zone in a  $\text{Fe}_3\text{Si}/\text{Zn}$  diffusion couple annealed for 121 h at 663 K in He; a) general view; b) view of the substrate, at point A the substrate touches point A in Fig. 5.12a;

Fig. 5.12 (continued) c) magnification of a band, showing it is two-phase;  
 d) magnified area close to the  $\text{Fe}_3\text{Si}$  substrate



To investigate the influence of the substrate ( $\text{Fe}_3\text{Si}$ ) thickness, thin substrate diffusion couples were prepared. Slices of  $\text{Fe}_3\text{Si}$  were ground to a thickness of less than  $200\ \mu\text{m}$ . A piece of zinc was welded on top a slice by melting in a high-frequency furnace. Fig 5.14 shows the reaction zone after welding for two minutes. The width of the weld does not exceed  $10\ \mu\text{m}$ . The couple does not show signs of bending after welding. From the slices rectangular couples were cut of approximately  $6 \times 2.5 \times 2\ (\text{l} \times \text{w} \times \text{t})\ \text{mm}^3$ . Those were annealed in a quartz tube with flowing He atmosphere at  $390\ ^\circ\text{C}$ . All diffusion couples treated in this way showed significant bending during the anneal, zinc being on the concave side (Fig. 5.15a), a sign of



stress relaxation. The reaction zone of the samples prepared in this way demonstrates strong deviation from that in the bulk diffusion couples. Some narrow bands of precipitates are seen on the zinc side (as in the bulk couples), followed by much broader bands on the  $\text{Fe}_3\text{Si}$  side (Fig. 5.15b). This behaviour was not always reproducible.

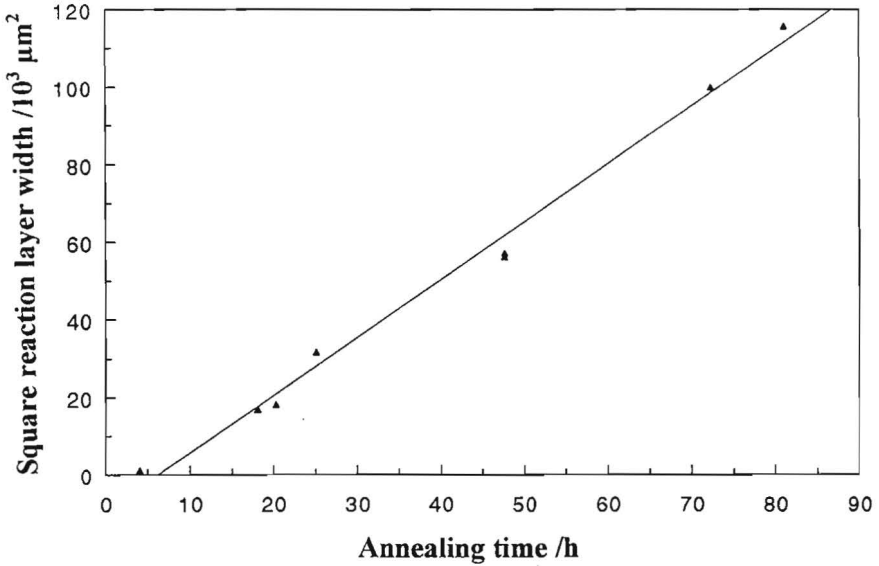


Fig. 5.13 Square reaction layer width of  $\text{Fe}_3\text{Si}/\text{Zn}$  couples as a function of annealing time at 663 K

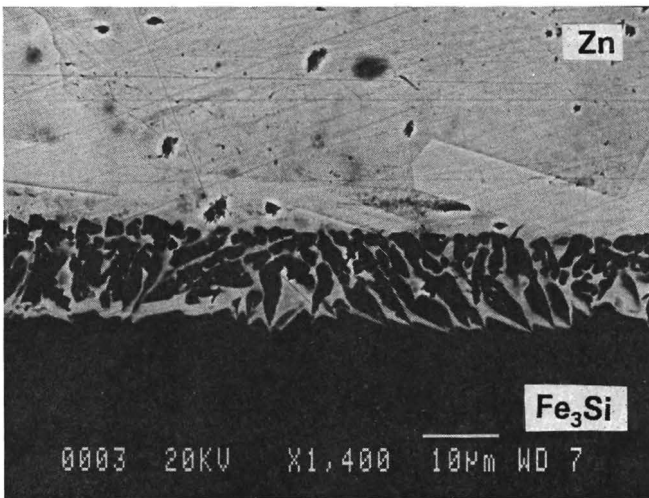


Fig. 5.14 Reaction zone of a  $\text{Fe}_3\text{Si}/\text{Zn}$  couple after welding for two minutes

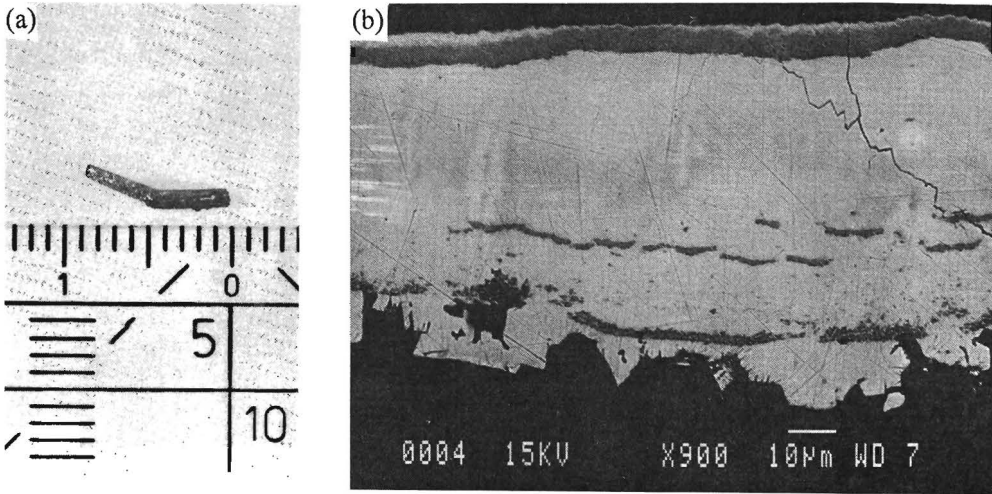


Fig. 5.15 "thin substrate"  $Fe_3Si/Zn$  couple after annealing for 8 h at 663 K in He; a) view of the bent couple; b) reaction zone

Bretez et al. [8] have observed a periodic layered morphology when  $Fe_{94}Si_6$  reacted with Zn vapour at 973 K. This structure consists of bands of  $\alpha$ -precipitates in a  $\Gamma$  matrix

### 5.3.2 Reactions of cobaltdisilicide with zinc

In this part we present our observations on reactions of  $Co_2Si$  with zinc. Apart from some common features with other systems showing periodic layer formation, there are some peculiar differences which deserve attention. Especially, the appearance of a pattern in a plane perpendicular to the diffusion direction is discussed. The pattern is similar to loops of dislocation emerging from a Bardeen-Herring source.

The reaction zone consists of a number of cells with different morphologies (Fig. 5.16). Some are regular and consist of parallel alternating layers (dark bands are slightly wavy), others are irregular but a certain kind of periodicity can still be observed.

The band spacing (or "wavelength") changes from cell to cell. It varies from 3.6  $\mu m$  (minimum) up to 20  $\mu m$ . Band width and -spacing occur in different proportions. In some zones we found a spacing of 4.4  $\mu m$  with a band of 0.8  $\mu m$  (ratio 5.5), in others a 9.0  $\mu m$  spacing with a 1.0  $\mu m$  wide band (ratio 9.0). With the minimum spacing a band width of 0.5-0.6  $\mu m$  occurs (ratio 6.5). In each cell the spacing is nearly constant.

The zones which have the smallest spacings are invariably the widest, i.e. they have grown fastest.

Along the zinc-side and extending over the complete zone there is always a very tiny band present. It is too thin to be analyzed by SEM. This we assume the first band to be formed.

Polarized light microscopy shows that cells of different morphology form on different grains of the orthorhombic [9] cobaltsilicide.

After etching with 2% nital the fine structure of the thin bands is revealed. They consist of small round grains, packed closely together in a matrix phase (Fig. 5.16b). The matrix phase consists of grains up to 5  $\mu\text{m}$  diameter.

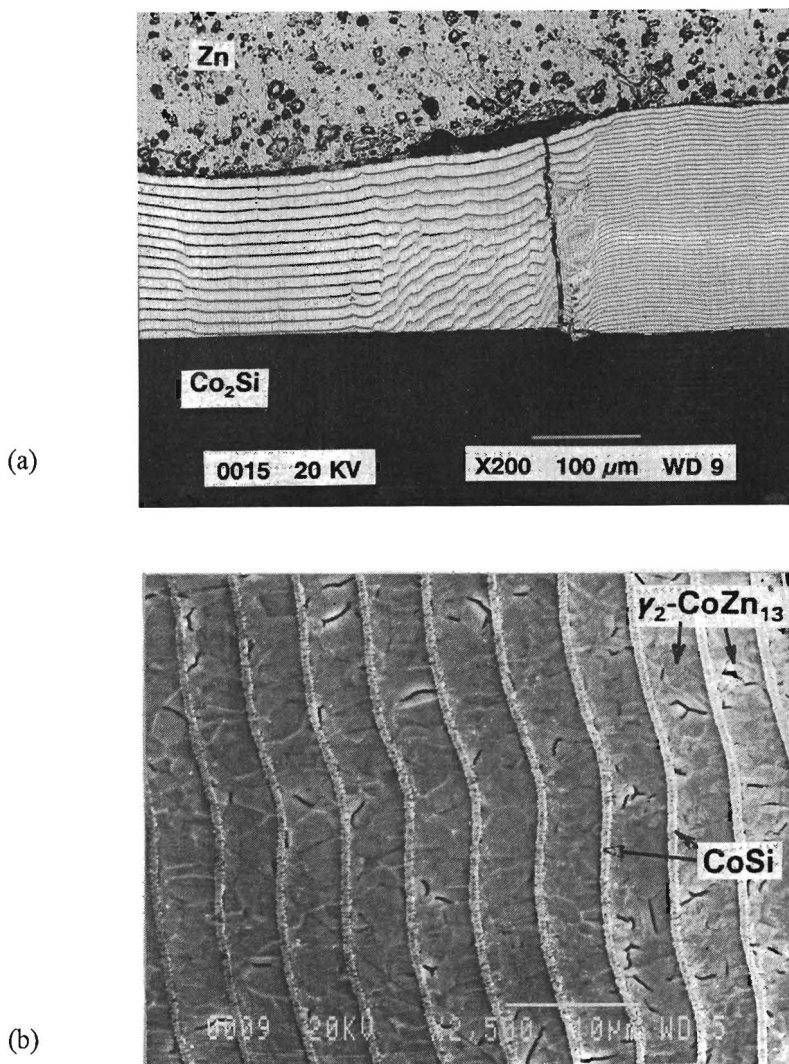


Fig. 5.16 Reaction zone of a  $\text{Co}_2\text{Si}/\text{Zn}$  diffusion couple after annealing for 28 h at 663 K in He; a) general view; b) magnification of etched sample

Cracks extending from the silicide to the zinc are observed after polishing (viz. Fig. 5.16a). They result from cooling. Frequently we find pieces of partly reacted  $\text{Co}_2\text{Si}$  inside the reaction layer.

A surprising morphology was observed when a  $\text{Co}_2\text{Si}/\text{Zn}$  couple was sectioned perpendicular to the diffusion direction (Fig. 5.17). The cross-section was taken close to the zinc-side of the couple. The image resembles the dislocation loops which emerge from a Bardeen-Herring source. To our knowledge, this kind of pattern formation has not been observed before in solid state systems.

Several of these cross-sections have been taken throughout the reaction zones of different couples. In general very chaotic patterns of dark bands in a light matrix phase are observed. The regular bands that we see in the "side view" are thus obviously not dense planes of grains, but rather a cross-section of apparently random patterns, which seem to form periodically. In the "top view" we can distinguish the grain boundaries of the underlying  $\text{Co}_2\text{Si}$  substrate. Different patterns are formed on different grains. The pattern of Fig. 5.17 has only been observed in some rare cases. Sometimes remains or parts of circles are observed.

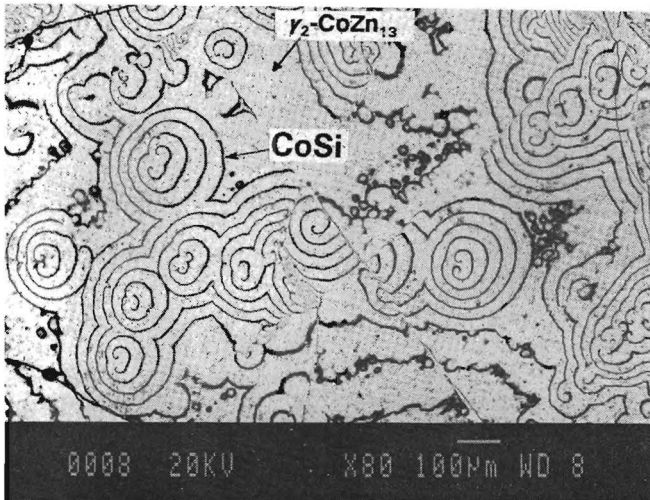


Fig. 5.17 Cross-section of the reaction zone of a  $\text{Co}_2\text{Si}/\text{Zn}$  diffusion couple perpendicular to the diffusion direction

From those observations it is clear that the morphology of the reaction zone is strongly dependent on the crystallographic orientation of the  $\text{Co}_2\text{Si}$ .

Patterns of circles of  $\text{CoSi}$  precipitates were also observed on the surface of a piece of  $\text{Co}_2\text{Si}$  when it was heated at  $390^\circ\text{C}$  together with a piece of zinc in an evacuated quartz capsule. The pieces were separated, so that the reaction resulted from interaction of  $\text{Co}_2\text{Si}$  with zinc vapour.

*Phase equilibria/composition*

The ternary Co-Si-Zn phase diagram has not been extensively investigated but a cross-section at 395 °C was tentatively described by Osinski [6]. No ternary compounds are present, so the system consists of five intermediate cobalt-zinc binaries and four intermediate cobalt-silicon binaries. The silicon-zinc system is a simple eutectic with no intermediate compounds or solid solutions. Silicon is only slightly soluble in the cobalt-zinc binaries (up to 1 at.-%) and zinc is only slightly soluble in the cobalt-silicon binaries.

Quantitative analysis was performed by EDS. In the  $\text{Co}_2\text{Si}/\text{Zn}$  couples three reaction products have been found:  $\gamma_1$  ( $11.0 < \text{at.-% Co} < 12.8$ ) at the  $\text{Co}_2\text{Si}$  side,  $\gamma_2$  ( $7.2 < \text{at.-% Co} < 8.7$ ) at the zinc side and CoSi. The latter is present as small grains inside either  $\gamma_1$  or  $\gamma_2$ . During the reaction of Zn with  $\text{Co}_2\text{Si}$  one mole of CoSi and one mole of  $\gamma_1$  are formed according to (approximately):  $8 \text{ Zn} + \text{Co}_2\text{Si} = \text{CoZn}_8 (\gamma_1) + \text{CoSi}$ .  $\gamma_2$  ( $\text{CoZn}_{13}$ ) is formed by conversion of  $\gamma_1$  by diffusing zinc. The molar volume ratio  $V_m(\gamma_2):V_m(\text{CoSi})$  is 9.2. The observation of different ratios in the diffusion couples supports our observation that the bands are not single-phase. The mixture of CoSi and  $\gamma_1$  or  $\gamma_2$  makes up the dark bands in Fig. 5.16. The lighter zones are  $\gamma_1$  or  $\gamma_2$  compounds with some CoSi.

*Kinetics*

The growth velocity of the reaction zone differs from cell to cell. As a measure of the growth rate we took the widest layer present in any investigated couple. This is always the zone with the smallest band spacing (about 4  $\mu\text{m}$ ), thus having the largest number of bands. The measurements are presented in Fig. 5.18.

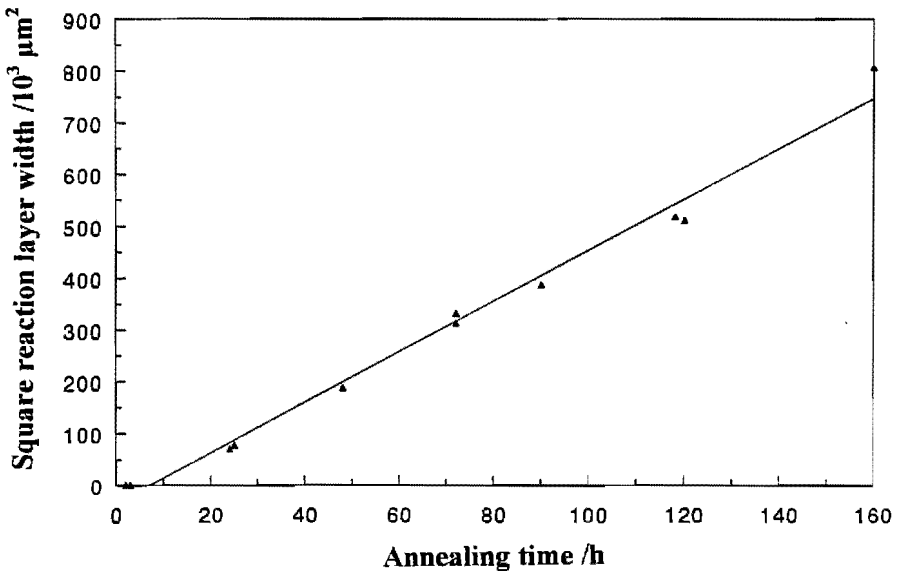


Fig. 5.18 Square reaction layer width of  $\text{Co}_2\text{Si}/\text{Zn}$  diffusion couples as a function of annealing time at 663 K

The growth is parabolic with time, indicating diffusion controlled kinetics. There seems to be an incubation period, the reason of which is not clear. The measured points can be fitted to a straight line  $d^2 = k.t - A$ , with  $k = 4128(\pm 106) \mu\text{m}^2.\text{h}^{-1}$  and  $A = 16768(\pm 56511) \mu\text{m}^2$ .

We did not observe a Kirkendall-plane in the couples, but earlier experiments in the related Fe-Zn [10] and Fe-Si-Zn systems have shown zinc to have a much higher mobility compared to the other components.

### 5.3.3. Reactions of nickel-silicides with zinc

A very fine periodic layered structure (with a spacing of  $\sim 1 \mu\text{m}$ ) was found in solid state diffusion couples of  $\text{Ni}_3\text{Si}_2$  with Zn annealed at 673 K (Fig. 5.19a). The morphology is characterized by a regular array of bands of particles of a Si-rich phase, probably  $\text{NiSi}_2$  (dark contrast in the backscattered electron images (BEI)) embedded in the matrix of a Ni-Zn intermetallic. It can be seen from the micrographs that spacing between bands slightly increases towards the Zn-side of the transition zone. Three two-phase layers consisting of Si-rich precipitates inside different intermetallic matrices can be distinguished just by their appearance in the BEI (fig. 5.19a).

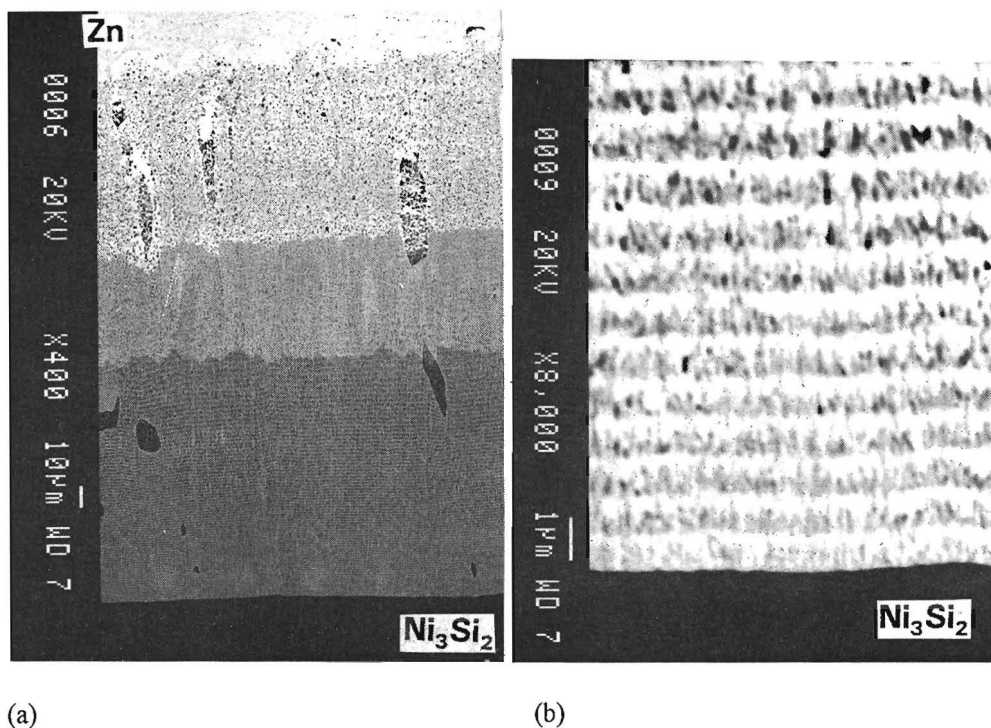


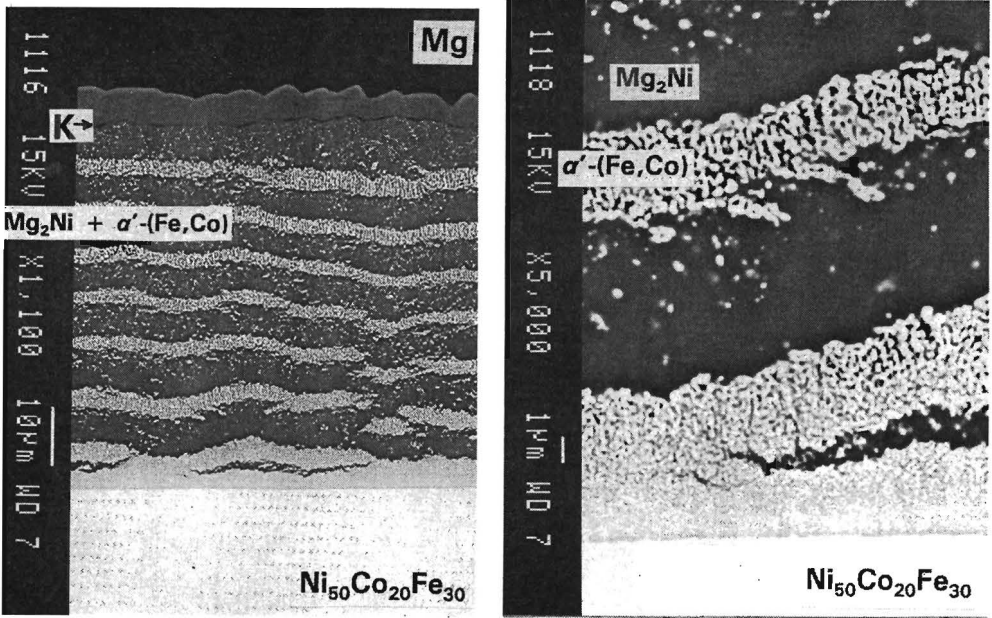
Fig. 5.19 Reaction zone of a  $\text{Ni}_3\text{Si}_2/\text{Zn}$  diffusion couple annealed for 72 h at 663 K in Ar (BEI); a) general view; b) magnified area close to the  $\text{Ni}_3\text{Si}_2$ /reaction layer interface

The formation of a periodic structure occurs only in the two-phase layer adjacent to the  $\text{Ni}_3\text{Si}_2$  substrate. In traversing the diffusion zone from the  $\text{Ni}_3\text{Si}_2$ /reaction layer interface, the periodic pattern disintegrates into randomly distributed particles of  $\text{NiSi}_2$  within the  $\delta\text{-NiZn}_8$  layer. A thin precipitate-free zone of  $\delta\text{-NiZn}_8$  was observed in the vicinity of the interface with Zn. Attempts to determine the chemical composition of the phases within the two-phase layers (except  $\delta\text{-NiZn}_8$ ) were inconclusive due to the limited spatial resolution of the Electron Probe Microanalysis.

The phase relations in the ternary Ni-Si-Zn system at 663 K are not known which makes it difficult to describe the morphological development in this diffusion couple. The low temperature of investigation, at which Ni and Si are supposed to be relatively immobile, makes it difficult to assess the phase relations by the usual means (powder pellets). Prohibitively long annealing times would be needed.

Several attempts to reproduce the periodic layered morphology in  $\text{Ni}_3\text{Si}_2$ /Zn couples have failed, indicating that in these couples the phenomenon may depend on subtle experimental parameter changes.

Reaction of  $\text{Ni}_2\text{Si}$  with Zn did not yield a periodic layered morphology.



(a)

(b)

Fig. 5.20 Reaction zone of a  $\text{Ni}_{50}\text{Co}_{20}\text{Fe}_{30}$ /Mg diffusion couple annealed for 72 h at 733 K in Ar; a) general view (K indicates Kirkendall plane); b) magnified area close to the alloy/reaction zone interface;

## 5.4 REACTIONS OF NICKEL-COBALT-IRON ALLOYS WITH MAGNESIUM

In 1980 Russian workers, in an attempt to join Fe-Ni alloys with the light-weight metal magnesium, inadvertently added some cobalt to the Fe-Ni. When this material was annealed together with Mg, a clear periodic structure was discovered. The results were not published until 1987 [11,12] and only in 1989 a paper appeared in a leading scientific journal [13].

We investigated Mg/Ni<sub>50</sub>Co<sub>20</sub>Fe<sub>30</sub> couples at 733 K and found the same type of periodic layered morphology (Fig. 5.20). There is a regular periodic array of bands (of width ~3  $\mu\text{m}$ ) of (Fe,Co) particles inside a Mg<sub>2</sub>Ni matrix phase. The band spacing is about 7  $\mu\text{m}$  and varies a little bit over the reaction zone. Many particles are also present in between the bands. TEM analysis of the particles (Fig. 5.20c, page 66) shows that they are  $\alpha'$ (Fe,Co) (i.e. ordered CsCl structure) and contain neither Ni nor Mg.

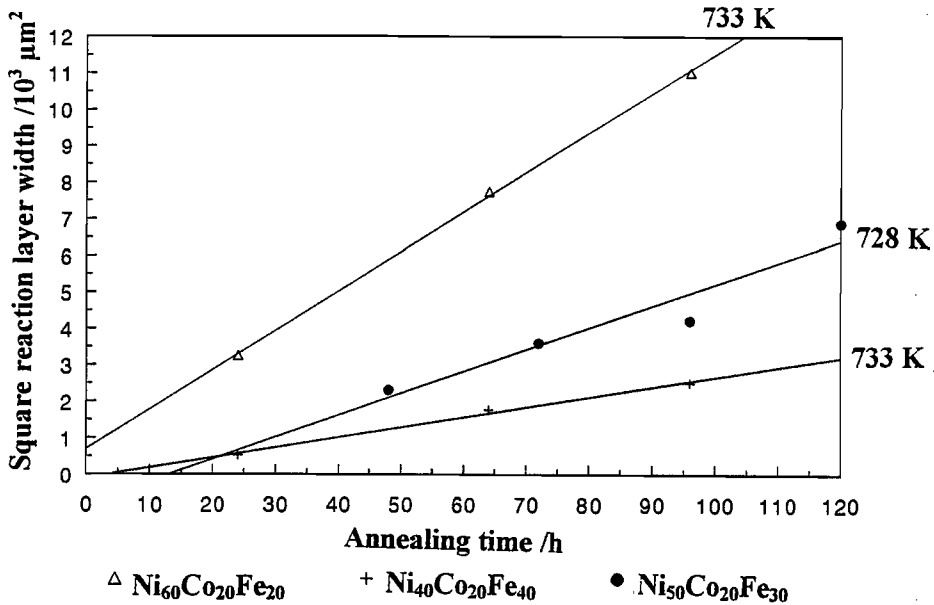


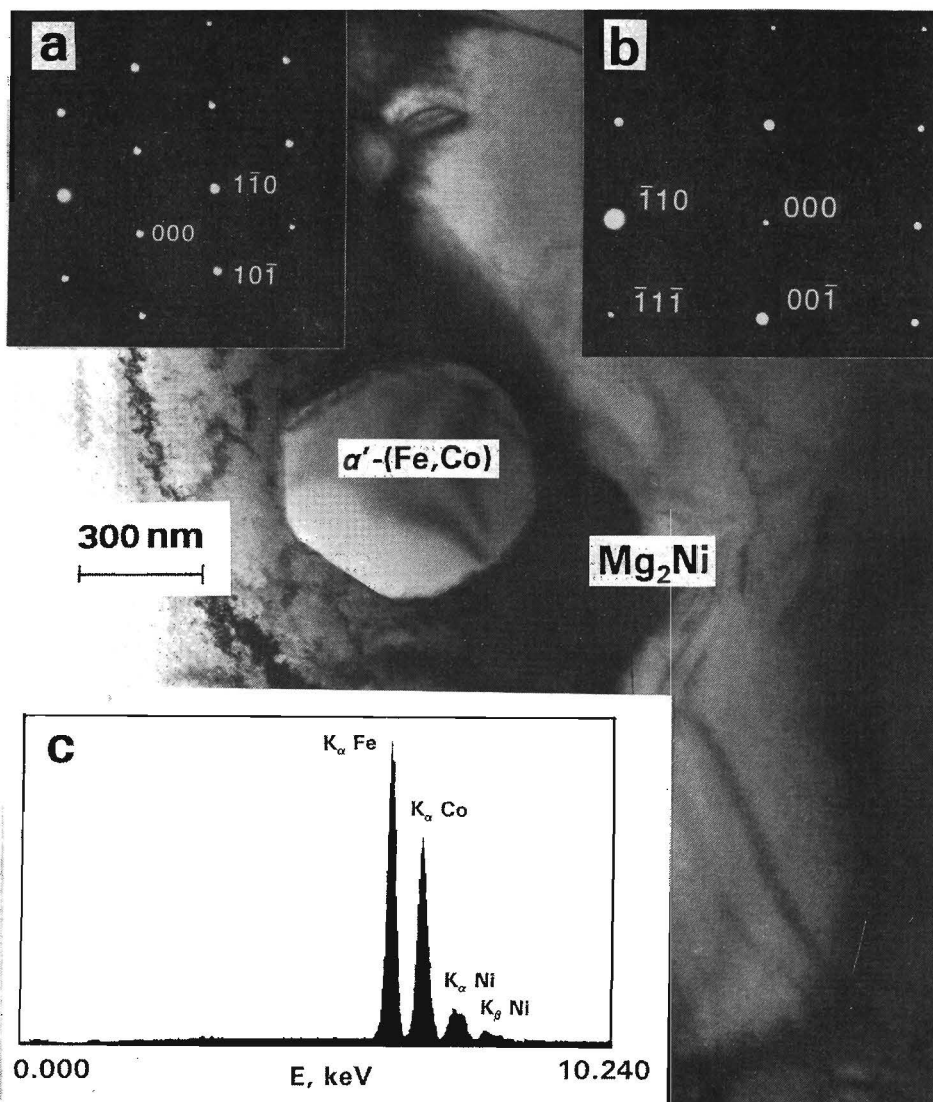
Fig. 5.21 Square reaction layer width of Ni-Co-Fe alloy/Mg diffusion couples as a function of annealing time. Data for Ni<sub>50</sub>Co<sub>20</sub>Fe<sub>30</sub> from [14]

The thickness of the total reaction layer in the Mg/Ni<sub>50</sub>Co<sub>20</sub>Fe<sub>30</sub> couple at 733 K follows the parabolic law, i.e. the reaction is diffusion controlled (Fig. 5.21). The Kirkendall plane is clearly visible inside the Mg<sub>2</sub>Ni intermetallic close to the Mg<sub>2</sub>Ni/Mg interface (Fig. 5.20a). This proves that Mg is the most mobile component in Mg<sub>2</sub>Ni although Ni atoms also diffuse appreciably. No (Fe,Co) precipitates are present on the Mg-side of the Kirkendall plane.



It can be seen from Fig. 5.20b that the appearance of the periodic structure originates from a repeated "cracking" of the interwoven (Fe,Co) bands close to the  $\text{Ni}_{50}\text{Co}_{20}\text{Fe}_{30}$  face. A lifting off occurs when the layer reaches a certain critical thickness. A relatively thick (a few  $\mu\text{m}$ ) two-phase layer still adheres to the initial alloy. We also see that the particles of the adhering band become coarser in the direction of Mg.

Fig. 5.20 (continued) c) TEM micrograph, electron diffraction patterns and X-ray spectrum of a particle



Varying the composition of the Ni-Co-Fe alloy can change the layered morphology drastically. Whereas  $\text{Ni}_{60}\text{Co}_{20}\text{Fe}_{20}$  gives a periodic layered structure (Fig. 5.22a), other compositions of the alloy result in less bands ( $\text{Ni}_{40}\text{Co}_{20}\text{Fe}_{40}$ , Fig. 5.22b) or no bands at all ( $\text{Ni}_{60}\text{Co}_{10}\text{Fe}_{30}$  and  $\text{Ni}_{40}\text{Co}_{30}\text{Fe}_{30}$ ). The latter two alloys rather give a two-phase reaction layer with precipitates. The layer growth is parabolic in all cases. We also found that the addition of 1 at.% tungsten to  $\text{Ni}_{50}\text{Co}_{20}\text{Fe}_{30}$  results in the total suppression of band formation (Fig. 5.23). The composition of the substrate alloys is given in fig. 5.24, which is a ternary cross-section of the Fe-Ni-Co phase diagram [15,16].

The Vickers hardness of the  $\text{Ni}_{50}\text{Co}_{20}\text{Fe}_{30}$  and the  $\text{Ni}_{50}\text{Co}_{20}\text{Fe}_{30}(\text{W})$  alloys was found to be identical within the experimental accuracy.

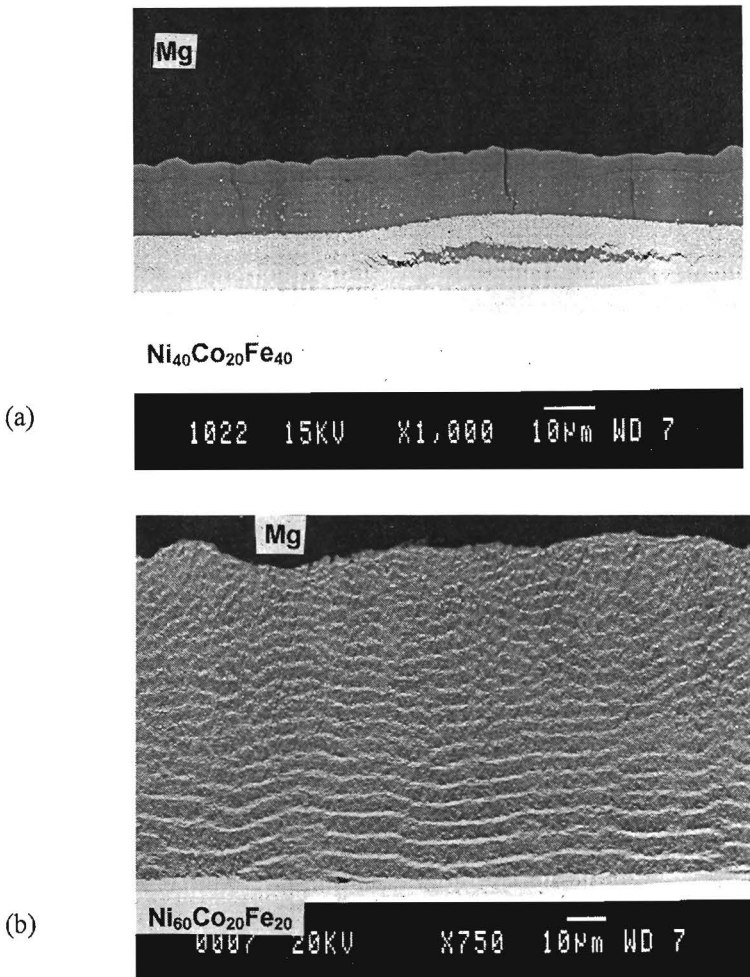


Fig. 5.22 BEI of the reaction zone between Ni-Co-Fe alloys and Mg: a)  $\text{Ni}_{40}\text{Co}_{20}\text{Fe}_{40}$ , 24 h, 733 K; b)  $\text{Ni}_{60}\text{Co}_{20}\text{Fe}_{20}$ , 64 h, 733 K

Fig. 5.23

Reaction zone of a  $Ni_{50}Co_{20}Fe_{30}(W)/Mg$  diffusion couple, annealed for 72 h at 726 K

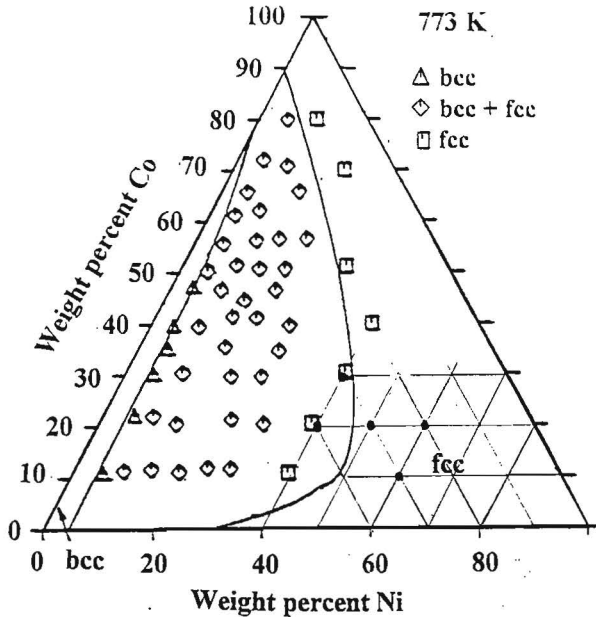
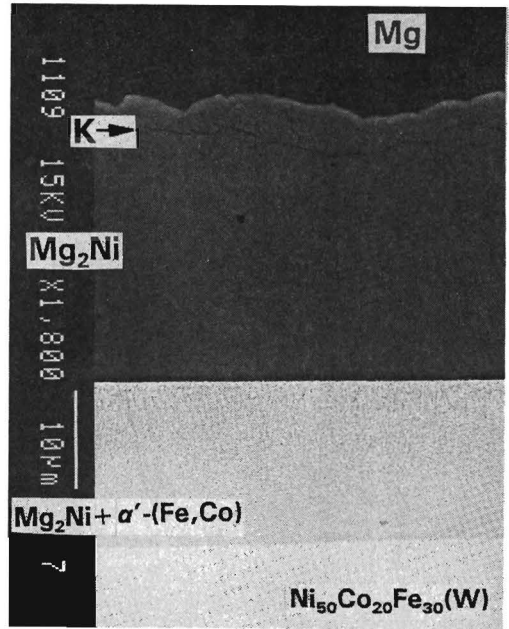


Fig. 5.24 Isothermal cross-section of the Fe-Ni-Co phase diagram at 773 K. (after [15], the solid lines are calculated bcc-fcc phase boundaries, the squares, diamonds and triangles are experimental points from Köster [16]). Alloy compositions used in our experiments are indicated by black dots. Grid was drawn for clarity

## 5.5 REACTIONS OF NON-CARBIDE FORMING METALS WITH SILICON CARBIDE

From the metallic systems we now turn to metal/ceramic systems. Joining of metals to ceramics is an important field in engineering. The combination of malleable metal and strong corrosion- and wear-resistant ceramic is especially useful in high-temperature structural applications. Application at high temperatures puts high demands on the stability of the joint. The chemical, physical and mechanical properties of the joint might influence the overall performance of the ensemble. It is thus useful to study growth and morphological development of the reaction zones between metal and ceramic.

Silicon carbide, SiC, is a very important non-oxide ceramic material. In whisker- or fibre-form, it is used as a reinforcement for both metals and ceramics (composite materials) to be used as high-temperature structural materials. Ohmic contacts to SiC are important in its application as a high-temperature, wide bandgap semiconductor. A morphologically stable contact is produced when the phase in contact with SiC is in equilibrium with it. This kind of information is provided by the metal-Si-C ternary phase diagrams.

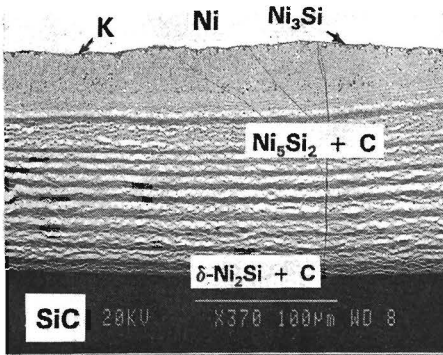
Metals that do not form (stable) carbides (i.e. Fe, Co, Ni and the platinum group metals) react with SiC at high temperatures to form silicides and leave (immobile) carbon as a side product. This results in a multiphase reaction layer existing of layers of silicide mixed with carbon. The actual morphology of the reaction layer varies from isolated precipitates of C to a distinct periodic structure, as we will see in the following sections.

### 5.5.1 Reactions of iron, cobalt or nickel with SiC

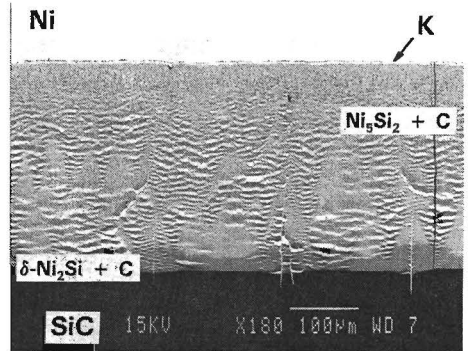
The first example of a banded morphology in metal/ceramic reactions was reported by Mehan and Jackson [17,18]. Their investigation concerned reactions of SiC with Ni and Ni-Cr-Al alloys (as a model for Ni-based superalloys). Bands of carbon particles were inside various silicide layers. This banded structure was later confirmed by Schiepers [19], Backhaus-Ricoult [20] and Chou et al. [21].

The reaction zone consists of  $\text{Ni}_3\text{Si}$ ,  $\text{Ni}_5\text{Si}_2 + \text{C}$  and  $\delta\text{-Ni}_2\text{Si} + \text{C}$ . The crystallographic orientation of the substrate has an obvious influence on the morphology of the reaction zone. Reactions of sintered SiC (grains of  $\sim 1 \mu\text{m}$ ) with Ni give a different morphology compared to reaction of coarse-grained polycrystalline SiC (Fig. 5.25a,b).

Reactions of SiC with pure Fe [19] or Co [21] produce zones with randomly distributed carbon particles (Fig. 5.26a,b). The distribution of carbon particles in the Fe/SiC couple is totally random, whereas in the Co/SiC couple a slight tendency to band formation can be seen. The reaction zone of Fe/SiC diffusion couples contains  $\alpha(\text{Fe,Si})$  as a matrix phase. That of Co/SiC couples consists of  $\text{Co}_2\text{Si} + \text{C}$ , and possibly a thin layer of  $\text{CoSi} + \text{C}$ .

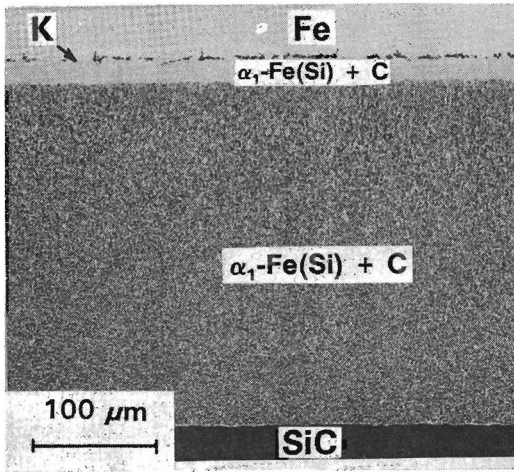


(a)

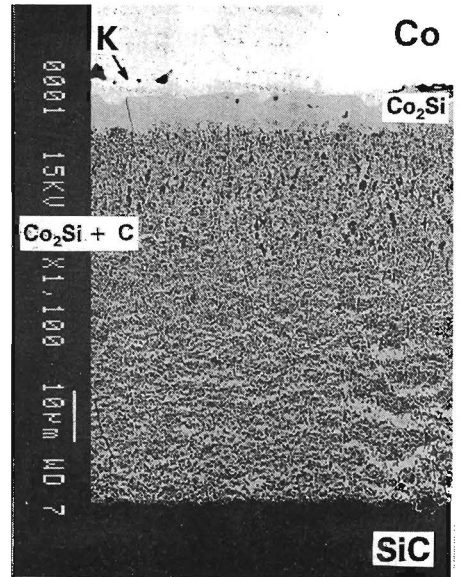


(b)

Fig. 5.25 Reaction zone of Ni/SiC diffusion couples; a) HIPSiC; b) polycrystalline SiC, 24 h, 1123 K



(a)



(b)

Fig. 5.26 Reaction zones of a) Fe/SiC, 22 h, 1123 K; b) Co/SiC, 87 h, 1123 K

### 5.4.2 Reactions of platinum with SiC<sup>2</sup>

In the study [21], Chou et. al. reported on the interaction between SiC and Pt over the temperature range 1173-1373 K which produces a very pronounced "banding" of the reaction zone. This periodic layered morphology (called by Chou a "modulated carbon precipitation zone") was left largely unexplained, except for the general statement that the C precipitation behaviour depends on "...several competing kinetic processes, e.g., overall nucleation and growth rate of silicide phases, rejection rate of C from the reaction front (...), growth (or condensation) rate of C clusters and diffusion rates of metals and Si".

Since the reaction studied by Chou involved liquid, we decided to study the *solid state* interaction between Pt and SiC in the temperature range 973 - 1023 K. It turns out that annealing of Pt/SiC diffusion couples produces a very pronounced periodic layered reaction zone. Study of the reaction zone morphology and reaction kinetics of Pt/SiC diffusion couples demanded more knowledge about the growth kinetics in the binary Pt-Si system and the phase relations in the Pt-Si-C system at the temperatures of interest. Therefore, we also investigated the growth kinetics of silicides in Pt/Si diffusion couples and the isothermal cross-sections of the Pt-Si-C diagram at 973 K and at 1023 K.

The study was carried out using conventional diffusion couple and pressed powder pellet techniques. Phase formation in the Pt-Si and in the Pt-SiC system and reaction zone morphology were studied using the diffusion couple technique. The materials for the diffusion couples were hot-isostatic pressed SiC with and/or without 0.25 wt.% alumina as a sintering aid (ESK, Germany), 0.25 mm platinum-foil (99.9%, ALFA products, Germany) and polycrystalline silicon (99.98, Hoboken, Belgium). The same experimental results were obtained with both types of SiC. Before use in a diffusion couple, Pt-foils of approximately 6x6 mm<sup>2</sup> were annealed in vacuum at 1400 K for 9 hours to improve their ductility. The foils were pressed flat and polished to a final finish with 0.05 µm alumina slurry. SiC and Si were machined to planparallel slices and a final finish of 10 µm. Sandwich couples of the type SiC/Pt-foil/SiC and Si/Pt-foil/Si were annealed for various times in vacuum under an external load of 4 MPa. The couples were allowed to cool to room temperature, cut with a slow-speed saw and prepared for microscopical examination by standard metallographic techniques. Polarized light microscopy, SEM and EPMA were used in investigating the samples.

Powders used for pressing pellets were Pt powder of 0.5-1.2 µm particle size (99.9%, ALFA products) and 325 mesh SiC-powder (>99.5%, ESK). Mixtures of the powders were cold-pressed into pellets and pre-sintered in vacuum at 973 K for 100 hours and at 1023 K for 48 hours. Further heat-treatment was conducted in an electroresistance furnace in evacuated quartz ampoules at 973 K and 1023 K for 400 hours. After preparation the pellets were investigated by EPMA and XRD. The surface of the pellets was studied by cylindrical texture

---

<sup>2</sup> Section 5.4.2 is a modified part of a paper which has been accepted for publication in *Solid State Ionics* [28]

camera. Other pellets were crushed, ground to a fine powder and investigated by powder diffraction.

### *Pt-SiC diffusion couples*

Fig. 5.27 shows the reaction zone morphology of a SiC/Pt/SiC diffusion couple annealed in vacuum for 36 hours at 1023 K.  $\text{Pt}_3\text{Si}$ ,  $\text{Pt}_7\text{Si}_3$ ,  $\text{Pt}_2\text{Si}$  and carbon are the reaction products. A periodic layered morphology is clearly present. Bands of carbon are embedded in the  $\text{Pt}_7\text{Si}_3$  phase up to the Kirkendall plane (see discussion section II). Adjacent to the SiC a two-phase carbon-containing zone ( $\text{Pt}_2\text{Si} + \text{C}$ ) is found (Fig. 5.27b).  $\text{Pt}_2\text{Si}$  has a very irregular interface with  $\text{Pt}_7\text{Si}_3$ . No carbon is found inside the  $\text{Pt}_3\text{Si}$  phase, which shows a wavy interface with Pt. Neither  $\text{Pt}_6\text{Si}_5$  nor  $\text{PtSi}$  are present in Pt/SiC diffusion couples.

The band width and the band spacing is increasing from Pt towards SiC. The carbon is present in the form of densely packed platelike grains embedded in a matrix of either  $\text{Pt}_7\text{Si}_3$  or  $\text{Pt}_2\text{Si}$ . The two-phase carbon bands are continuous over almost the total reaction zone. When the thickness of the  $\text{Pt}_2\text{Si}$  layer exceeds the thickness of the carbon-containing zone the formation of bands stops. The number of bands formed is the same in both reaction zones of the SiC/Pt/SiC couple (Fig. 5.27a).

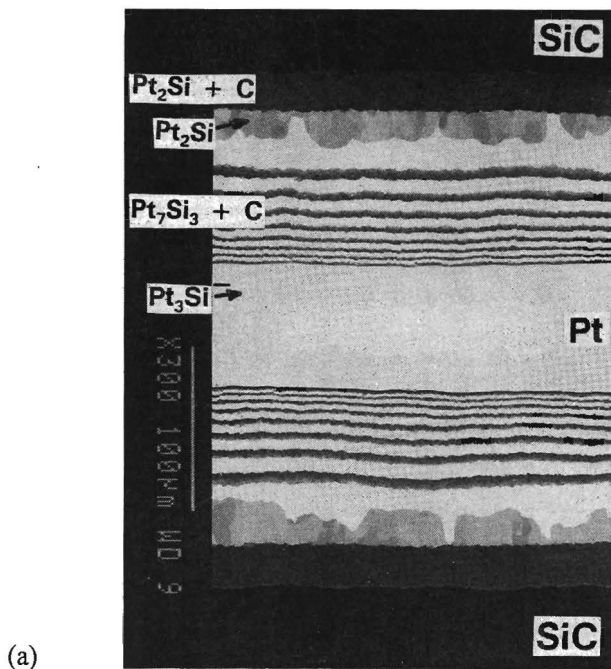
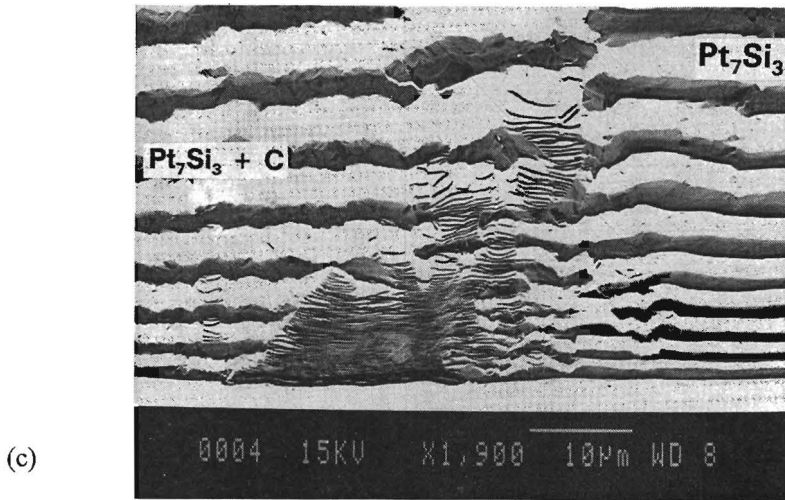
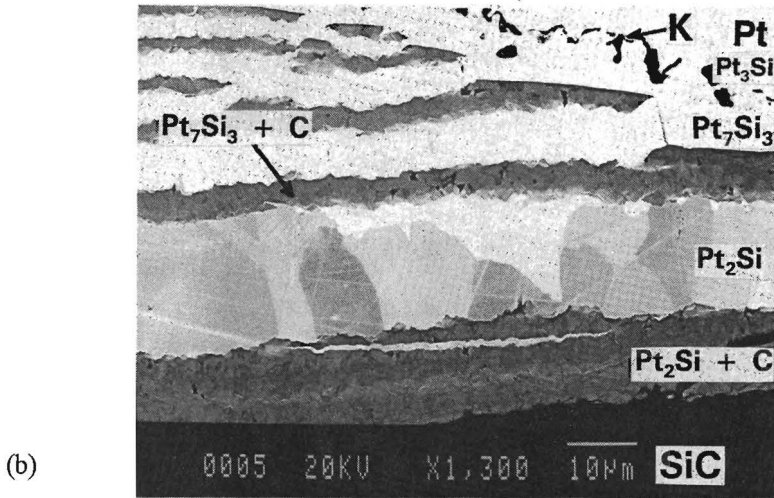


Fig. 5.27 Diffusion zone of a SiC/Pt/SiC diffusion couple annealed for 36 h at 1023 K (BEI); a) general view; b) area near the end of the reacted part; c) degradation of carbon bands in the old part of the reaction zone

Fig. 5.27 (continued)



The Kirkendall plane is situated inside  $Pt_7Si_3$ , close to the interface with  $Pt_3Si$ , as is revealed by a row of pores (Fig. 5.27b). This proves that Pt is the fastest diffusing component inside  $Pt_7Si_3$  at 1023 K.

A rather peculiar "degradation" of the carbon bands can be seen in fig. 5.27c. In a part of the reaction zone the bands are broken up into tiny ribbons of carbon.

Fig. 5.28 shows the reaction zone morphology of Pt/SiC diffusion couple annealed in vacuum for 16 hours at the lower temperature of 973 K. A morphology rather similar to the one previously described developed in this couple.  $Pt_3Si$ ,  $Pt_7Si_3$  and carbon are the directly visible



reaction products. Again we find bands of carbon embedded in  $\text{Pt}_7\text{Si}_3$  with an increasing spacing and thickness in the direction of SiC. A two-phase carbon-containing zone is found adjacent to the SiC. There is also degradation of bands in some part of the diffusion zone. In the vicinity of cracks in the diffusion zone which run parallel to the diffusion direction, carbon is found as finely dispersed particles (Fig. 5.28c)

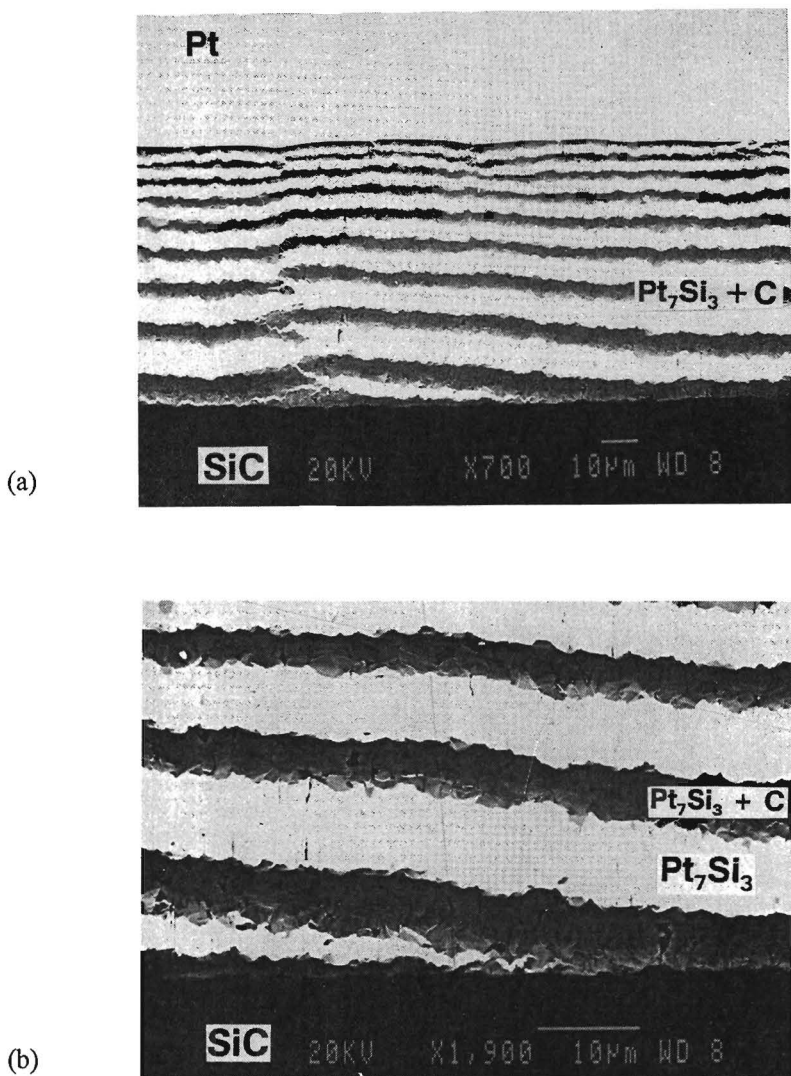
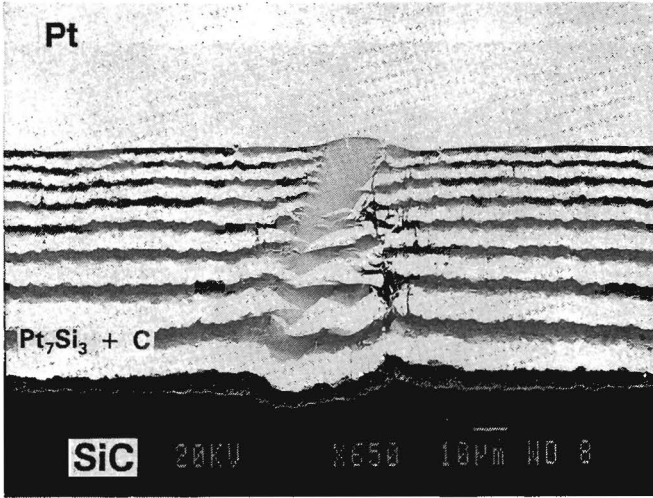


Fig. 5.28 Diffusion zone of a SiC/Pt diffusion couple annealed for 25 h at 973 K (BEI); a) general view; b) magnified area close to the SiC interface;

Fig. 5.28 (continued) c) area near a crack parallel to the diffusion direction



(c)

Although the growth of intermetallics in the reaction zone is irregular, the overall growth rate of the reaction zone is found to obey the parabolic law both at 973 K and 1023 K (Fig. 5.29). This indicates that the reaction is diffusion controlled.

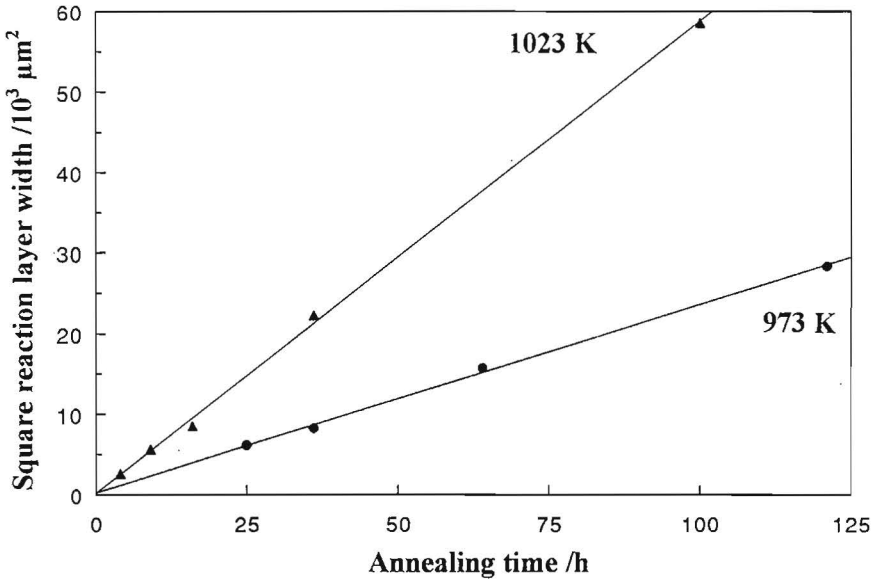


Fig. 5.29 Square reaction layer width in SiC/Pt diffusion couples as a function of time

An important feature of the band formation can be seen from Fig. 5.28b. After the two-phase zone adjacent to SiC reaches a critical thickness, cracking in the interwoven graphite band occurs. The shape of the interface between  $\text{Pt}_7\text{Si}_3$  and the newly formed mixed  $\text{Pt}_7\text{Si}_3 + \text{C}$

band is an exact replica of the ( $\text{Pt}_7\text{Si}_3 + \text{C}$ ) layer that remains at the SiC interface. This is true for all graphite-containing bands.

No single-phase  $\text{Pt}_2\text{Si}$  can be directly observed in the reaction zone of couples annealed at 973 K, not even after long annealing times (121 hours, Fig. 5.30). However, the Pt:Si ratio (as measured by EPMA) inside the carbon-containing zone close to the SiC was found to be 2:1, while a ratio of 7:3 was measured within the same zone but close to the  $\text{Pt}_7\text{Si}_3$  side. This indicates that also at 973 K  $\text{Pt}_2\text{Si}$  is formed, but as a thin layer. The  $\text{Pt}_2\text{Si}/\text{Pt}_7\text{Si}_3$  interface is "hidden" inside the carbon-containing layer.

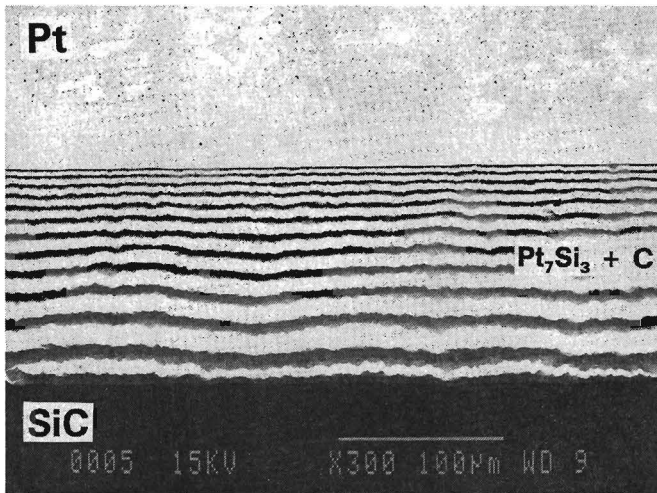


Fig. 5.30 Reaction zone of a Pt/SiC diffusion couple annealed for 121 h at 973 K

According to [22]  $\text{Pt}_2\text{Si}$  exists in two modifications: high-temperature (HT)  $\beta\text{-Pt}_2\text{Si}$  and low-temperature (LT)  $\alpha\text{-Pt}_2\text{Si}$ , with a transition temperature of  $968 \pm 5$  K. The HT phase has the hexagonal crystal structure, whereas the LT phase is tetragonal [23]. Thus the conspicuous difference in growth kinetics of  $\text{Pt}_2\text{Si}$  in the present case might be due to the formation of the  $\beta$ -modification at 1023 K and the formation of the  $\alpha$ -modification at 973 K.

In order to study the growth kinetics of  $\text{Pt}_2\text{Si}$ , binary platinum/silicon diffusion couples were annealed at 973 K and 1023 K. In Fig. 5.31 two couples annealed at these respective temperatures for four hours are compared. It is clear that at 1023 K,  $\text{Pt}_2\text{Si}$  is the predominant compound in the diffusion zone, whereas at 973 K it grows very slowly. In the latter case PtSi is the predominant compound. In both cases the Kirkendall plane is found inside  $\text{Pt}_7\text{Si}_3$ . The growth of most of the intermetallics in those Pt/Si diffusion couples is rather irregular, i.e. no straight interfaces are observed.

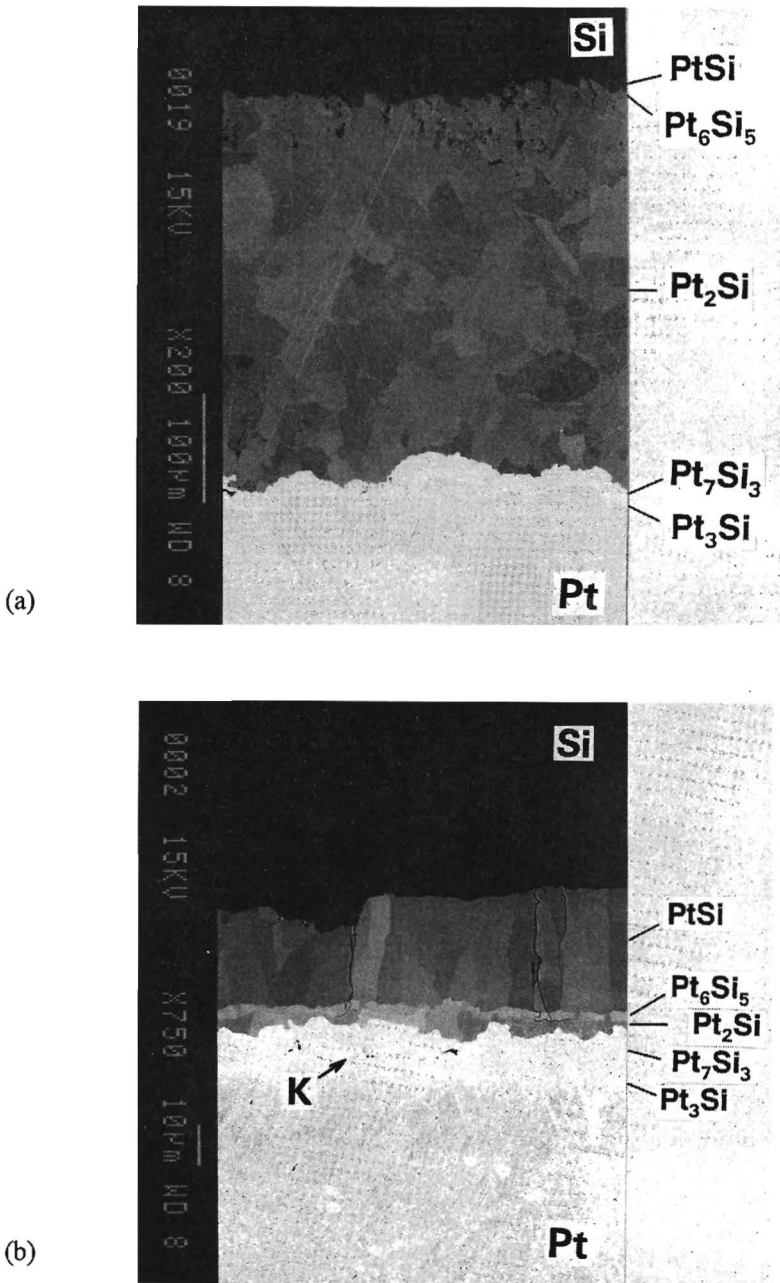


Fig. 5.31 Binary bulk Pt/Si couples annealed for 4 h; a) at 1023 K; b) at 973 K

For comparison some diffusion couples were made of Pt-foil with single crystalline SiC. Annealing of these couples results in an irregular periodic layered arrangement of the phases (Fig. 5.32).

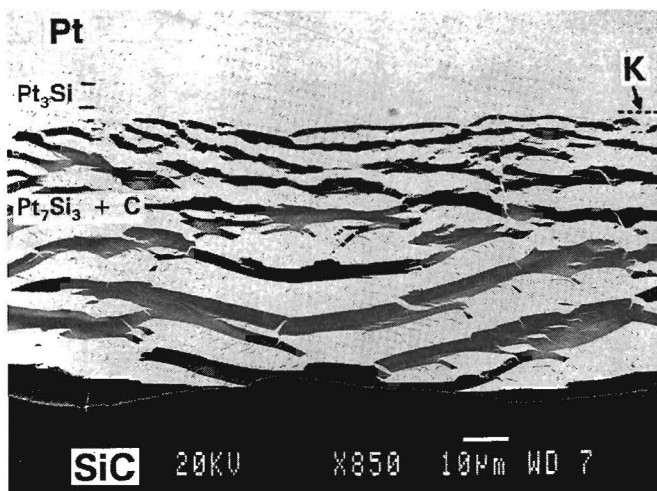


Fig. 5.32 Reaction zone of a diffusion couple of Pt with single crystal SiC, annealed for 25 h at 973 K in vacuum

In order to interpret the presence (or absence) and sequence of the phases in the diffusion couples, knowledge about the Pt-Si-C diagram is needed. This diagram will be discussed in the following section.

#### *Isothermal cross-sections of the Pt-Si-C phase diagram*

A first attempt towards a description of the phase relations in the Pt-Si-C system was published by Searcy and Finnie ([24], reproduced in [25]). Their data are rather uncertain. No temperature was specified and not all binary Pt-Si compounds as we know them nowadays are present, i.e. Pt<sub>6</sub>Si<sub>5</sub> and Pt<sub>7</sub>Si<sub>3</sub> are missing. There is still some uncertainty as to the composition of the latter platinum silicide, which may also be found in literature as Pt<sub>12</sub>Si<sub>5</sub>, e.g. in [23]. A metastable phase, Pt<sub>2</sub>Si<sub>3</sub>, is also known [23].

The three binary phase diagrams involved in the Pt-Si-C system provide us with a specific type of cross-section. There are no binary Pt-C compounds and between Si and C only the line-compound SiC exists. Since platinum is a non-carbide forming metal, it is highly unlikely that ternary platinum-carbosilicides are present in the Pt-Si-C system. Moreover, in the studies of Chou it was shown by Raman spectroscopy that pure carbon is formed in the reactions between Pt and SiC, either in amorphous state or in the form of graphite and no ternary phases were reported. This topology of the cross-section allows us to determine the isothermal cross-section of the Pt-Si-C phase diagram by just one well-equilibrated pellet, as shown in Fig. 5.33. The dotted lines indicate all possible equilibrium triangles in the Pt-Si-C

system. If we find the silicide that is in equilibrium with both C and SiC, the other equilibria will immediately be known. We can achieve this by choosing the composition of the pellet in the upper right triangle of Fig. 5.33. We chose  $\text{Pt}_{30}\text{Si}_{35}\text{C}_{35}$  (a mixture of Pt and SiC) as the initial pellet-composition, indicated by A in Fig. 5.33.

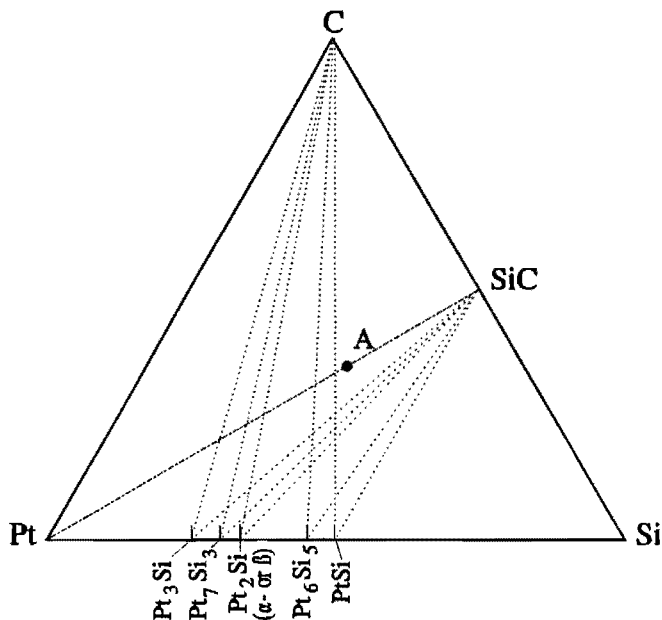


Fig. 5.33 Diagram showing how to choose the composition of a Pt/SiC pellet in order to determine the complete isothermal cross-section of the Pt-Si-C phase diagram

Cylindrical texture camera measurements [26] revealed the presence of coarse SiC particles,  $\alpha$ - $\text{Pt}_2\text{Si}$  and graphite at both annealing temperatures. The data were corroborated by the powder diffraction measurements.  $\text{Pt}_2\text{Si}$  was the only silicide phase present in the pellets.

Fig. 5.34 shows the cross-section of equilibrated pellets. Coarse-grained SiC is visible together with single-phase  $\text{Pt}_2\text{Si}$  and two-phase ( $\text{Pt}_2\text{Si}$  + graphite) regions. Only SiC, carbon and  $\text{Pt}_2\text{Si}$  were found both at 973 K and 1023 K. We conclude that PtSi,  $\text{Pt}_6\text{Si}_5$  and  $\text{Pt}_2\text{Si}$  are in equilibrium with SiC and  $\text{Pt}_7\text{Si}_3$ ,  $\text{Pt}_3\text{Si}$  and  $\text{Pt}_2\text{Si}$  are in equilibrium with carbon at both temperatures. This confirms the presence of  $\text{Pt}_2\text{Si}$  in the Pt/SiC diffusion couples annealed at 973 K. No ternary phases have been found. The experimentally determined cross-section of the phase diagram is given in Fig. 5.35.

### 5.4.3 Reactions of palladium with SiC

Because of its chemical similarity to both Ni and Pt, we investigated reactions of Pd-foil with HIPSiC (Fig. 5.36). Not surprisingly, a kind of periodic layered reaction zone developed in these diffusion couples. The reaction products are  $\text{Pd}_5\text{Si}$ ,  $\text{Pd}_3\text{Si}$ ,  $\text{Pd}_2\text{Si}$  and carbon which is

present as thick "broken pieces" inside  $\text{Pd}_3\text{Si}$ . Fig. 5.36b shows a very peculiar morphology of carbon found close to the  $\text{Pd}_5\text{Si}$  which may be related to the degradation of carbon bands as shown in Fig. 5.27c. Very recently, an extensive study of the Pd/SiC reaction [27] confirmed these results.

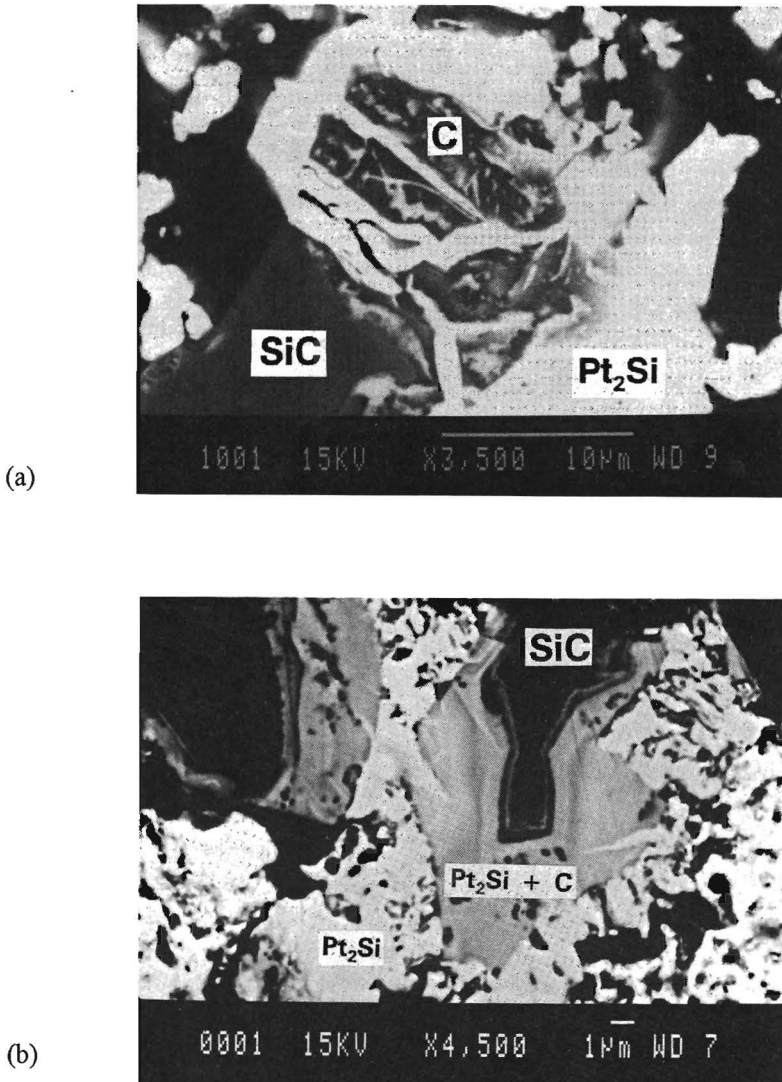


Fig. 5.34 Cross-sections of the equilibrated Pt/SiC pellets annealed in vacuum  
a) 448 h at 1023 K; b) 500 h at 973 K

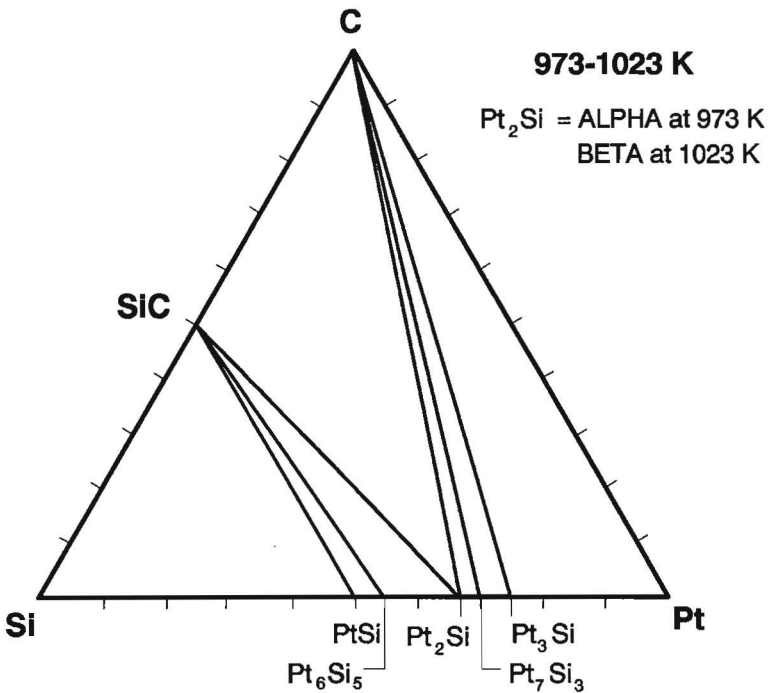


Fig. 5.35 Experimentally determined cross-section of the Pt-Si-C phase diagram.  $Pt_2Si$  is present as  $\alpha$  at 973 K and as  $\beta$  at 1023 K

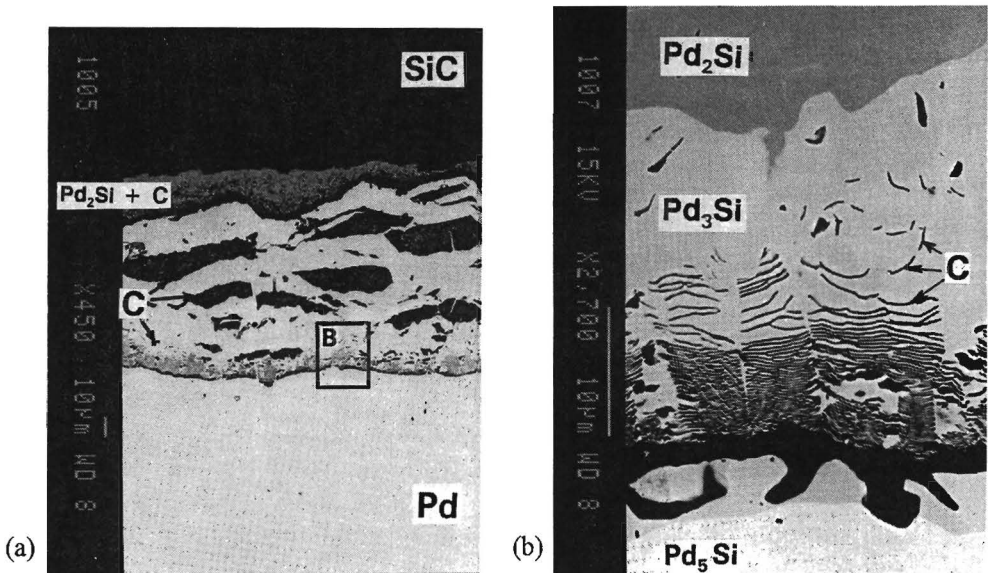


Fig. 5.36 Morphology of the reaction zone between Pd and HIPSiC, annealed for 64 h at 1003 K in vacuum (BEI); a) general view; b) magnification of area B in 5.36a



## References to Chapter 5

- [1] Binary alloy phase diagrams, T.B. Massalski, J.I. Murray, L.H. Bennett et al., eds., American Society for Metals, Metals Park, Ohio, 1986
- [2] C. Vahlas, P.Y. Chevalier, E. Blanquet: A thermodynamic evaluation of four Si-M (M = Mo, Ta, Ti, W) binary systems, *CALPHAD* **13** (1989), 273-292
- [3] J.A. van Beek, A.A. Kodentsov, F.J.J. van Loo: Phase relations in the Fe-Ag-Ti system at 1123 K, *J. Alloys Compounds* **221** (1995), 108-113
- [4] W. Wakelkamp: Diffusion and phase relations in the systems Ti-Si-C and Ti-Si-N, *PhD Thesis*, Eindhoven University of Technology, Eindhoven, the Netherlands, 1991
- [5] J.H. Gülpen, A.A. Kodentsov, F.J.J. van Loo: Growth of silicides in Ni-Si and Ni-SiC diffusion couples, *Z. Metallkde.* **86** (1995), 530-539
- [6] K. Osinski: The influence of aluminium and silicon on the reaction between iron and zinc, *PhD Thesis*, Eindhoven University of technology, Eindhoven, the Netherlands, 1983
- [7] K. Osinski, A.W. Vriend, G.F. Bastin, F.J.J. van Loo: Periodic formation of FeSi bands in diffusion couples Fe(15 wt.%Si)-Zn, *Z. Metallkde.* **73** (1982), 258-261
- [8] M. Bretez, J.-Y. Dauphin, J. Foct, P. Perrot: Phase relations and diffusion paths in the system zinc vapor - iron silicon alloys at 773 and 973 K, *Z. Metallkde.* **78** (1987), 137-140
- [9] S. Geller: The crystal structure of Co<sub>2</sub>Si, *Acta Cryst.* **8** (1955), 83-87
- [10] M. Onishi, Y. Wakamatsu, H. Miura: Formation and growth kinetics of intermediate phases in Fe-Zn diffusion couples, *Trans. Jap. Inst. Met.* **15** (1974), 331-337
- [11] E.M. Slyusarenko, S.F. Dunaev: Nonequilibrium effects in diffusion zones, *Vestn. Mosk. Univ., Ser. 2: Khim.* **28** (1987), 79-82
- [12] A. Zver'kov, S.F. Dunaev, E.M. Slyusarenko: Interaction of magnesium with alloys of the Co-Ni system, *Vestn. Mosk. Univ., Ser. 2: Khim.* **29** (1988), 182-184
- [13] S.F. Dunaev, S.A. Zver'kov: Influence of high pressure on the formation of periodic regular structures in multicomponent diffusion zones, *J. Less Comm. Metals* **153** (1989), 143-150
- [14] P. Adriaansens: Research on the morphology of the reaction layer in the diffusion pairs: Ni<sub>50</sub>Co<sub>20</sub>Fe<sub>30</sub>/Mg & Ni<sub>70</sub>Co<sub>30</sub>/Mg at 455 °C, *Student report*, Eindhoven University of Technology, Eindhoven, the Netherlands, 1990
- [15] A. Fernández Guillermet: Assessing the thermodynamics of the Fe-Co-Ni system using a calphad predictive technique, *CALPHAD* **13** (1989), 1-22
- [16] W. Köster, W.D. Haehl: Das Realschaubild und die Gleichgewichtseinstellung im Dreistoffsystem Eisen-Kobalt-Nickel, *Arch. Eisenhüttenw.* **40** (1969), 569-574
- [17] R.L. Mehan, M.R. Jackson: A study of solid metal/ceramic interactions, final report, General Electric Co. New York, 1982
- [18] M.R. Jackson, R.L. Mehan, A.M. Davis, E.L. Hall: Solid state SiC/Ni alloy reaction, *Met. Trans. A* **14A** (1983), 355-364
- [19] R.C.J. Schiepers, F.J.J. van Loo, G. de With: Reactions between a-SiC and nickel or iron, *J. Am. Ceram. Soc.* **71** (1988), C-284-C-287
- [20] M. Backhaus-Ricoult: Solid state reactions between silicon carbide and various transition metals, *Ber. Bunsenges. Phys. Chem.* **93** (1989), 1277-1281
- [21] T.C. Chou, A. Joshi, J. Wadsworth: Solid state reactions of SiC with Co, Ni, and Pt, *J. Mater. Res.* **6** (1991), 796-809
- [22] Binary alloy phase diagrams, T.B. Massalski, J.I. Murray, L.H. Bennett et al., eds., American Society for Metals, Metals Park, Ohio, 1986
- [23] Pearson's handbook of crystallographic data for intermetallic phases, P. Villars, L.D. Calvert, eds., American Soc. for Metals, Metals Park, Ohio, 1985

- [24] A.W. Searcy, L.N. Finnie: Stability of solid phases in the ternary systems of silicon and carbon with rhenium and the six platinum metals, *J. Am. Ceram. Soc.* **45** (1962), 268-273
- [25] H.J. Goldschmidt: Interstitial alloys, Butterworth & Co., Ltd. London, 1967
- [26] C.A. Wallace, R.C.C. Ward: An X-ray cylindrical texture camera for the examination of thin films, *J. Appl. Cryst.* **8** (1975), 255-260
- [27] K. Bhanumurthy, R. Schmid-Fetzer: Experimental study of ternary Pd-Si-C phase equilibria and Pd/SiC interface reactions, *Z. Metallkde.* **87** (1996), 244-253
- [28] M.R. Rijnders, A.A. Kodentsov, J.A. van Beek, J. van den Akker, F.J.J. van Loo: Periodic pattern formation in Pt/SiC diffusion couples, *Sol. St. Ionics*, accepted for publication

## CHAPTER 6

### MECHANISMS OF PERIODIC LAYER FORMATION DURING SOLID STATE REACTIONS

The previous chapter describes our observations on periodic layer formation. Two kinds of diffusion couples were considered: the finite thin foil (Ag/Ti-foil/Si) couples and bulk diffusion couples. In the thin foil couples single-phase periodic layers were observed in the reaction zone, whereas in the bulk couples the periodic layers exist of interwoven two-phase bands. The observed phenomena lead us to the conclusion that the two cases of periodic layer formation are fundamentally different. In this chapter we will demonstrate two mechanisms that lead to periodic layer formation in solid/solid diffusion couples.

#### 6.1 PROPOSED REACTION MECHANISM LEADING TO PERIODIC PATTERN FORMATION IN Ag/Ti-foil/Si DIFFUSION COUPLES

The series of events with increasing annealing time for a sandwich couple Ag/Ti-foil/Si is schematically depicted in Fig. 6.1. As long as pure  $\alpha$ -Ti is present in the transition zone between the Ti-silicides and  $Ti_2Ag$ , the growth of intermetallic phases is governed by the bulk diffusion kinetics of the respective binary systems Ti-Si and Ti-Ag (Fig. 6.1a). As soon as the Ti-foil is completely converted into intermetallic compounds, the binary Ti/Si and Ti/Ag couples constituting the sandwich couple are not semi-infinite anymore. In fact  $Ti_3Si$  and  $Ti_2Ag$  will meet (Fig. 6.1b). According to the phase diagram (Fig. 5.5) these phases can exist in equilibrium, but the reaction will proceed because of the Si- and Ag activity gradients which are still present in the diffusion couple. Silver diffuses through the TiAg-layer and reacts with  $Ti_2Ag$  until the entire layer of  $Ti_2Ag$  is converted into TiAg (Fig. 6.1c). The same holds for the Ti/Si couple: Si-atoms are still moving through the reaction product layers.  $Ti_3Si$  will transform into  $Ti_5Si_3$  and onwards into  $Ti_5Si_4$ . This process will eventually bring the  $Ti_5Si_4$  layer into contact with the TiAg layer. Since those layers cannot be in equilibrium, Si-atoms diffusing through the product layer will react at the TiAg/ $Ti_5Si_4$  interface according to the reaction:  $5 TiAg + 4 [Si] \rightarrow Ti_5Si_4 + 5 Ag$ . As a result a continuous layer of silver will form at the TiAg side, separating the TiAg and  $Ti_5Si_4$  layers (Fig. 6.1d).

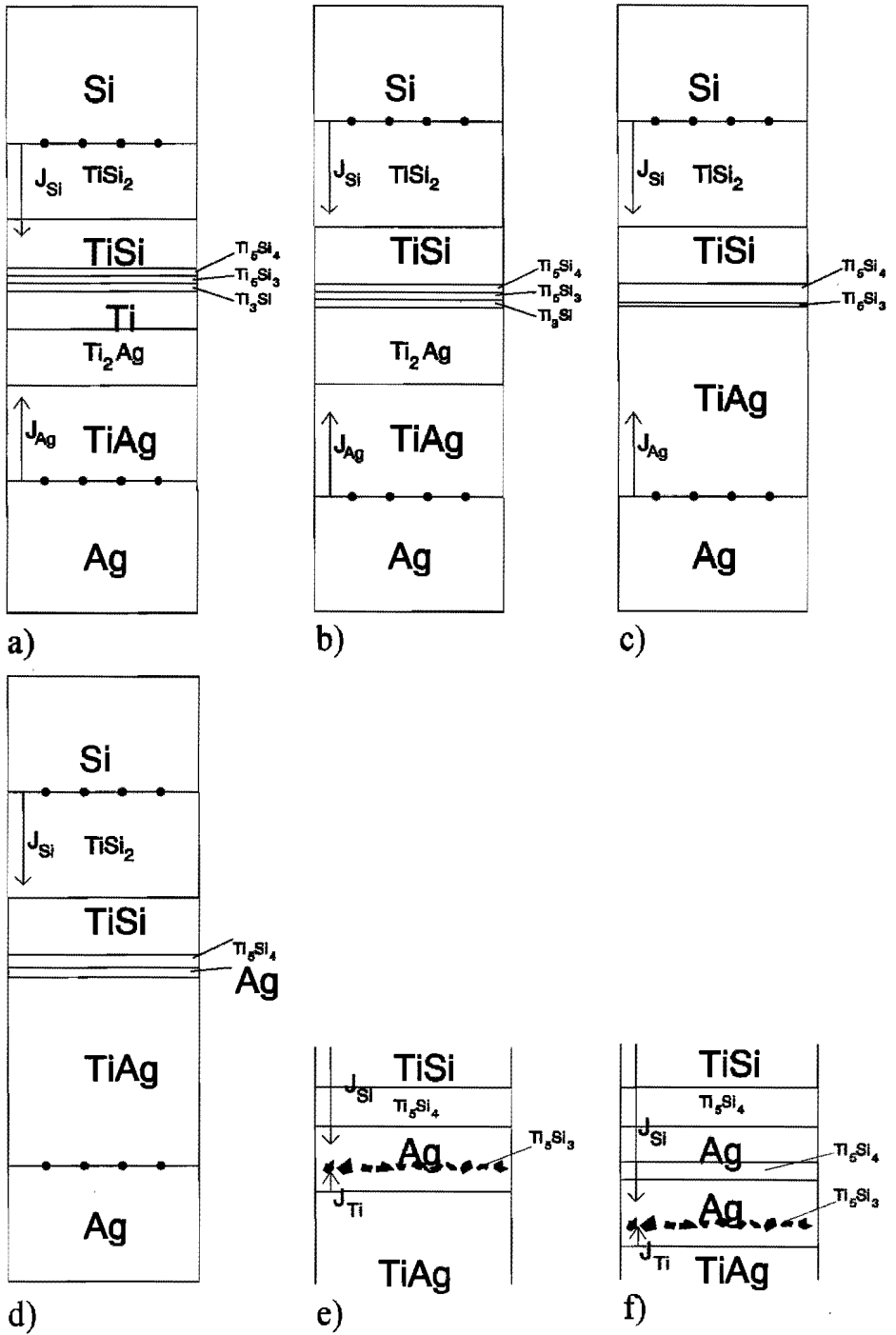


Fig. 6.1 Schematic illustration of reaction stages in the sandwich couple Ag/Ti-foil/Si

These phase sequences were experimentally observed in the transition zone of the sandwich sample Ag/Ti-foil(50  $\mu\text{m}$ )/Si after annealing in vacuum at 1073 K for 100 h (Fig. 6.2). In the part of the diffusion zone designated A (Fig. 6.2a)  $\alpha$ -Ti is not completely exhausted, in region B (enlarged in Fig. 6.2b) the Ti-foil was consumed and TiAg is indeed separated from  $\text{Ti}_5\text{Si}_4$  by a thin band of Ag. The point is now to explain the observed periodic structure, i.e. the transition from the morphology in Fig. 6.2b to that shown in Fig. 6.2c (region C in Fig. 6.2a).

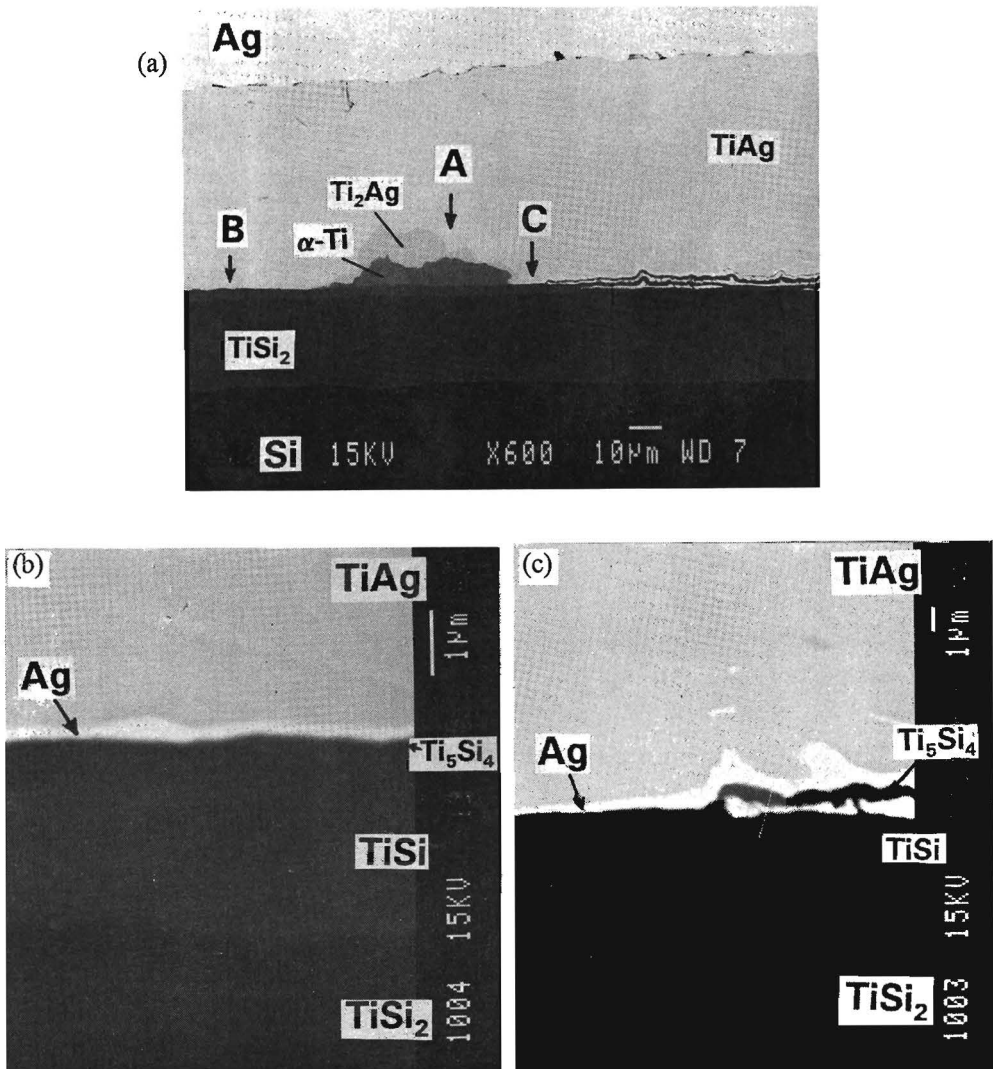
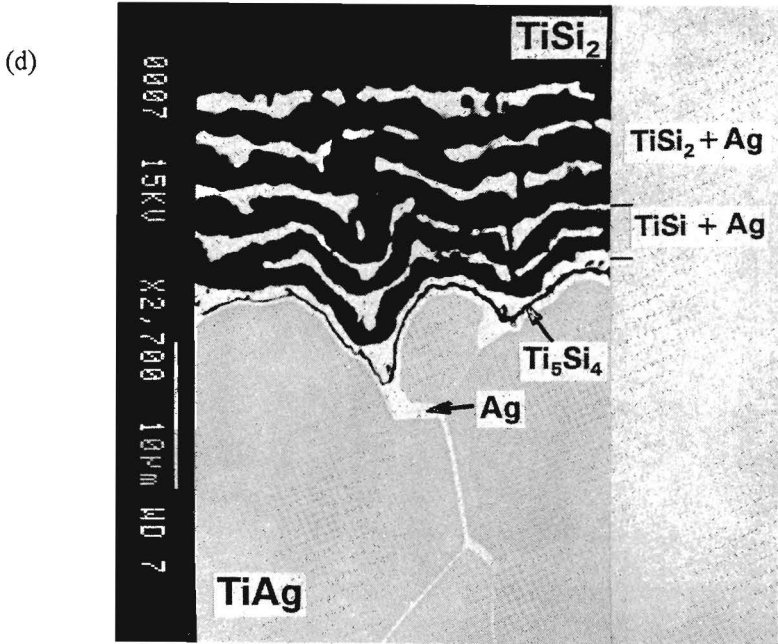


Fig. 6.2 Reaction zone in the sandwich couple Ag/Ti-foil(50 $\mu\text{m}$ )/Si, annealed for 100 h at 1073 K in vacuum; a) general view; b) magnified area pointed at by B in Fig. 6.2a, showing the formation of a continuous silver layer between Ti-silicides and TiAg

Fig. 6.2 (continued); c) magnified area pointed at by C in Fig. 6.2a, showing the initial stage of periodic layer formation; d) formation of silver along grain boundaries of TiAg



A number of mechanisms has been put forward to explain the formation of resembling periodic layered structures found in different solid state systems like  $\text{Fe}_3\text{Si}/\text{Zn}$ ,  $\text{Co}_2\text{Si}/\text{Zn}$  and  $\text{SiC}/\text{Ni}$ , either based on a periodic build-up and relaxation of stresses [1], on a periodic instability of the substrate/reaction product interface [2] or nucleation of bands through composition fluctuations [3].

Periodic layered zones of precipitates have also been observed in internal oxidation [4,5] and internal reduction [6] of solids and were explained as a Liesegang phenomenon [7], where the authors adopted Ostwald's supersaturation theory [8]: solute depletion at the precipitation front periodically arrests the nucleation process followed by recovery of supersaturation by subsequent diffusion (see also section 3.2). Although Kirkaldy and others developed a more general model for the spontaneous evolution of spatiotemporal patterns [9,10], we will follow Wagner's and Ostwald's line of reasoning [11] to show that the phenomena found by us are related to the Liesegang mechanism. In explaining the observed morphology in Ag/Ti-foil/Si couples we should, however, keep in mind that in the present system, contrary to the classical Liesegang phenomena, the "inert" matrix phase (in which precipitation takes place, in our case silver) itself grows as a new phase during the reaction.

The appearance of the silver layer between  $Ti_5Si_4$  and TiAg (Fig. 6.1d, 6.2b) creates a situation in which silicon atoms and titanium atoms (from TiAg, note depletion of the grain boundaries in Fig. 6.2d) can diffuse from opposite directions into the "inert" Ag-solvent and react to form titanium silicide inside the silver (somewhat similar to the Ti/Ag-foil/Si couple shown in Fig. 5.8). This reaction takes place close to the TiAg-side when the solubility product of the silicide reaches a critical supersaturation value. The internal reaction creates a band of precipitates (Fig. 6.1e). Probably first  $Ti_5Si_3$  will form, because this phase is, according to the experimentally determined phase diagram, Fig. 5.5, in equilibrium with nearly the whole range of Ag(Ti) solid solution. As precipitation continues, the silver layer grows at the expense of the dissociating TiAg. The increasing distance between the Ag/TiAg interface and the precipitation zone will cause the flux of Ti to decrease. This will lead to depletion of Ti and since the silicon flux keeps at a practically constant level (Si is a very fast diffuser through Ag), the  $Ti_5Si_3$  precipitates will transform into a band of  $Ti_5Si_4$ . This first band is shown in Fig. 6.2c, which is the enlarged area C of Fig. 6.2a. Subsequently Si can diffuse further into the freshly formed silver layer and the whole process will repeat, forming distinct bands inside the reaction zone, as is shown schematically in Fig. 6.1f and as observed in Fig. 6.2d. In the latter micrograph 6 bands are seen to have formed, of which the "youngest" is still very thin. Later on the bands of  $Ti_5Si_4$  can be converted into TiSi and finally into  $TiSi_2$  (Fig. 5.9d). The process keeps going until the entire layer of TiAg is converted in titanium silicides and silver.

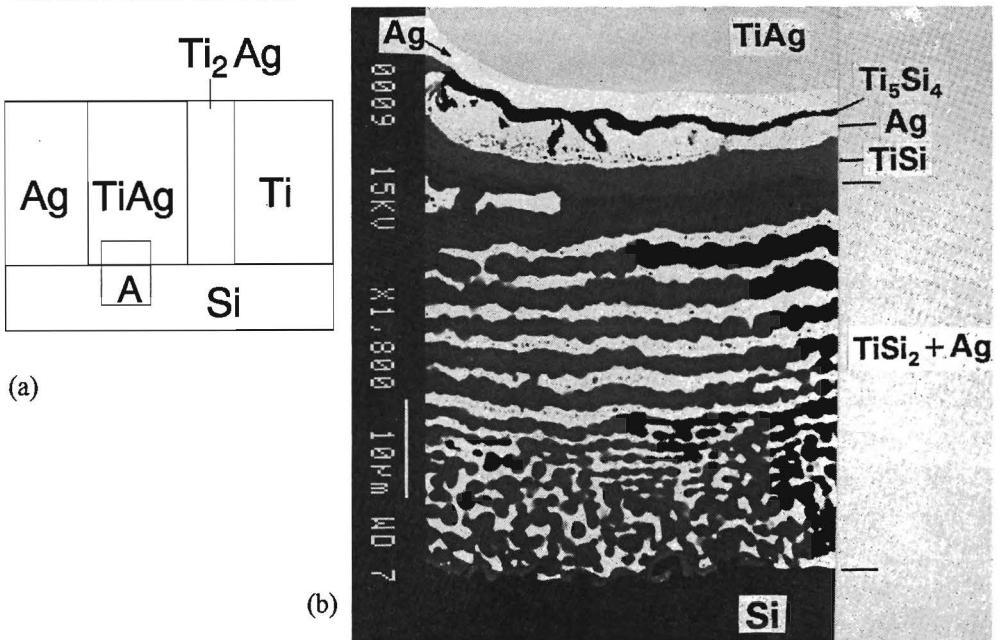


Fig. 6.3 *Reaction zone of a TiAg/Si diffusion couple annealed for 64 h at 1103 K in vacuum; a) schematic illustration of the diffusion couple; b) reaction zone between TiAg and Si, BEI of the part indicated by A in Fig. 6.3a*

If this mechanism is valid a same type of periodic structure can be expected for a diffusion couple of the type TiAg/Si. It was technically difficult to prepare a pure TiAg compound as a starting material, therefore the experiment was performed in the following manner: a Ti/Ag diffusion couple was annealed in order to form a layer of TiAg and afterwards a slice of silicon was joined to the cross-section of this couple (Fig. 6.3a). Between the silicon and the TiAg indeed alternating bands of silver and Ti-silicides were formed (Fig. 6.3b)

## **6.2 PERIODIC LAYER FORMATION AND THE KIRKENDALL EFFECT**

### **6.2.1 Evidence for Kirkendall-effect driven periodic layer formation; Pt/SiC diffusion couples**

In diffusion couples with components of unequal diffusivities mass flow occurs relative to the original interface (the Kirkendall plane, s. 2.5). The position of the Kirkendall plane relative to its original position (the Matano plane) gives information about the relative mobilities of the components. This is especially true for binary diffusion couples, but also for higher order systems.

The Kirkendall plane, i.e. the original contact surface between Pt and SiC, was found to lie within the Pt<sub>7</sub>Si<sub>3</sub> phase, close to Pt<sub>3</sub>Si. From this, we conclude that in Pt<sub>7</sub>Si<sub>3</sub> platinum is by far the most mobile element. In Pt/SiC diffusion couples a periodic layered structure is exclusively found in the Pt<sub>7</sub>Si<sub>3</sub> phase. Other systems known to exhibit a periodic layered reaction zone also contain an element that is relatively mobile in the reaction zone. Since no periodic layers were found in Pt<sub>2</sub>Si, the question arose whether the ratio of the mobilities of Pt and Si in this phase differed appreciably from that in Pt<sub>7</sub>Si<sub>3</sub>. In order to gain qualitative information about the relative mobilities of Pt and Si in Pt<sub>2</sub>Si, a many-foil couple of platinum with silicon was annealed. The use of this technique is described in [12]. Four foils of platinum of about 200 μm were clamped and annealed at 1023 K between two slices of silicon. Since the contact between foils can never be perfect, pores existing prior to annealing may serve to identify the original contact interfaces. The photomicrograph (Fig. 6.4) shows one half of the diffusion couple. The first foil of Pt is already completely consumed by the reaction. The second foil has been partly consumed. Pt<sub>2</sub>Si is the dominant phase in the diffusion zone, the other four Pt-Si intermetallics are present as very thin layers. The original interface between the first and second Pt-foil was determined by extrapolating the straight interface between the unreacted ends of the couple. This interface is marked M. The original interface between the Pt-foils two and three is marked by B. The row of pores marked by K' constitutes the second Kirkendall plane, i.e. the plane which was originally situated at M. It shows that this plane has shifted just a few microns from its original position in the direction of Si.

The situation is schematically depicted in Fig. 6.5. This figure shows the parabolic growth of a single compound (in this case, Pt<sub>2</sub>Si) in a binary system between two foils (Pt) and a bulk couple half (Si). The width of the Pt<sub>2</sub>Si layer at  $t = t^*$  has doubled at  $t = 4t^*$ . The position of



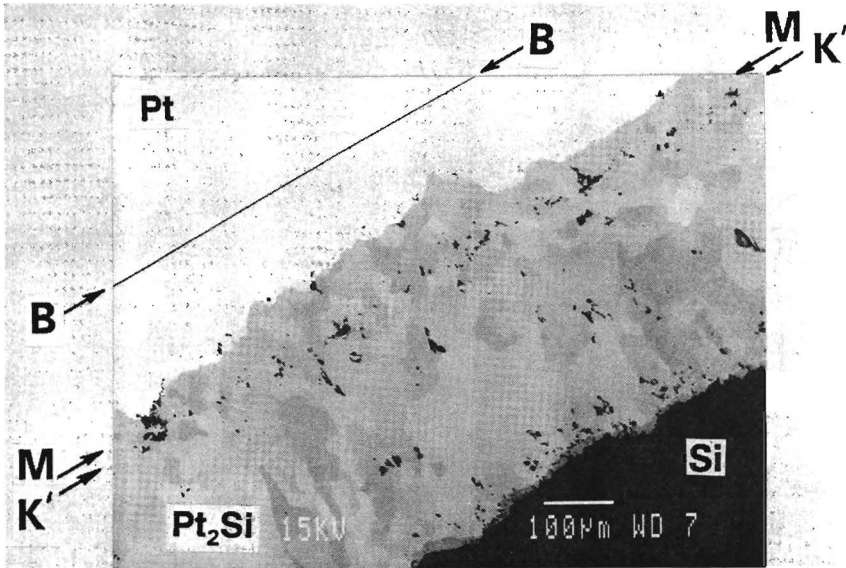


Fig. 6.4 "Multi-foil" couple of Pt and Si, annealed for 4h at 1023 K in vacuum

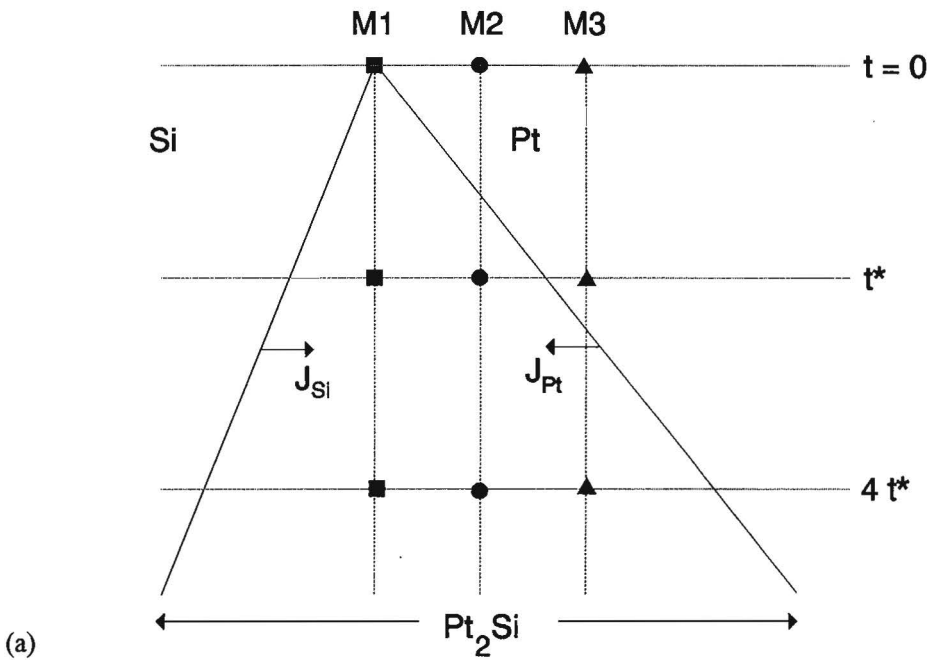
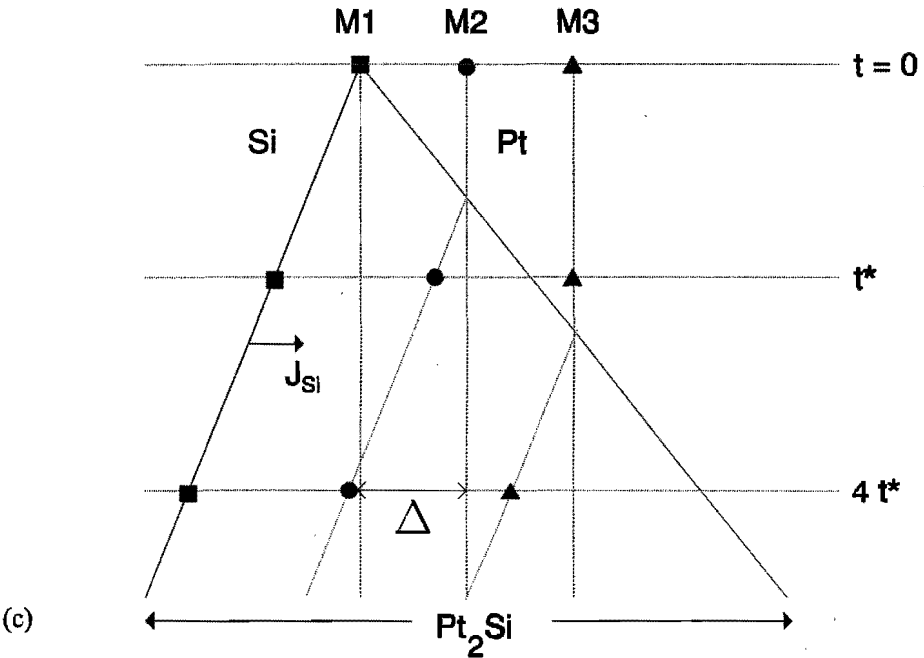
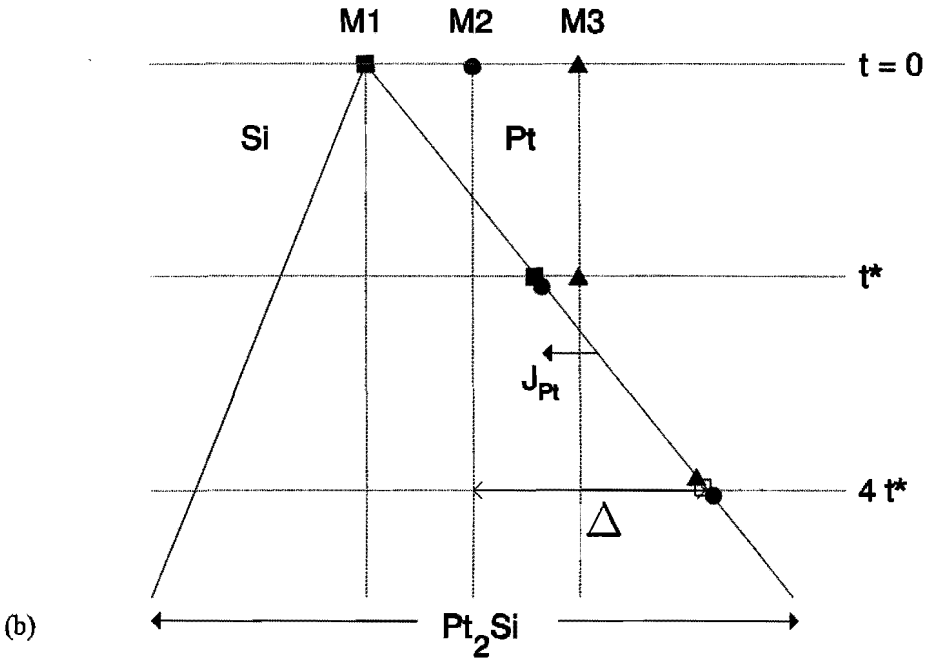


Fig. 6.5 Schematic view of interface motion in a multi-foil Pt/Si diffusion couple. For explanation, see text

Fig. 6.5 (continued)



markers is shown as a function of time for different kinetic situations. At time  $t = 0$  the markers are situated at their original positions between the bulk and the foil (M1) or between the foils (M2, M3, those markers are "buried" inside Pt). Clearly, if Pt and Si were equally mobile (i.e. there would be no net vacancy flux), the markers would not move from their position (Fig. 6.5a). On the Pt-side twice as much  $\text{Pt}_2\text{Si}$  would be formed as on the Si-side. The limiting cases are shown in Fig. 6.5b and c. If only Pt was mobile,  $\text{Pt}_2\text{Si}$  would grow at the Si/ $\text{Pt}_2\text{Si}$  interface and all markers would be found at the  $\text{Pt}_2\text{Si}/\text{Pt}$  interface (Fig. 6.5b). If only Si was mobile,  $\text{Pt}_2\text{Si}$  would be formed at the  $\text{Pt}_2\text{Si}/\text{Pt}$  interface and the markers would be "overtaken" by the  $\text{Pt}_2\text{Si}$  phase (Fig. 6.5c). In the latter two cases the markers show a maximum displacement from their original position, indicated by  $\Delta$  for the circular markers in Fig. 6.5. For intermediate situations the markers will have a displacement somewhere in between the two extremes and this is exactly what we found in the Si/Pt(multi-foil) diffusion couple of Fig. 6.4. The slight displacement of the K' plane from M towards Si indicates that in  $\text{Pt}_2\text{Si}$  the mobility of Si is somewhat higher than that of Pt. This observation supports the fact that the formation of a periodic layered reaction zone needs components with widely different mobilities inside this zone.

Considering the flux-balance at the  $\text{Pt}_2\text{Si}/\text{Pt}_7\text{Si}_3$  interface in connection with these observations, we note that this interface must be a source of vacancies. There is a large flux of vacancies from this interface in the direction of Pt, and a small flux in the direction of SiC. The formation of carbon bands may be explained by this situation.

At the SiC/ $\text{Pt}_2\text{Si}$  interface the following reaction takes place:  $\text{SiC} + 2 [\text{Pt}] = \text{Pt}_2\text{Si} + \text{C}$ , where  $[\text{Pt}]$  stands for diffusing Pt atoms.

At the  $\text{Pt}_2\text{Si}/\text{Pt}_7\text{Si}_3$  interface  $\text{Pt}_7\text{Si}_3$  is formed by conversion of  $\text{Pt}_2\text{Si}$ :  $3 \text{Pt}_2\text{Si} + [\text{Pt}] = \text{Pt}_7\text{Si}_3$ . This interface is moving towards the SiC, into the carbon-containing zone. As long as the carbon remains inside  $\text{Pt}_2\text{Si}$  it will experience a "Kirkendall force" in the direction of SiC, whereas when it is located inside  $\text{Pt}_7\text{Si}_3$  it experiences a force in the opposite direction. These oppositely directed forces will eventually tear the interwoven carbon band apart at the  $\text{Pt}_2\text{Si}/\text{Pt}_7\text{Si}_3$  interface. That inert markers may be split in a solid state diffusion couple was already demonstrated by Bastin [28]. Van Loo et al. have considered the splitting of markers in binary diffusion couples theoretically [13]. After this splitting the process will repeat. As the reaction layer growth continues the fluxes at this interface will diminish and consequently the time needed to separate another carbon layer is greater. This explains why the band width increases in the direction of SiC. Since continuing band formation was observed at 700 °C, the fluxes as observed in the multi-foil experiment at 750 °C are expected to be qualitatively the same at this temperature.

At 750 °C the band formation was observed to cease after a number of bands had been formed. The  $\text{Pt}_2\text{Si}/\text{Pt}_7\text{Si}_3$  interface is then located outside the carbon-containing zone (Fig. 5.27). This indicates a change in reaction kinetics during the reaction. Whereas at first the mechanism described above may be operative and the  $\text{Pt}_2\text{Si}$  remains relatively thin, there must, in a later stage, be a changeover to  $\text{Pt}_2\text{Si}$  formation at the  $\text{Pt}_2\text{Si}/\text{Pt}_7\text{Si}_3$  interface so that

the motion of this interface is reversed. As the interface then moves away from the carbon containing zone, no more carbon layers can be separated.

It may be observed from Fig. 5.27 that the relative thicknesses of  $\text{Pt}_2\text{Si}$  and  $\text{Pt}_7\text{Si}_3$  differ from the binary case. Whereas in the binary case  $\text{Pt}_2\text{Si}$  is by far the fastest growing phase, in the case of Pt/SiC couples the thicknesses of  $\text{Pt}_2\text{Si}$  and  $\text{Pt}_7\text{Si}_3$  are almost equal after 36 hours of annealing. As argued above, in order to form bands, the  $\text{Pt}_2\text{Si}$  should be even smaller in the beginning of the reaction. This may be explained by the fact that in the ternary case  $\text{Pt}_2\text{Si}$  is not able to grow over its entire homogeneity region, since it is in part in equilibrium with C and in part with SiC (Fig. 6.6), and only the first part gives rise to a diffusion potential. The same difference can be observed for the growth of  $\delta\text{-Ni}_2\text{Si}$  in Ni/SiC or Ni/Si diffusion couples [14].

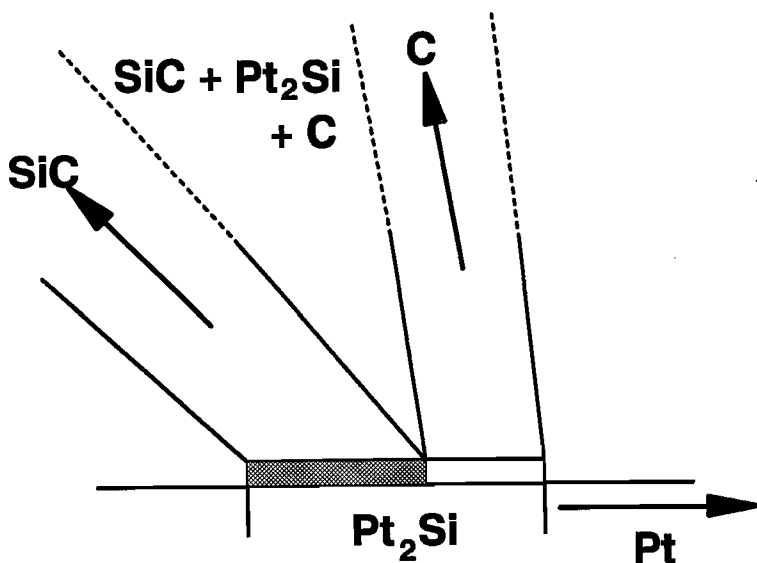


Fig. 6.6 *Magnified region of a cross-section of the Pt-Si-C phase diagram, showing that  $\text{Pt}_2\text{Si}$  is not able to grow over its entire homogeneity region*

Recently a paper has been published on the reaction of NiO with Al [15]. The reaction zone consisted of bands of  $\text{Al}_2\text{O}_3$  embedded in a matrix of the Ni-aluminides  $\text{NiAl}_3$  and  $\text{Ni}_2\text{Al}_3$ . Neither  $\text{NiAl}$  nor  $\text{Ni}_3\text{Al}$  were found in the reaction zone. The NiO was separated from this zone by a pure Ni-layer. From binary Ni-Al diffusion couple experiments [16] it is known that  $\text{NiAl}_3$  and  $\text{Ni}_2\text{Al}_3$  are the dominant phases, whereas  $\text{NiAl}$  and  $\text{Ni}_3\text{Al}$  grow as very thin layers. Moreover, Al is the only diffusing species in the first two compounds, whereas Ni is the only diffusing species in the other two. It appears therefore, that in accord with our theory for periodic layer formation, in NiO/Al diffusion couples the  $\text{Ni}_2\text{Al}_3/\text{NiAl}$  interface acts as the separating interface for the inert  $\text{Al}_2\text{O}_3$  layers.

### 6.2.2 Fluxes in metal-silicide/Zn diffusion couples

At the relatively low temperature (390 °C) of the experiments with solid zinc, the reaction is totally dominated by the diffusion of zinc through the reaction zone. Marker experiments with Fe/Zn [17] and Fe/ $\zeta$  [18] diffusion couples have shown that Zn is the only mobile element in those binary solid-solid couples. The presence of Kirkendall pores on the Zn-side in Fe<sub>3</sub>Si/Zn diffusion couples proves that Zn is also the only mobile component in  $\zeta$  in those couples. We suppose that this is also true for Zn in the  $\delta$ -phase. Therefore the reaction takes place at the Fe<sub>3</sub>Si/reaction layer interface and is characterized by an uptake of Fe from Fe<sub>3</sub>Si by Zn and a redistribution of the remaining Fe and Si to form FeSi at the reaction front. Since the layer growth is parabolic, the diffusion of Zn must be rate-limiting.

Si-rich particles have been observed to drift off into the reaction zone as inert markers in a  $\zeta$ /Fe(1.3 at.%Si) diffusion couple [18].

Vasilev and Budurov investigated the growth kinetics of Co-Zn [19] and Ni-Zn [20] diffusion couples in the temperature range of 420 °C to 1000 °C. The interdiffusion coefficients and activation energies for growth of the intermediate phases were calculated. However, no statements on the separate mobilities of Co, Ni or Zn were given. We consider, in view of the low temperature in our experiments, that zinc is the only mobile component in such couples, analogous to the Fe-Zn case. In Co<sub>2</sub>Si/Zn couples, the Kirkendall plane is situated on the zinc side, proving that Zn is the most mobile component in  $\gamma_2$ . In the fastest growing cells the growth of the reaction layer is not hindered by the bands of CoSi particles. The growth is even faster than in the binary case.

In view of the mechanism for periodic layer formation given in the previous section, in transition metal silicide/zinc couples, the substrate/reaction layer interface must act as the separating interface for band formation.

### 6.2.3 Periodic layer formation in Ni-Co-Fe alloy/Mg diffusion couples

In Section 5.4 it was shown that alloys Ni<sub>x</sub>Co<sub>y</sub>Fe<sub>z</sub> (indicated by X-Y-Z in the following) react with magnesium to give, in some cases, a periodic layered reaction zone. The appearance of the zone varies according to the composition of the alloy. The 50-20-30 gives a clear periodic structure, the 40-20-40 gives coarse and irregular bands (onset of band formation is seen in Fig. 5.22a), the 60-20-20 (Fig. 5.22b) and the 60-10-30 give a "foggy" periodic appearance [21], i.e. precipitates are more spread throughout the reaction zone, and the 40-30-30 gives a "normal" layered reaction zone [21]. Two phases are clearly present in all cases; Mg<sub>2</sub>Ni, which forms the matrix and precipitates of (Fe,Co) solid solution. At the temperatures of interest, Mg shows the highest mobility in Mg<sub>2</sub>Ni, Ni shows some mobility and Fe and Co show none.

The point of interest in these diffusion couples is the breakaway of the bands, which occurs at a relatively large distance away from the substrate/reaction layer interface, i.e. the substrate is always covered with a thick and dense band of precipitates. We therefore expected a "hidden phase" to be present (as in the Pt/SiC diffusion couples), namely MgNi<sub>2</sub>. The MgNi<sub>2</sub>/Mg<sub>2</sub>Ni interface would then act as the "Kirkendall separator", as the Pt<sub>2</sub>Si/Pt<sub>7</sub>Si<sub>3</sub> interface does in

Pt/SiC diffusion couples, if Ni would be diffusing faster in this phase than Mg. The fact that the bands grow quite thick may be due to their dense growth, making the process of mechanical separation harder than in other cases of periodic layer formation.

We could not detect this MgNi<sub>2</sub> phase, however, and the presence of it remains speculative. The alloy that failed to give periodicity might have a different diffusion path as the others, i.e. the MgNi<sub>2</sub> phase could be skipped. Since the Mg-Ni-Co-Fe phase diagram is not known, no certain conclusions can be drawn as yet.

#### **6.2.4 Sintering behaviour and band formation**

We have seen that the bands in the periodic layered structure consist of interwoven particles. Two conditions have to be met in order to reach the interwoven state. First, the fresh nuclei must reside at the reaction interface for a sufficiently long time. Second, the volume fraction of this product phase must exceed a critical value.

We cannot a priori determine whether a reaction layer will consist of isolated precipitates or interwoven precipitates. However, the sintering of particles is crucial to periodic layer formation, as we can see from experiments with Fe(Si)/Zn diffusion couples. Osinski has shown that there is a transition between a zone of isolated precipitates and a periodic layered zone when the Si-content of the Fe(Si) solid solution is increased from 17.9 at.% Si to 23.2 at.%. At the latter concentration, bands of FeSi start to develop, although they are not continuous over such long distances as in the Fe<sub>3</sub>Si/Zn couples. The ability of the reaction products to form a continuous interwoven two-phase layer at the reaction interface is therefore important for the formation of a periodic layered morphology.

#### **6.2.5 Single-crystal vs. polycrystalline substrate**

The reaction zone morphology of a solid state reaction may differ depending on whether a single crystal or a powder compact is used as a couple half. For instance, the reaction between powder compacted NiO and Fe gives an interwoven morphology [22]. When single crystal NiO is used, the morphology is still interwoven, but a kind of periodicity may be observed [23].

We found a very conspicuous difference when single crystalline SiC instead of hot isostatically pressed SiC (HIPSiC) was annealed with platinum (compare Figs. 5.27a and 5.32b, see also [24]). Single crystal, polycrystalline or powdered materials are not chemically different. Indeed the reaction products found will be the same with all of these. It is the arrangement of those products which differs and the reason for this must be physical in nature. The experiments with coarse-grained Co<sub>2</sub>Si show that the crystallographic orientation of the substrate grain determines the morphology of the reaction zone.

Both growth velocity and morphology of the reaction layer are dependent on the orientation of the Co<sub>2</sub>Si grains in the substrate. Co<sub>2</sub>Si is orthorhombic, hence its properties are anisotropic. This can affect the reaction in the following way:

The crystals at the surface present different crystallographic planes to the zinc. Those planes differ in surface energy and nucleation of a new phase is influenced. Since we found the

reaction to be diffusion controlled (in some parts, perhaps not in all) nucleation problems do not play a major role. Moreover, the small band present along the zinc-side indicates that growth of all the cells starts at the same time. However, newly nucleated product phases may show preferential orientation of growth (i.e. texture). If the various cells in the reaction layer possess different textures, the diffusion rate of zinc to the reaction front (which is rate-determining for the growth velocity) will vary from cell to cell and hence some cells grow faster than others. This is illustrated in Fig. 6.7. The direction of maximum diffusion velocity inside the diffusion zone is indicated by  $J_{\perp}$ .

The effect will become small when the grain size of the substrate is small (like with the HIPSIC), when diffusion in the reaction products is not very anisotropic or when the orientation relationship of the substrate and the product is not very strong.

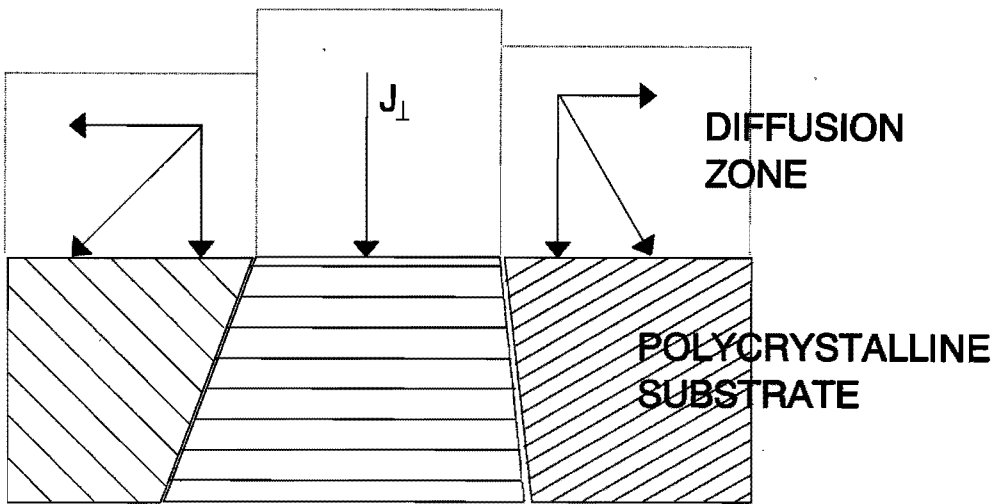


Fig. 6.7 *Schematic view of diffusion fluxes through the reaction zone in cells on differently oriented substrate grains.  $J_{\perp}$  is at a maximum in the middle, so this part of the reaction zone will grow fastest*

### 6.3 APPEARANCE OF LOOPS

The pattern which is shown in Fig. 5.17 is a top view of the reaction layer. The pattern is very similar to dislocation loops emerging from a Bardeen-Herring source [25]. In the Bardeen-Herring mechanism dislocations are multiplied by climb. This kind of climb source had an antecedent in the Frank-Read source for glide loops [26] and is configurationally similar to it. We suggest that macroscopic deformation loops, which are a result of the action of what we call a "super Bardeen-Herring source", are present in the  $\text{Co}_2\text{Si}$ . The source could be a result from the arc-melting procedure, whereby the rapid cooling introduces all kinds of imperfections into the lattice. A long stretch of dislocation line, possibly resulting from stacking faults, is running parallel to the  $\text{Co}_2\text{Si}$  surface. We have observed the presence of stacking faults in  $\text{Co}_2\text{Si}$  by etching the material. A section of the line is pinned. It extends over a length of about 30  $\mu\text{m}$  (Fig. 5.17). The subsequent heat treatment then could cause the source to expand by climb, curing the missing planes, and form several rings of deformed  $\text{Co}_2\text{Si}$ , the distance between the loops ranging from 20  $\mu\text{m}$  up to 45  $\mu\text{m}$ . Macroscopic dislocation spirals with comparable spacing have been observed in silicon (see, e.g. [27]). When this faulted  $\text{Co}_2\text{Si}$  is joined with zinc and annealed we suggest that when a Co-Zn phase nucleates, the remaining Co and Si are segregated out of the growing Co-Zn phase and precipitate as  $\text{CoSi}$  on the dislocation loops, i.e. the dislocation loops are covered by small  $\text{CoSi}$ -nuclei. In the course of reaction those nuclei grow out to macroscopic particles, decorating the places where used to be the dislocation loops.

Because of the polycrystalline nature of the substrate we can only observe this pattern in its purest form in some rare cases. Unfavourable orientations of the substrate grains and/or differently oriented dislocations will probably lead to the chaotic patterns that we commonly observe in cross-sections perpendicular to the diffusion direction.

### References to Chapter 6

- [1] F.J.J. van Loo, K. Osinski: Periodic structures in multicomponent diffusion couples, in: Proc. Int. Symp. on fundamentals and applications of ternary diffusion, G.R. Purdy, ed., Pergamon Press, (1990), 109-118
- [2] C.R. Kao, Y.A. Chang: A theoretical analysis for the formation of periodic layered structure in ternary diffusion couples involving a displacement type of reaction, *Acta Metall. Mater.* **41** (1993), 3463-3472
- [3] S.F. Dunaev, S.A. Zver'kov: Influence of high pressure on the formation of periodic regular structures in multicomponent diffusion zones, *J. Less Comm. Metals* **153** (1989), 143-150
- [4] V.A. van Rooijen, E.W. van Royen, J. Vrijen, S. Radelaar: On Liesegang bands in internally oxidized AgCd-based ternary alloys, *Acta Met.* **23** (1975), 987-995
- [5] Y.S. Shen, E.J. Zdanuk, R.H. Krock: The influence of additives on the formation of periodic precipitation (Liesegang bands) in the Ag-Cd system, *Met. Trans.* **2** (1971), 2839-2844
- [6] R.L. Klueh, W.W. Mullins: Periodic precipitation (Liesegang phenomenon) in solid silver, *Acta Met.* **17** (1969), 59-76
- [7] R.E. Liesegang: Ueber einige Eigenschaften von Gallerten, *Naturw. Wochenschr.* **11** (1896), 353-362



- [8] W. Ostwald: Lehrbuch der allgemeinen Chemie, An.Engelman Verlag, Leipzig (1897), 778
- [9] J.S. Kirkaldy: A continuum theory of Liesegang phenomena, *Scripta Met.* **20** (1986), 1571-1574
- [10] J.S. Kirkaldy: Spontaneous evolution of spatiotemporal patterns in materials, *Rep. Prog. Phys.* **55** (1992), 723-795
- [11] C. Wagner: Mathematical analysis of the formation of periodic precipitations, *J. Colloid Sci.* **5** (1950), 85-97
- [12] Y. Adda, J. Philibert: La diffusion dans les solides, Tome I & II, Institut National des Sciences et Techniques nucléaires, Saclay (1966)
- [13] F.J.J. van Loo, B. Pieraggi, R.A. Rapp: Interface migration and the Kirkendall-effect in diffusion-driven phase transformations, *Acta Metall. Mater.* **38** (1990), 1769-1773
- [14] J.H. Gülpen: Reactive phase formation in the Ni-Si system, *PhD. Thesis*, Eindhoven University of Technology, Eindhoven, the Netherlands (1995)
- [15] D.W. Song, R. Subramanian, R. Dieckmann: Displacement reactions in the Ni-Al-O system resulting in periodic layer structures, *Mat. Res. Soc. Symp. Proc.* **365** (1995), 59-64
- [16] M.M.P. Janssen, G.D. Rieck: Reaction diffusion and Kirkendall-effect in the nickel aluminum system, *Trans. Met. Soc. AIME* **239** (1967), 1372-1385
- [17] M. Onishi, Y. Wakamatsu, H. Miura: Formation and growth kinetics of intermediate phases in Fe-Zn diffusion couples, *Trans. Jap. Inst. Met.* **15** (1974), 331-337
- [18] K.A. Lichti, P. Niessen: The effect of silicon on the reactions between iron and zeta (FeZn<sub>13</sub>), *Z. Metallkde.* **78** (1987), 58-62
- [19] G. Wassilew, S. Budurov: Growth kinetics of Co-Zn intermediate phases, *J. Alloys Compounds* **199** (1993), 197-201
- [20] S. Budurov, G. Wassilew, N.T. Kuck: Die Wachstumskinetik von Schichten intermetallischer Phasen im System Nickel-Zink, *Z. Metallkde.* **68** (1977), 226-230
- [21] C. Cserhádi: Periodic layer formation in the Ni-Co-Fe-Mg and Ni-Si-Zn system, *Internal report*, Eindhoven University of Technology, Eindhoven, the Netherlands, 1994
- [22] R.A. Rapp, E. Ezis, G.Y. Yurek: Displacement reactions in the solid state, *Met. Trans.* **4** (1973), 1283-1292
- [23] C. Tangchitvittaya, J.P. Hirth, R.A. Rapp: Mechanism of the solid-state displacement reaction between iron and nickel oxide at 1000 °C, *Met. Trans. A* **13A** (1982), 585-594
- [24] K. Bhanumurthy, R. Schmid-Fetzer: Experimental study of ternary Pd-Si-C phase equilibria and Pd/SiC interface reactions, *Z. Metallkde.* **87** (1996), 244-253
- [25] J. Bardeen, C. Herring: Diffusion in alloys and the Kirkendall effect, in: Imperfections in nearly perfect crystals, W. Shockley, et al. eds., Wiley, New York (1952), 261-288
- [26] F.C. Frank, W.T. Read, jr. Multiplication processes for slow moving dislocations, *Phys. Rev.* **79** (1950), 722-723
- [27] S. Amelinckx: The direct observation of dislocations, *Solid State Physics*, suppl. 6, Academic Press, (1964)
- [28] G.F. Bastin, G.D. Rieck: Diffusion in the titanium-nickel system: I. Occurrence and growth of the various intermetallic compounds, *Met. Trans.* **5** (1974), 1817-1826

**LIST OF SYMBOLS AND ABBREVIATIONS**

a	activity	
B	mobility	( $\text{m s}^{-1} \text{N}^{-1}$ )
$C_i$	concentration of species i	( $\text{mol m}^{-3}$ )
d	reaction layer width	(m)
$D_i$	intrinsic diffusion coefficient	( $\text{m}^2 \text{s}^{-1}$ )
$D_{\text{int}}$	integrated diffusion coefficient	( $\text{m}^2 \text{s}^{-1}$ )
$\bar{D}$	interdiffusion coefficient	( $\text{m}^2 \text{s}^{-1}$ )
F	force	(N)
G	Gibbs energy	(J)
H	enthalpy	(J)
$J_j$	flux	(number/ $\text{m}^2 \text{s}$ )
$k_p$	parabolic rate constant	
K	Kirkendall plane	
$K_r$	equilibrium constant for a reaction	
$L_i$	transport coefficient	( $\text{mol}^2 \text{N}^{-1} \text{m}^{-2} \text{s}^{-1}$ )
M	Matano plane	
$n_i$	number of species i per unit volume	( $\text{m}^{-3}$ )
p	pressure	(Pa)
$P_i$	product species	
R	gas constant	( $8.314 \text{ J K}^{-1} \text{ mol}^{-1}$ )
$R_i$	reactant species	
S	entropy	( $\text{J K}^{-1}$ )
t	time	(s)
T	absolute temperature	(K)
$T_m$	melting temperature	(K)
v	velocity	( $\text{m s}^{-1}$ )
$\bar{V}_i$	partial molar volume of species i	( $\text{m}^3 \text{mol}^{-1}$ )
$V_m$	molar volume	( $\text{m}^3 \text{mol}^{-1}$ )
x	distance coordinate	(m)
$x_i$	atomic fraction of species i	
$\bar{x}$	total composition (= $x_1, x_2, x_3, \dots$ )	
$\gamma$	activity coefficient	
$\Delta G_r^\ominus$	standard Gibbs energy of reaction	( $\text{J mol}^{-1}$ )
$\Delta G_f^\ominus$	standard Gibbs energy of formation	( $\text{J mol}^{-1}$ )
$\mu$	chemical potential	( $\text{J mol}^{-1}$ )
$\mu_i^p$	chemical potential of species i in phase p	( $\text{J mol}^{-1}$ )
$\mu_i^\ominus$	chemical potential of pure i in its standard state	( $\text{J mol}^{-1}$ )
v	stoichiometric coefficient in chemical reaction equation	
$\xi$	distance coordinate	(m)
$\perp$	perpendicular to, edge dislocation	
Eq.	Equation	
Fig.	Figure	
SEM	Scanning Electron Microscopy	
TEM	Transmission Electron Microscopy	
EPMA	Electron Probe MicroAnalysis	
XRD	X-ray Diffraction	

## SUMMARY

This work deals with a peculiar phenomenon in solid state chemistry: the formation of a periodic layered reaction zone in diffusion couples. Four basic reaction layer morphologies may be found in ternary diffusion couples: simple layered, layered with isolated precipitates, interwoven and periodic layered. The first three types occur in the majority of solid state reactions. Their mechanism of formation is reasonably well understood. The periodic layered morphology, which was discovered fairly recently, is much less understood.

It is clear that the morphology of a reaction zone depends on the interplay between thermodynamic, kinetic, mechanical and other physical factors. A basic survey of those factors is given in Chapter 2. The Kirkendall-effect, present in all diffusion couples, and the role of diffusion and stresses in the reaction zone are discussed.

Periodic phenomena and periodic structures are encountered in other areas of chemistry. Well-known examples are Liesegang rings (colloid chemistry) and oscillating reactions (organic chemistry) which are discussed shortly in Chapter 3. From the literature survey it is concluded that Liesegang phenomena exist in the solid state. The theory for oscillating reactions is not thought to be adequate to explain the phenomena encountered in this research.

Two forms of periodic layered morphology are discerned in this thesis. One consists of alternating single-phase layers (occurring in Ag/Ti-foil/Si "sandwich" diffusion couples) and the other of a periodic array of two-phase bands in a single-phase matrix (occurring in, e.g., Pt/SiC diffusion couples). The experimental observations are presented in Chapter 5. In Chapter 6, the origin of the periodicity is shown to be different in both cases.

The formation of titanium-silicide bands in a silver matrix in Ag/Ti-foil/Si diffusion couples is described as a Liesegang phenomenon, the difference with the "classical" Liesegang band formation being that periodic precipitation takes place in a matrix formed *in situ* by the reaction.

The bulk of the experimentally observed periodic layered reaction zones in this work results from a different mechanism. They are found in diffusion couples of transition metal-silicides with zinc, non-carbide forming metals with silicon carbide and nickel-cobalt-iron alloys with magnesium. The periodic layers consist of interwoven bands of particles. In the part of the reaction zone in which periodic layers are found, one of the components has a high mobility, whereas the others have a small to negligible mobility. The bands are considered as inert markers. Periodicity results from a repeated "breaking" of the interwoven band covering the substrate, induced by a separation of Kirkendall planes at the interface between two phases. Remarkable patterns of loops appearing in Co<sub>2</sub>Si/Zn diffusion couples are explained to be resulting from the action of Bardeen-Herring sources (forming dislocation loops) in Co<sub>2</sub>Si.

## **SAMENVATTING**

Dit proefschrift behandelt een opmerkelijk verschijnsel in de vaste stof chemie: de vorming van een periodiek gelaagde reactiezone in diffusiekoppels. Er bestaan vier basis-morfologieën die gevormd kunnen worden in ternaire diffusiekoppels. Deze kunnen worden gerangschikt naar de onderlinge ligging van de fasen in de reaktielaag: 1) éénfasige lagen achter elkaar; 2) lagen met geïsoleerde precipitaten van een tweede fase; 3) twee fasen die met elkaar verweven zijn en 4) periodiek gelaagde fasen. Over de vorming van de eerste drie typen is veel bekend. Zij komen voor in het overgrote deel van de vaste stof reacties. De recentelijk ontdekte periodiek gelaagde morfologie is veel minder goed begrepen.

De morfologie van een reaktielaag wordt bepaald door een samenspel van thermodynamische, kinetische, fysische en mechanische factoren. Hoofdstuk 2 behandelt deze factoren en hun invloed op de reaktielaagvorming. Het Kirkendall-effect, aanwezig in alle diffusiekoppels, wordt toegelicht en de rol van diffusie en mechanische spanningen in de reaktielaag wordt verduidelijkt.

Periodieke verschijnselen en structuren zijn bekend in andere deelgebieden van de scheikunde. Bekende voorbeelden zijn Liesegangringen (colloidchemie) en oscillerende reacties (organische chemie). Een kort overzicht hiervan wordt gegeven in Hoofdstuk 3. Uit literatuurstudie blijkt dat het Liesegang-verschijnsel ook voorkomt in vaste stoffen. De huidige theorie voor oscillerende reacties wordt niet geschikt geacht om de verschijnselen uit het onderhavige onderzoek te verklaren.

In dit proefschrift worden twee periodiek gelaagde morfologieën onderscheiden. De ene bestaat uit eenfasige lagen die elkaar afwisselen (dit komt voor in Ag/Ti-folie/Si "boterham" diffusiekoppels), de andere uit een gelaagde structuur van tweefasige banden in een éénfasige matrix. Deze laatste vorm vinden we o.a. in diffusiekoppels van platina met siliciumcarbide. De experimentele waarnemingen worden gepresenteerd in Hoofdstuk 5. In Hoofdstuk 6 wordt aangetoond dat aan de vorming van de beide morfologieën een verschillend mechanisme ten grondslag ligt.

De vorming van banden van titaniumsilicides in een zilvermatrix in Ag/Ti-folie/Si diffusiekoppels wordt geïnterpreteerd als een Liesegang verschijnsel. Het verschil met de klassieke Liesegang bandvorming is dat de matrix, waarin de deeltjes periodiek neerslaan, zelf ook gevormd wordt door de reactie.

Het merendeel van de in dit proefschrift bestudeerde periodieke morfologieën vloeit voort uit een ander reaktiemechanisme. Deze morfologie vinden we in diffusiekoppels van overgangsmetaalsilicides met zink, metalen met silicium-carbide en nikkel-kobalt-ijzer legeringen met magnesium. De periodieke lagen bestaan uit banden van twee fasen die met elkaar verweven zijn. In het deel van de reactiezone waar de periodieke lagen worden aangetroffen heeft één van de componenten een grote mobiliteit, terwijl de andere een verwaarloosbare mobiliteit hebben. De banden worden beschouwd als inerte

*Periodic layer formation during solid state reactions*

markeringen. Herhaald "breken" van de band die het substraat bedekt wordt veroorzaakt door twee in tegengestelde richting bewegende Kirkendall vlakken in twee aan elkaar grenzende fasen. Dit zorgt voor periodieke banden in de reaktielaag.

De buitengewone patronen die zijn waargenomen in de reaktielaag van  $\text{Co}_2\text{Si}/\text{Zn}$  diffusiekoppels worden verklaard door de aanwezigheid van Bardeen-Herring bronnen (die patronen van dislocatielijnen veroorzaken) in  $\text{Co}_2\text{Si}$ .

## NAWOORD

Na de worstelpartij met wetenschappelijke materie rest mij de plezierige taak dit werk van een dankwoord te voorzien. Natuurlijk is dit niet volledig, maar de niet genoemden zullen waarschijnlijk net zoveel hebben bijgedragen aan de totstandkoming van dit boekwerk als diegenen die ik hier expliciet bedank. Zij weten zelf wie ze zijn.

Ten eerste wil ik mijn ouders bedanken die mij altijd hebben gestimuleerd om kennis te verwerven op allerlei gebied.

Mijn eerste promotor, Ruud Metselaar, bedank ik voor de vrijheid die hij mij gelaten heeft om het onderzoek naar mijn eigen inzicht in te richten. Veel dank ben ik verschuldigd aan mijn tweede promotor, Frans van Loo. Zijn enorme ervaring op het gebied van diffusie, zijn heldere uitleggen, zijn geduld en de nuttige discussies met hem hebben mij van het enthousiasme voorzien om dit project tot een goed einde te brengen.

I would like to thank Csaba Cserháti for introducing me to the principles of the art of diffusion-couple making, - baking and - breaking.

Alexander Kodentsov en Han van Beek heb ik leren kennen als de onvermoeibaar overuren makende experimentele tandem van onze groep, samen van onschatbare waarde voor een deel van de uitvoering van het werk. Nooit klopte ik tevergeefs bij hen aan voor een goed advies of zomaar een gesprek. Naar hen gaat mijn speciale dank uit.

Als a-technicus ben ik ook blij dat de technische staf van TVM ervoor heeft gezorgd dat de benodigde apparatuur meestentijds in staat van paraatheid was.

Through the years I have met and worked with many foreign colleagues and I will not try to address them in their respective languages; we always found common ground in speaking English. I have enjoyed their company and would like to thank them for the much wider view of the world they have given me.

Belangrijk voor mij is de steun en collegialiteit geweest van diverse AIO-collega's en studenten in onze groep. Vooral de laatste jaren ben ik dit steeds meer gaan waarderen. De buitenwetenschappelijke activiteiten die we samen ondernamen verlenen de broodnodige meerwaarde aan het werk. Naast de vaste stof chemie werd ook de chemie van vloeistof met gas grondig bestudeerd. Zij worden bij deze hartelijk bedankt.

Tenslotte gaat mijn dank ook uit naar mijn vrienden bij Nayade. Hoewel niet direct betrokken bij het werk hebben ze er toch voor gezorgd dat het leven in Eindhoven voor mij aangenamer en gezonder is geworden.

## CURRICULUM VITAE

Marco Rijnders werd geboren op 1 september 1966 te Andijk. Na het met goed gevolg doorlopen van zes leergangen aan het prof. ter Veen Lyceum te Emmeloord begon hij in 1984 aan een studie scheikunde aan de Rijksuniversiteit Groningen, met als hoofdvak chemie van de vaste stof. Zijn afstudeerwerk bestond uit het synthetiseren en meten van fysische eigenschappen van een aantal intercalatieverbindingen. De titel drs. werd hem toegekend op 27 september 1990.

In de anderhalf jaar daarop volgend volbracht hij zijn vervangende dienstplicht bij de Chemiewinkel van de Rijksuniversiteit Groningen.

In juli 1992 begon hij als onderzoeker in opleiding (OIO) in dienst van de Nederlandse Organisatie voor Wetenschappelijk Onderzoek (NWO) aan een promotie-onderzoek aan de Technische Universiteit Eindhoven, onder leiding van de promotoren prof.dr. R. Metselaar en prof.dr. F.J.J. van Loo. Uiteindelijk heeft dit werk geleid tot dit proefschrift.

Marco Rijnders was born on the 1<sup>st</sup> of September, 1966, in Andijk, the Netherlands. After secondary school he studied chemistry at the University of Groningen. His main subject concerned solid state chemistry. His graduation work consisted of the synthesis of some intercalation compounds and measurement of the physical properties thereof. He became a Master of Science in September 1990.

In the one-and-a-half year following this, he fulfilled his alternative national service at the "Chemiewinkel" of the University of Groningen.

In July 1992 he started research as a PhD. student at the Eindhoven University of Technology, in the pay of NWO (the Dutch organization for scientific research) and under the guidance of prof.dr. R.Metselaar and prof.dr. F.J.J. van Loo. The work finally resulted in this thesis.

**Stellingen**

behorende bij het proefschrift

**Periodic layer formation during solid state reactions**

door

**Marco Raymond Rijnders**

**16 december 1996**



1. De term "vervangingsreactie", zoals hij wordt gebruikt door Kao en Chang, is niet goed gedefinieerd en kan als zodanig worden gebruikt voor elke willekeurige chemische reactie.

C.R. Kao, Y.A. Chang, *Acta Metall. Mater.* **41** (1993), 3463-3472

2. Het is niet nodig om het bestaan van ternaire Co-Si-C verbindingen te postuleren om de periodieke structuren in Co/SiC diffusiekoppels te verklaren.

C.S. Lim, H. Nickel, A. Naoumidis, E. Gyarmati, *J.Mat.Sci.* **31** (1996), 4241-4247

3. Er is geen ternaire fase aanwezig in  $\text{Ni}_{50}\text{Co}_{20}\text{Fe}_{30}/\text{Mg}$  diffusiekoppels.

S.F. Dunaev, S.A. Zver'kov, *J.Less Common Metals* **153** (1989), 143-150;  
*Dit proefschrift*

4. Het niet vermelden van de gasdruk bij isotherme doorsneden van het fasendiagram van ternaire gas-vast systemen geeft verwarring die het mogelijk maakt om in de literatuur verschillende van deze isotherme doorsneden van hetzelfde systeem te vinden.

M. Paulasto, J.K. Kivilahti, F.J.J. van Loo, *J.Appl.Phys.* **77** (1995), 4412-4416;  
W. Wakelkamp: Diffusion and phase relations in the systems Ti-Si-C and Ti-Si-N, *PhD thesis*, Eindhoven University of Technology, Eindhoven, the Netherlands

5. Het inzetten van de Mobiele Eenheid tijdens vreedzame bijeenkomsten leidt vaak tot rellen.

6. Het *Journal of Materials Science* heeft een zeer brede opvatting van het begrip "materialen". Dit blijkt o.a. uit de volgende publikaties:

M.N. Charalambides, J.G. Williams, S.Chakrabarti: A study of the influence of ageing on the mechanical properties of Cheddar cheese, *J.Mat.Sci.* 30 (1995), 3959-3967

F.X. Hart, B.Bodakian: The dielectric spectra of heated potatoes, *J.Mat.Sci.Lett.* 14 (1995), 1214-1217

7. Het stimuleren van overheidswege tot het nemen van kinderen, door het verstrekken van kinderbijslag, zou moeten worden omgezet in een negatieve financiële prikkel ("kinderheffing") teneinde de bevolkingsgroei te keren.

8. Het schrappen van de evolutietheorie als leerstof voor het centraal schriftelijk eindexamen door de politiek getuigt van gebrekkig inzicht in de wetenschappelijke methode.

9. De technische ontwikkeling zoals die ons getoond wordt in SF films is gebaseerd op wat men denkt dat voortkomt uit de huidige stand van wetenschap en techniek. Films als Robocop, Terminator en Star Wars zijn daarom nog slechts een klein voorproefje van wat de mensheid te wachten staat.

10. Perfectie wordt slechts bereikt bij  $t = \infty$

11. Het is navrant dat sommige diersoorten door mensen vertroeteld en vereerd worden, terwijl diezelfde mensen met een gerust hart andere diersoorten opeten.

12. Liefhebbers van "hard rock" en "heavy metal" zijn bij uitstek geschikt voor onderzoek aan materialen.